KINETIC ANALYSIS OF HOMOGENEOUS CATALYTIC REACTIONS

Lynzi M. Robb

A Thesis Submitted for the Degree of PhD
at the
University of St. Andrews

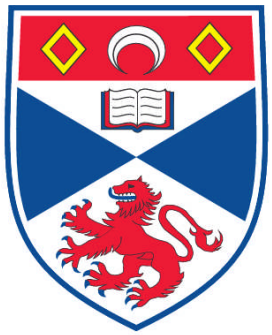

2011

Kinetic Analysis of Homogeneous Catalytic Reactions

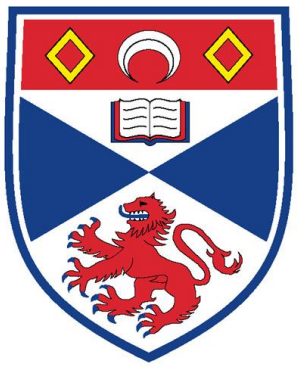

University
of
St Andrews

A thesis presented by

Lynzi M. Robb

To the

University of St Andrews

In application for

THE DEGREE OF DOCTOR OF PHILOSOPHY

April 2011

This thesis is dedicated to:

Robert Robertson Robb
I will love you always.

Anybody who has been seriously engaged in scientific work of any kind realises that over the gates of the temple of science are written the words “Ye must have faith”

– Max Planck

Declaration

I, Lynzi Marie Robb, hereby certify that this thesis, which is approximately 35,000 words in length, has been written by me, that it is the record of work carried out by me and that it has not been submitted in any previous application for a higher degree.

I was admitted as a research student in [October 2005] and as a candidate for the degree of Doctor of Philosophy in [October, 2005]; the higher study for which this is a record was carried out in the University of St Andrews between [2005] and [2011].

Date ……. signature of candidate …….

I hereby certify that the candidate has fulfilled the conditions of the Resolution and Regulations appropriate for the degree of Doctor of Philosophy in the University of St Andrews and that the candidate is qualified to submit this thesis in application for that degree.

Date ……. signature of supervisor ……

In submitting this thesis to the University of St Andrews I understand that I am giving permission for it to be made available for use in accordance with the regulations of the University Library for the time being in force, subject to any copyright vested in the work not being affected thereby. I also understand that the title and the abstract will be published, and that a copy of the work may be made and supplied to any bona fide library or research worker and that my thesis will be electronically accessible for personal or research use.

The following is an agreed request by candidate and supervisor regarding the electronic publication of this thesis:

Access to printed copy and electronic publication of thesis through the University of St Andrews.

Date …….. signature of candidate …….

Date …….……..signature of supervisor …….

Acknowledgements

Firstly I would like to thank my supervisor and friend, Professor David J. Cole-Hamilton for all his unwavering and infectious enthusiasm; his kind words as well as all his help and support throughout some of the most difficult times I have had to face, both within and out with my PhD. You are the true definition of a gentleman and it has been an honour and a privilege to know you and work for you. I would also like to thank Mrs Rosemary Cole-Hamilton for being so welcoming, loving and caring. If, in life I can become half the woman you are, I will have surpassed my highest expectations. A special mention also goes to Romeo.

I would like to thank the EPSRC and Lucite International for allowing me to work on this project and for the funding provided. In particular, I thank Dr Graham Eastman, for all his advice, input and good company.

My special thanks go to Mr Peter Pogorzelec. I would not have managed to complete this without you. When necessary you have kept me grounded, smiling, optimistic and very often sane and I am sincerely appreciative of all you have done for me. My regards and thanks also go to Mrs Wilma Pogorzelec for being such a friend these last four years.

To all the Cole-Hamilton group members, past and present, who made life and day to day life so much fun, who always went out of their way to help and advise when they could. My special thanks go to Dr Paul Webb, who was never to busy to take the time to answer all my silly questions. My particular thanks to Dr Gavin Hill, Dr Jennifer Amey, Dr Bianca Munoz, Jacorien Coetzee, Jan Hendrik and Ruben Duque for being such good friends over the last two years.

To all the additional academics and staff who made my time at St Andrews so enjoyable. Particular mentions go out to Mr Bobby Cathcart, I would never have got anything done without your help. Others I would like to thank include: Mr Arnot Williamson, Mrs Sylvia Williamson, Dr Nigel Botting, Dr Chris Baddeley, Dr Iain Smelley, Ian, Colin, George, Colin, Marjory and the office staff.

To all my friends, who have made my time in St Andrews so special and memorable. In particular Dr Lyndsey Ritchie, living proof that there is such a thing as a “posh fifer”, Dr Sara-Jane Dickson, the adopted St Andrews student, Dr Lynn Power, Dr Dave “The Shirt” Aldous, Jacqueline Garland, Dr Sneh Jain, Dr Charlotte Jones, Dr Aoife Trant, Dr Ben Parnham, Dr Steve Francis, Dr Lydia Hill, the honorary “C” word, Mr Stephen Shakespeare and his “th words”, Neal McLoughlin, Dr David “Mildred” Miller, Dr Mark Cassidy, Dr Ed Milton, Dr Laura Boyd, Dr Stewart Warrander and Julie Nairn.

Additional thanks go to my friends and colleagues at Johnson Matthey for constantly asking how the thesis is getting on. Thanks to Dan, Jamie, Ruth, Alex, Andrew, Jan, Lee, Marie, Giorgios, Richard, Jason and Louise. Special thanks go to Dr Colin Newman for pushing me when I needed it most.

To Gail Mallarkey, truly the best friend anyone could ever ask for. I doubt anyone else would drop everything to take me for Chinese food and wine when I have “blown something up.” Laura Steen, no matter how little I see you, I know I can always depend on you to be there when I need you. Ashleigh Day, my oldest friend and constant, having you around has always kept me grounded.

To Dr Jonathan Kearney, you truly are a special friend and I thank you from the bottom of my heart for taking the time to keep me company throughout my PhD, even if it did mean you got one yourself in the process. Dr Stuart Miller, you were my rock through the toughest parts of my PhD and I will always appreciate that and be thankful for it. I really couldn’t have done this without you. I would also like to acknowledge Andrew Mack for giving me the faith in myself to apply and take on a PhD in the first place. Your continual faith in me and your constant support have always been appreciated.

Lastly I would like to thank my family for all their love and support. I truly am gifted to have you as part of my life. You are the people who have made me who I am and I would be nothing without you. I love you more than you can ever imagine.

Table of Contents

List of Abbreviations

BDTB PMB	1,2-bis(di-*tert*-butylphosphinomethyl)benzene
VAM	vinyl acetate monomer
CO	carbon monoxide
MeOH	methanol
MsOH/MSA	methane sulphonic acid
$Pd_2(dba)_3$	tris(dibenzylideneacetone)dipalladium(0)
PPh_3	triphenylphosphine
TOF	turn over frequency
NMR	nuclear magnetic resonance spectroscopy
Pt	platinum
Pd	palladium
MeP	methyl propanoate
P	phosphorus
C	carbon
OMe	methoxy
PPh_2py	diphenylphosphinopyridine
MMa	methyl methacrylate
Co	cobalt
$HCo(CO)_4$	tetracarbonylhydrocobalt
α	alpha
ω	omega
D	deuterium
Au	gold
ROH	alcohol group
OAc	acetate group
Me	methyl group
R	functional group
PLA	poly lactic acid
FDA	United States food and drug administration
$	US dollar
$PdCl_2/PPh_3$	palladium (II) dicholride/triphenylphosphine

b:l	branched to linear ratio
ml	millilitres
s	seconds
k	rate constant
mol	mole
ln	natural log
p	partial pressure
β	beta
Ar	aromatic (aryl) group
Ph	phenyl group
napht	naphthalene group
Hg	mercury
H_2SO_4	sulphuric acid
P-N	aminophosphine ligand
h	hours
X	counter ion
RPKA	reaction progress kinetic analysis
FTIR	Fourier transform infra-red spectroscopy
Al_2O_3	aluminium oxide
K	Kelvin
mmoles	millimoles
H_2	hydrogen
H^+	hydride
UV-vis	ultraviolet-visible spectroscopy
GCMS	gas chromatography mass spectroscopy
$RhCl(PPh_3)_3$	chlorotris(triphenylphosphine)rhodium(I)
$RhCl_3(PPh3)_3$	trichlorortris(triphenylphosphine)rhodium(III)
NO_2	nitrogen dioxide
GC-FID	gas chromatography flame ionisation detector
MS	mass spectroscopy
PTFE	poly tetra fluoro ethane
$Rh(CO)_2(acac)_2$	dicarbonyl-diacetylacetone-rhodium (I)
µl	micro litre
cm^3	cubic centimetre

mg	milligram
tpp	triphenylphosphine
$RhH(PPh_3)_3CO$	Carbonyl triphenylphosphine rhodium hydride
Rh	rhodium
ae	axial-equatorial coordination
ee	equatorial-equatorial coordination
C_3H_6	propene
rpm	revolutions per minute
L	ligand
atm	atmospheres

Abstract

Reaction progress kinetic analysis (RPKA) is a powerful tool for determining kinetic parameters of catalytic reactions. Many of the published articles that have used RPKA have employed reaction calorimetry for obtaining sufficient data to be reliable. The use of gas uptake measurements, in place of calorimetry is explored in this Thesis.

Chapter 2 details the use of gas uptake measurements in establishing the order with respect to substrate and gas for the rhodium catalysed hydrogenation of 1-octene. Previous studies have used initial rate measurements to establish these orders and the reaction cycle is well known. The use of RPKA allows the same information to be established in two reactions.

Chapter 3 focuses on the rhodium catalysed hydroformylation of 1-octene as it involves the reaction of one substrate with two gases. Using RPKA it is possible to determine the order in substrate and the overall order in gas, but it was found difficult to determine the order with respect to the individual gases using RPKA alone.

Chapter 4 shows the palladium catalysed methoxycarbonylation of vinyl acetate. The reaction has two substrate concentrations changing simultaneously as well as a gas. This chapter shows that by careful design of experiments the orders with respect to each of these substrates and CO can be determined in minimal numbers of experiments.

Chapter 5 focuses on the methoxycarbonylation of alkynes, which uses RPKA in complex multistep reactions, to establish if RPKA can be used to determine the kinetics with respect to the individual reacting components for each step. This study focuses on the methoxycarbonylation of phenylacetylene to produce methyl cinnamate as well as the methoxycarbonylation of both terminal and internal linear alkynes. These linear alkynes carbonylate to produce an α,β-unsaturated ester. The double bond is isomerised from its conjugated position along the chain to the terminal position where it is trapped and carbonylated to produce an α,ω-dieter product.

1. Introduction and Aims

1.1 Catalysis

The concept of a catalyst was first recognised by Berzelius in 1836.[1] He concluded that the effect was brought on by a special force applied to the reaction by the catalyst. Oswald,[2] conducted studies into catalysis between 1888 and the early 20th century. Within this time he defined a catalyst as being *"a substance that alters the velocity of a chemical reaction without modification of the energy factors of the reaction."* [2] There have been several definitions since then which are equivalent to one another but the definition approved in 1981 by the International Union of Pure and Applied Chemistry states that *"a catalyst is a substance that increases the rate of a reaction without modifying the overall standard Gibbs free energy change in the reaction; the process is known as catalysis, and a reaction which a catalyst is involved in is known as a catalysed reaction."* [3]

There are numerous organic reactions which can be catalysed by both heterogeneous and homogeneous catalysts; a good example of this would be the hydrogenation of alkenes; using Wilkinson's catalyst, palladium on carbon or Raney nickel. Each system has advantages and disadvantages but upon comparison, there are many advantages of homogeneous catalysts over heterogeneous catalysts.[4]

Homogeneous catalysts are known to be more active than heterogeneous catalysts.[4] The surface only coordination within heterogeneous catalysts allows for a very limited diffusion and restricts the number of catalytically active sites available. As homogeneous catalysts tend to be in solution, or in the gas phase, they have higher rates of diffusion and are less susceptible to poisoning, which can often be problematic and costly in heterogeneous catalysis.

As a result of this high affinity for diffusion, homogeneous catalysts often have a greater efficiency as smaller catalyst loadings and milder conditions are required compared to heterogeneous systems.[5] This has many advantages in industry such as; lower running costs, lower temperature requirements and pressure requirements. The ability to "tune" the

electronic and steric properties of a homogeneous catalyst allows for a greater efficiency and selectivity over heterogeneous catalysts.

There are certain drawbacks to homogeneous systems, such as their sensitivity, which can often lead to short catalytic lifetimes.[4] The use of precious metals and expensive ligands required to "tune" catalysts, can also make them very expensive. Once a reaction has taken place, additional problems can arise owing to the need to remove the catalyst from the system. In heterogeneous catalysis the removal of the catalyst by filtration is simple in comparison to some of the methods required to remove catalysts from homogeneous systems.[6] High catalyst recovery is important owing to the greater cost of homogeneous systems. This can often be problematic, owing to the low thermal stability of most homogeneous catalysts.

Newly emerging applications in fine chemicals and pharmaceuticals are placing a greater demand on homogeneous catalysts as a result of their selectivity, and the increasing need for efficient and environmentally friendly processes. Homogeneously catalysed hydrogenations, carbonylations and hydroformylations, utilising precious metal catalysts are looked at in more detail herein.

1.2 Catalysis and Kinetics

In order to gain a more thorough and comprehensive understanding of catalysis and catalytic reactions, reaction mechanisms must be studied, rate determining steps and possible competing side reactions must be elucidated to allow for a greater understanding of the reaction pathways. Kinetics is frequently a fundamental tool employed in the mechanistic study of catalytic multi-step reactions in order to gain a more comprehensive understanding of reactions pathways. "*Kinetic measurements are essential for the elucidation of any catalytic mechanism since catalysis, by definition and significance, is purely a kinetic phenomenon*".[7] Although it is not possible to *prove* a reaction mechanism via the use of kinetics alone, the ability to define and describe quantitative dependencies between reacting components, which in turn can exclude specific reaction sequences or mechanisms makes kinetics an invaluable asset within any mechanistic investigation.[8]

When chemical reactions are examined from a kinetic perspective, a chemical reaction can be defined as a journey which is narrated and dictated by the reaction rate law. It is also used to define concentration dependencies of the individual components within the reaction in addition to defining rate and equilibrium constants for the elementary steps taking place within a reaction network.[8]

Kinetics can be described as one of a number of different "languages" for relating chemical events. Other such examples include drawing out a reaction mechanism or constructing an energy flow diagram. Reaction progress can be shown readily in an energy flow diagram with a reaction coordinate axis. Kinetics can also be shown in this manner, although it is less commonly employed.[9]

1.3 Complications with Kinetics

There can be several complicating factors when catalytic reactions are studied. Difficulties in the analysis and interpretation of experimental data has often resulted in kinetic studies being performed once reaction mechanisms have been determined using various other methods, as a route to confirming already firm ideas

The majority of catalytic reactions involve multiple steps and often involve several reaction component concentrations changing simultaneously. Multi-step reactions are often problematical owing to the dependence on the reaction rate law characteristics of these reactions. Kinetic experiments where more than one reacting component changes simultaneously are very rare as there are very few ways in which both can be monitored concurrently. This is because the most commonly used methods for collecting kinetic data are decades old.

1.4 Methods of Simplification

As a result of these problems, simplified means of representing data have been sought. Some of the more commonly used methods focus on linearising rate equations for simple catalytic networks in order to extract kinetic parameters from the derived slopes and intercepts. One of the better known methods for simplifying kinetic data was the use of the

Michaelis-Menten equation,[10] which was utilised as a straightforward means of linearising enzymatic reaction rates.

The Michaelis-Menten equation can be used to describe simple mechanisms. It does this by defining a relationship between rate and substrate concentration (1.1).

$$\upsilon = \frac{\upsilon_{\max} [S]}{K_{MM} + [S]} \qquad (1.1)$$

ν_{max} is a numerical constant representing the maximum velocity obtained when substrate A exists completely in the active catalyst species (AB) form, ($\nu_{max} = k(A_{total})$) and K_s is the Michaelis constant. This type of analysis is suitable for reactions where the rate is first order in substrate concentration at low substrate concentrations, but becomes zero order at high substrate concentrations. Such a system is said to exhibit saturation kinetics.[11]

One of the most commonly used examples of this is the construction of a double reciprocal plot detailed by Lineweaver and Burk.[12] This describes a straightforward means for linearising reaction rates and has been focused on enzymatic reactions.

In 1934, Lineweaver and Burk illustrated that in enzyme kinetics there were dissociation intermediate complexes formed from reactants and enzymes.[12] In the case of the simplest equilibrium dissociation, equation (1.2):

$$K_s = \frac{[A][B]}{[AB]} \qquad (1.2)$$

Lineweaver and Burk concluded that for most reactions the kinetics involved do not correspond to the Michaelis-Menten equation. They outlined 7 different reaction types and undertook experiments in each of these cases, they combined the results and produced the Lineweaver-Burk equation, which turned the Michaelis-Menten equation upside down (1.3).[12]

$$\frac{1}{\upsilon} = \frac{1}{\upsilon_{\max}} + \frac{K_{MM}}{\upsilon_{\max}} \frac{1}{[S]} \qquad (1.3)$$

This equation has allowed more chemists to make sense of experimental kinetic data for both enzymatic and non enzymatic catalyst systems.

1.5 Reaction Progress Kinetic Analysis

As a result of the dramatic improvements in experimental measurement techniques and computer analysis tools, there have been advances in the ways in which experimental data can be recorded, stored, manipulated and presented. The ability to accurately monitor reactions continuously for increasingly longer periods of time allows for reactions to be followed from start to finish, resulting in the generation of voluminous data sets. This data allows for fewer reactions to be carried out in order to acquire the same amount of information.

As a result of all these advances, a new methodology for mechanistic studies of complex catalytic reactions has been established, called reaction progress kinetic analysis, RPKA.[9] Reaction progress kinetic analysis is defined as "*the analysis of experimental data acquired over the course of the reaction under synthetically relevant (non-pseudo zero order) substrate conditions.*"[9]

These reactions usually involve the concentration of two or more reacting components decreasing simultaneously over the course of the reaction. This method aims to provide a "*rapid and comprehensive understanding of the concentration driving forces operating on a steady state catalytic cycle from the outset, as opposed to at the end of, the mechanistic investigation*."[9]

The aim of this methodology is to produce visual and graphical approaches to "phenomenological" [9] or global kinetics, by taking advantage of a wealth of information derived from voluminous data sets, which are readily attained via accurate *in-situ* monitoring of reaction progress. The manipulation of this information allows for the construction of plots of various functions which contain information on the reaction rate against substrate concentration to produce "graphical rate equations." [9]

The depth of study in this area is dependent on the depth of information desired; the complexity of the reaction being studied, the quality of the data measured and the time commitments of the analyst.

In its most comprehensive form RPKA "*uses detailed modelling to asses quantitatively the relative likelihood of different proposed reaction mechanisms*." [9] In cases where only minimal investigation is required, RPKA can rapidly make available a "*qualitative fingerprint of reaction behaviour for streamlining practical exploration of new chemistry*."[9] It also gives insights which are useful in further mechanistic study, such as which avenues require further study and which techniques can be used to best achieve the desired outcome.

In between these cases, the graphical approach can be used to apply simple manipulations to data from a series of tailored experiments, which in turn can be manipulated to yield comprehensive mechanistic information, which requires minimal amounts of mathematical prowess to achieve.

1.6 Benefits of Reaction Progress Kinetic Analysis

There are several benefits of this technique over the traditionally used methods for extracting kinetic data. This methodology can be utilised using any experimental technique that can provide an accurate measure of how concentration changes as a function of reaction progress. It allows for the rapid extraction of kinetic information with a number of carefully designed experiments, where two or more substrate concentrations are changing. It is faster; requires fewer experiments, owing to the continual monitoring throughout the reaction; provides enhanced mechanistic elements and is debatably more accurate than classical kinetic techniques.[9]

The ability to monitor time evolution allows data to provide significant indication on classical catalytic reaction problems such as: catalyst activation and deactivation, as well as product inhibition and acceleration. When this technique is used to elucidate mechanistic information, it limits the number of plausible reaction pathways under consideration as well as allowing for a more informed decision on the direction of the mechanistic tools to employ for the further characterisation and extrapolation of information. For example, the

initial experiments can highlight which species within the reaction may be isolable and/or which key steps within the reaction can be practicable to study in further detail.

1.7 Requirements of Reaction Progress Kinetic Analysis

The two key requirements for this methodology are: an *in-situ* method for continuous and accurate experimental data collection as well as the computational means for manipulating the data. This includes a spreadsheet package, such as Excel and if possible a curve fitting software.

The *in-situ* method used can be an integral or a differential method of data collection. Integral methods, such as Fourier Transform Infrared (FTIR) show a relationship between a measurable parameter and the species concentration. This means that the concentration of the reactant species is proportional to the integral of the reaction rate. The reaction rate may be determined by differentiating the experimental concentration versus time data. Within integral methods the rate is a processed parameter derived from a primary parameter, such as concentration or conversion of substrate.

Differential methods, also known as derivative measurements, measure the reaction rate directly. A common method utilised for these measurements is calorimetry. This relates the reaction rate to the heat flow q through the thermodynamic heat of reaction ΔH_{rxn}. In differential methods the rate is the primary measured parameter, and concentration or conversion of the substrate is proportional to the integral of the rate versus the time.

Despite its common use throughout kinetics, plotting the reaction progress against time is not the best way to extract kinetic information from a reaction. As was shown previously, the Michaelis-Menten and Lineweaver-Burk equations define a relationship between rate and substrate concentration. This is where the combination of integral and differential methods is particularly beneficial.

When considering any reaction undertaken, if the differential measurement is plotted against the integral measurement (concentration and conversion of substrate) on the y and x-axis respectively, this does not include time. The resulting plot is known as a graphical rate equation.[9] Plotting the concentration on the x-axis will result in the reaction progress being

given from right to left, owing to the decrease in substrate concentration over the course of the reaction. The key to the success of this graphical method is collecting sufficient amounts of data which is of high quality and accuracy.

Using several orthogonal techniques means that it is possible to confirm that the reaction is going on as is expected, as well as giving more information on the reaction than is possible with one technique alone.

In order to utilise this method, reaction progress is determined using an integral method and a differential method and both are plotted as a function of time. Once these plots are calculated, it is then possible to plot the differential measurement on the y-axis and the integral measurement on the x-axis to give a Michaelis-Menten kinetic model and plotting the double reciprocal model gives a classic Lineweaver-Burk plot.[9]

1.8 Basic Ideas and Key Terminology of Reaction Progress Kinetic Analysis

Reaction progress kinetic analysis has been comprehensively reviewed by Donna Blackmond,[9] therefore only the fundamental principles of the methodology and the key elements relevant to the work herein will be explained in more detail.

Blackmond [9] illustrates a straightforward example; the asymmetric hydrogenation of ethyl pyruvate using cinchona-modified Pt/Al_2O_3 catalyst, figure 1.1, to illustrate how data can be extracted, compared and contrasted using reaction progress kinetic analysis.

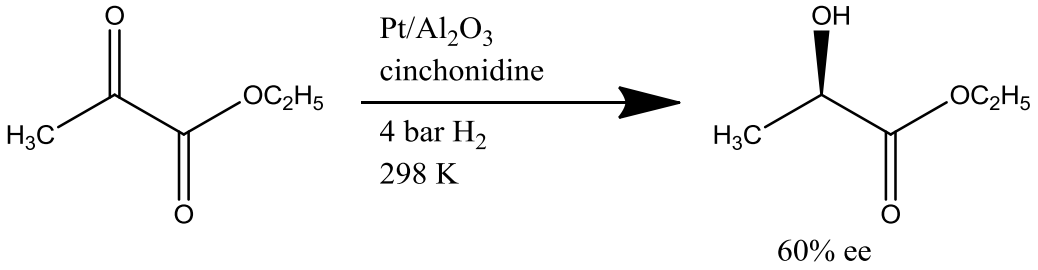

Figure 1.1: Asymmetric hydrogenation of ethyl pyruvate mediated by cinchona-modified Pt/Al_2O_3. [9]

The reaction was carried out in two different solvents and the reaction progress was followed using both a differential and integral method and the resulting data was plotted as a function of time. These are shown in figure 1.2

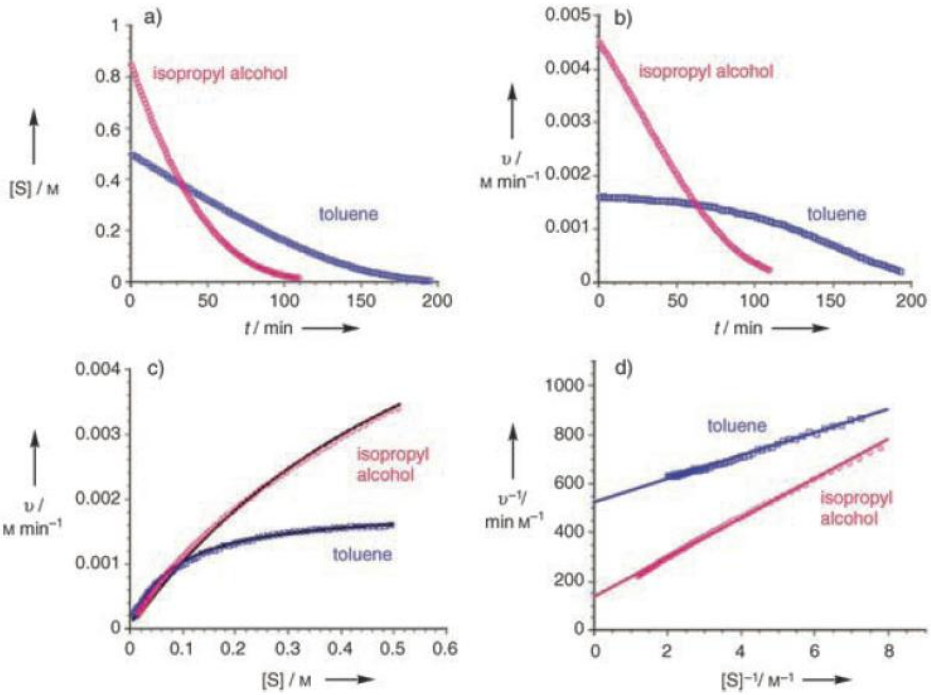

Figure 1.2: Graphs showing kinetic analysis (by differential and integral methods) of the hydrogenation reaction shown in figure 1.1 carried out in isopropyl alcohol (red) and toluene (blue): a) Substrate concentration versus time (integral method). b) Reaction rate versus time (differential method). c) Rate versus substrate concentration; d) Reciprocal rate versus reciprocal substrate (Lineweaver–Burk plot). [9]

This example illustrates how two reactions, monitored via two methods can produce both a qualitative comparison of the same reaction in two solvents as well as a quantitative analysis of the kinetics of each reaction. Simple observations show that the reaction is slower in toluene than isopropyl alcohol. This is inferred from the greater degree of flatness in the direct rate measurements of the toluene reaction.

The graphical rate equation, graph c, reiterates this, as the more horizontal the rate equation appears, the closer the reaction is to zero order conditions. Therefore it can be concluded that the reaction is almost zero order in toluene and almost first order in isopropyl alcohol.

1.9 Excess

Conventional kinetic studies are carried out by maintaining the concentration of one reacting component whilst the other is investigated. Most commonly, this is accomplished via using initial rate measurements or by utilising pseudo zero-order conditions to ensure only one of the reacting component concentrations changes. This often results in numerous experiments being undertaken. Reaction progress kinetic analysis aims to significantly reduce the number of experiments required. In order to accomplish this, it is required to make use of the reaction stoichiometry.

In basic reactions where the concentration of only one reacting component changes, reactions such as isomerisations or decompositions, a simple Michaelis-Menten equation, (1.1) can be used to define the rate for the reaction. This can then be turned upside-down to produce a Lineweaver-Burk plot, (1.3). A simple cycle for this is shown in figure 1.3.

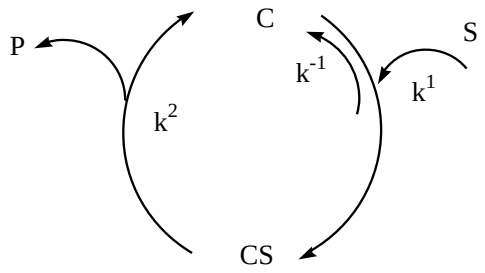

Figure 1.3: Catalytic cycle for a simple reaction which involves the conversion of one substrate. C = catalyst, S = substrate, CS = catalytic intermediate species, P = product. [9]

In reality, chemists tend to study reactions which have a greater order of complexity, and often contain two or more reacting components which change simultaneously under synthetically relevant conditions. Figure 1.4, shows how the diagram for a simple decomposition reaction can be modified to incorporate the addition of a second substrate. Within this reaction the first substrate reacts with the catalyst to produce a catalytic intermediate. The addition of the second substrate to the catalytic intermediate species allows for the product formation and the regeneration of the original catalyst species. This rate expression for a reaction like this is shown in equation 1.4 and simplified in equation 1.5.

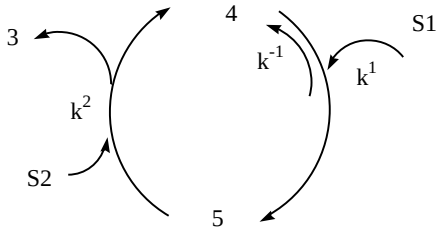

Figure 1.4: Reaction scheme showing the addition of a second substrate to the catalytic intermediate species formed by the addition of substrate one. S1/2 = substrate, 3 = product, 4 = catalyst, 5 = catalytic intermediate species. [9]

$$\upsilon = \frac{k_1 k_2 [S2][4]_{total}}{k_{-1} + k_1[S1] + c[S2]} \tag{1.4}$$

$$\upsilon = \frac{a[S1][S2][4]_{total}}{1 + b[S1] + c[S2]}$$

$$a = \frac{k_1}{k_{-1}} k_2, b = \frac{k_1}{k_{-1}}, c = \frac{k_2}{k_{-1}} \tag{1.5}$$

The kinetic parameters within this equation become more complex and are no longer constants as they now have a dependency on the second substrate concentration. In order to counteract this using conventional kinetic means, a Lineweaver-Burk plot for a two substrate reaction must be constructed, wherein the concentration of the second substrate remains constant. The drawback in this situation is that the constants obtained from this plot are only relevant to the specific conditions in which the reaction was carried out. This results in numerous experiments being run, using varying reaction conditions, in order to establish a relationship between the Michaelis-Menten constant and the second substrate concentration.

Using reaction progress kinetic analysis helps reduce the time in which this data can be derived. This is because it allows for a situation where both substrate concentrations can

change simultaneously. This relies on the reaction stoichiometry for the reaction. An example of this would be in an equimolar reaction, such as the example of the simple Diels-Alder reaction shown in figure 1.5, within which, for every mole of substrate A converted to product, one mole of substrate B is also required.

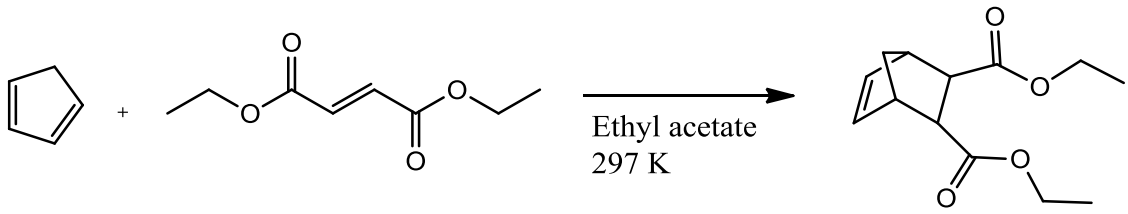

Figure 1.5: Diels-Alder reaction of cyclopentadiene with a diethyl fumarate. [9]

The parameter which defines the relationship between both substrates is known as "excess" and is defined as being "equal to the difference in the initial concentrations of the two substrates." [9] The relationship is shown in equation 1.6.

The units for this parameter are the same as those for both substrates, which are usually moles or *m*moles. The "excess", also shown throughout as ["excess"] to define the excess concentration, does not change as the reaction progresses for constant volume reactions. Similarly it is not the same as the number of equivalents or the percent excess concentration, both of which change throughout a reaction. Once the excess concentration is known, the reactions can be carried out with synthetically relevant conditions and all that is required between reactions is that the excess concentration remains constant.

$$[\,] = [\,]_0 - [\,]_0 \Rightarrow [\,] = [excess''] + [\,] \qquad (1.6)$$

If the excess expression is substituted into equation 1.5, the resulting equation is given by equation 1.7. In this equation the total catalyst concentration and the excess concentration remain constant, as well as k^1, k^{-1} and k^2. This means that the only variable within the reaction is the concentration of substrate 1. Therefore, as long as the excess concentration is known, none of the reacting component concentrations are required to be fixed as pseudo-constant high values throughout the reaction.

$$\upsilon = a' \frac{[excess'][A]^2}{1 + b'[A]^2} [A]_{total} \qquad (1.7)$$

$$a' = \frac{k_1 k_2}{k_{-1} + k_2 [excess']}, \quad b' = \frac{k_1 + k_2}{k_{-1} + k_2 [excess']}$$

The use of excess in kinetic analysis is two fold. Experiments which employ reactions with the same ["excess"] are the equivalent of carrying out the same reaction from several different staring points and are useful in probing reactions for complexities such as product inhibition and catalyst deactivation. The other option is carrying out reactions which have different ["excess"]. As is shown in equation 1.7, a' and b' are the adjustable parameters within the reaction. Carrying out the reaction at two or more different excess concentrations allows the three independent rate constants, k_1, k_{-1} and k_2, to be derived via the use of simultaneous equations.

1.10 Previous studies

Reaction progress kinetic analysis is a relatively new methodology and as such there are only a few papers which show the methodology applied within catalyst systems. The majority of these studies have been performed by Donna Blackmond and co-workers at Imperial College, London. [13-17] This section highlights some of the systems which have utilised this methodology to look more in depth at reactions and their mechanisms. Having a greater insight into the kinetics of the reaction also allows the reactions to be optimised more easily to enhance the overall performance.

Blackmond discusses the details and concepts of reaction progress kinetic analysis in great depth within her review of the methodology itself [18] and highlights key points throughout other papers such as the "Investigations of Pd-Catalyzed ArX Coupling Reactions Informed by Reaction Progress Kinetic Analysis" [19] within this, four case studies are analysed:

1. Heck coupling of butyl acrylate with 4-bromobenzaldehyde catalyzed by Pd(P(*t*-Bu)$_3$)$_2$
2. Palladacycle-catalyzed Heck coupling of butyl acrylate with 4-bromobenzaldehyde.

3. $Pd(P(t\text{-}Bu)_3)_2$-catalyzed Sonogashira coupling of phenyl acetylene with 4-bromoacetophenone.
4. Pd/(binap)-catalyzed amination of 3-trifluoromethylbromobenzene

The first reaction was found to show a first order dependence on the 4-bromobenzaldehyde concentration and a zero order dependence on the butyl acrylate concentration. However, the second reaction was found to have a zero order dependence on the 4-bromobenzaldehyde concentration and a first order dependence on the butyl acrylate concentration. As the results from the reaction catalysed by the palladacycles shows the opposite dependencies to those of the reaction catalysed by $Pd(P(t\text{-}Bu)_3)_2$. This gives an example of how different catalysts can produce different rate determining steps for the same reaction.

The third reaction was found to show first order kinetics in phenyl acetylene and a complex order in 4-bromoactetophenone. It was also found that the system was showing indications of saturation kinetics in the 4-bromoactetophenone. This was postulated as the concentration as a function of time plots showed curves which overlay but did not exhibit straight lines. This is shown in figure 1.6. Plotting the rate divided by the phenyl acetylene concentration as a function of the 4-bromoacetophenone concentration showed the complex order in aryl halide concentration, shown in figure 1.7. The double reciprocal plot of this reaction was then produced to determine the Michaelis constant. This is shown in figure 1.8 [19] The fourth reaction was zero order in 3-Trifluoromethylbromobenzene and zero order in amine and therefore the global rate expression is equal to the constant, k.

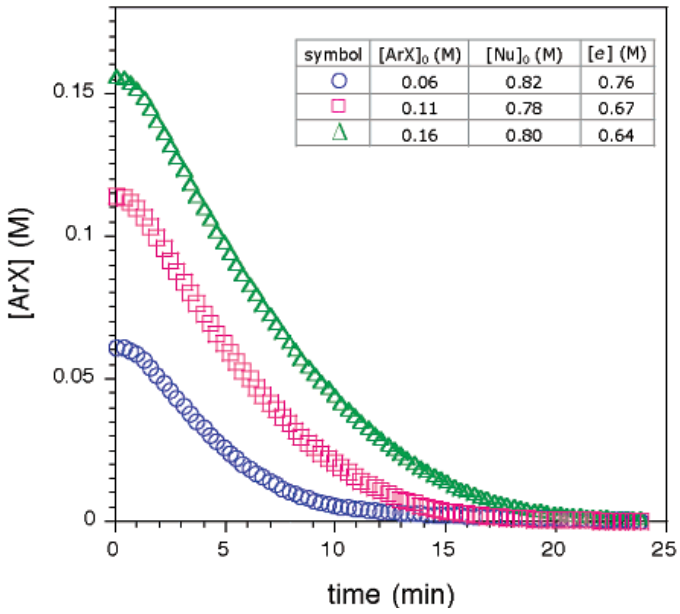

Figure 1.6: Plots of concentration as a function of time for the $Pd(P(t\text{-}Bu)_3)_2$-catalyzed Sonogashira coupling of phenyl acetylene with 4-bromoacetophenone. Two of the reactions have the same excess (red and green) and one has a different excess (blue). [19]

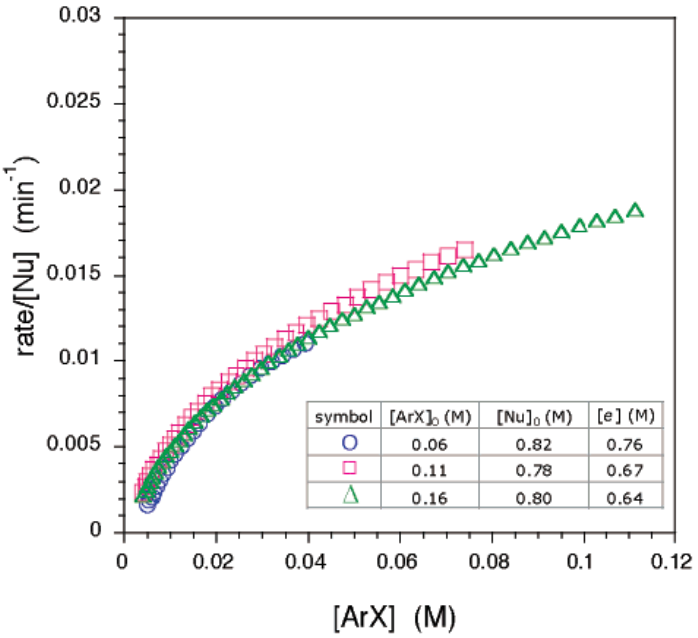

Figure 1.7: Graphical rate equations showing the rate divided by the phenyl acetylene concentration as a function of the 4-bromoacetophenone concentration to establish the order with respect to 4-bromoacetophenone. [19]

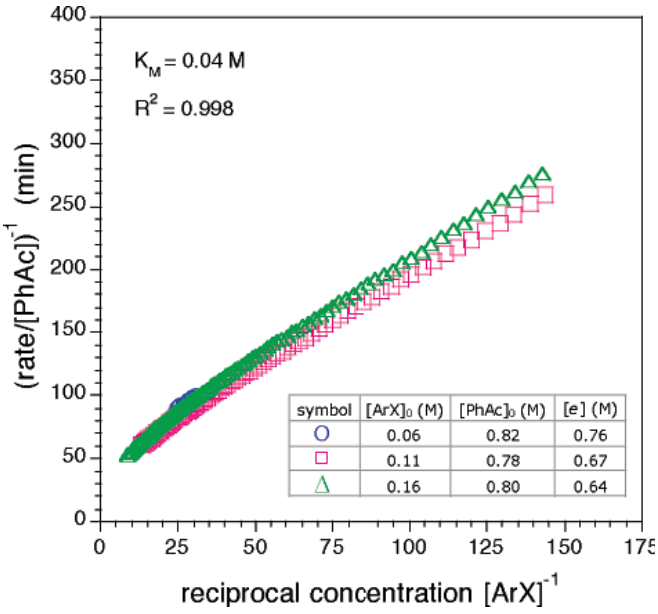

Figure 1.8: The data from figure 1.7 plotted in double reciprocal form. [19]

Further study into these reactions has proposed mechanisms, rate determining steps and catalyst resting states for each of the reactions. In the first reaction it is postulated that oxidative addition is the rate limiting step and the resting state of the catalyst in this system would be the palladium (0) species at the entrance of the cycle, shown in figure 1.9. In reaction 2 the rate limiting step is the addition of the nucleophile to the oxidative addition complex. As there is an overall zero order in aryl halide concentration, it can be postulated that the nucleophilic attack is rate determining and the species before the rate determining step is the major species observable spectroscopically. Theses steps are highlighted in figure 1.9.

In reaction 3, it can be put forward that the reaction of the nucleophile with the oxidative addition complex is the rate limiting step. Saturation kinetics could be applied as in reaction 2, but the curves shown in the graphical rate equation suggest that the species is not saturated. The catalyst resting state within this reaction is divided between the palladium species at the entrance of the reaction cycle and the oxidative addition complex. This results in the complex order in the [ArX]. In the 4th reaction, as there is a zero order in both nucleophile and aryl halide, any step which occurs after the addition of both substrates can be rate limiting. From this it is postulated that the resting state of the catalyst is the species containing the nucleophile added to the oxidative addition complex.

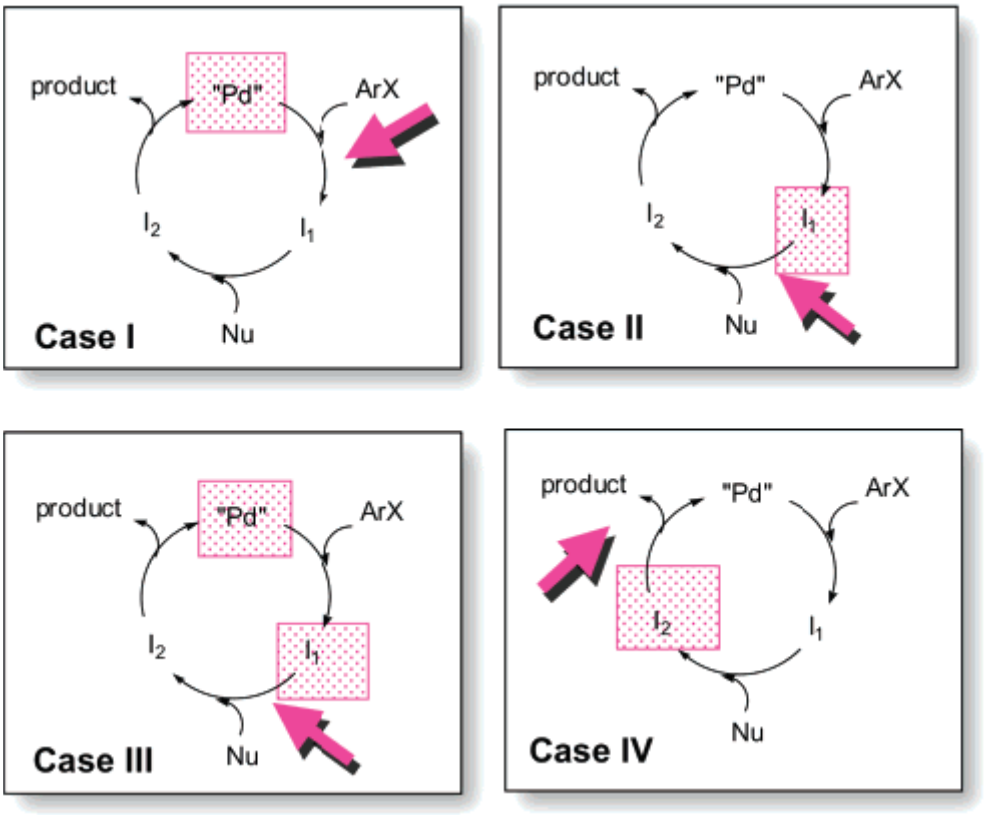

Figure 1.9: The proposed rate determining step and catalyst resting states (shown in pink) for the aryl halide coupling reactions as described by Blackmond et al. [19]

In a recent collaborative study Hii and Blackmond [20] undertook mechanistic studies for the palladium-catalysed asymmetric aza-Michael addition of aniline to α,β-unsaturated *N*-imide. They monitored the mechanism for this reaction via a number of different characterisation techniques including kinetic studies, XRD, NMR and UV-vis spectroscopy.

The dicationic palladium(II) species used to catalyse the reaction was [((R)-BINAP)Pd-$(OH_2)_2$]$^{2+}$ [TfO]$^-_2$ which is shown below in figure 1.10.

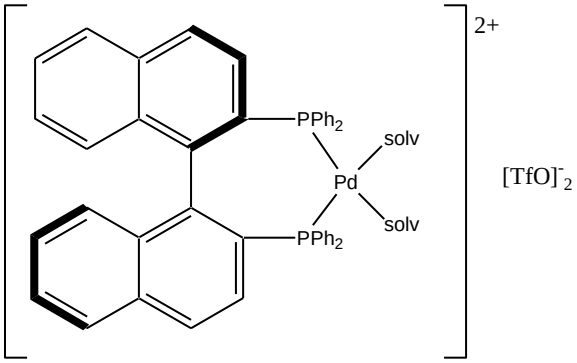

solv = CH_2CN or H_2O

Figure 1.10: Schematic representation of [((R)-BINAP)Pd-$(OH_2)_2$]$^{2+}$ [TfO]$^-_2$.[20]

This was used because of its ability to effect the highly enantioselective addition of aromatic amines to several Michael acceptors which contain chelating carbonyl moieties, such as *N*-carbamates, shown in figure 1.8.[20]

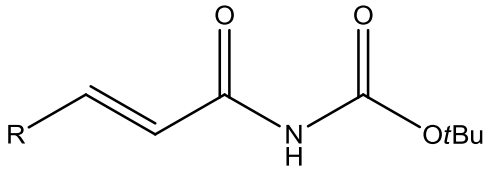

Figure 1.11: Schematic representation of tert-butyl acryloylcarbamate (R=H). [20]

Hii *et al* [20] believe that the catalyst acts as a chiral Lewis acid, activating the unsaturated double bond towards nucleophilic attack through the chelation of the 1,3-dicarbonyl functionality.[20] They also established that only dicationic species which contain diphosphine ligands gave good turnovers and that the species which contained a C_2- symmetrical biaryl unit, gave high enantioselectivities. [21] They also compared selectivity and catalyst turnover when using *N*-oxazolinone, *N*-benzoyl and *N*-carbamate. They concluded overall that the reaction outcome is dependent on the electronic nature of the aromatic amine.

It was proposed that nucleophilic amines deactivate the dicationic palladium catalyst, and to preserve the atom economy within the reaction, the reaction protocol was adjusted. As a result of this, a study to explain key steps of the reaction was undertaken, as this would

allow for a clearer understanding of the reasons behind the catalyst deactivation process and its relation to the catalytic turnover.

Using UV-vis spectroscopy they were able to determine that the addition of the amine to the catalyst species occurred in a two stage process where the coordination of the first aniline is facile and reversible whereas the second aniline addition occurs more slowly. However, once the diamine complex is formed it is kinetically stable and does not readily dissociate. This is shown schematically in figure 1.12.

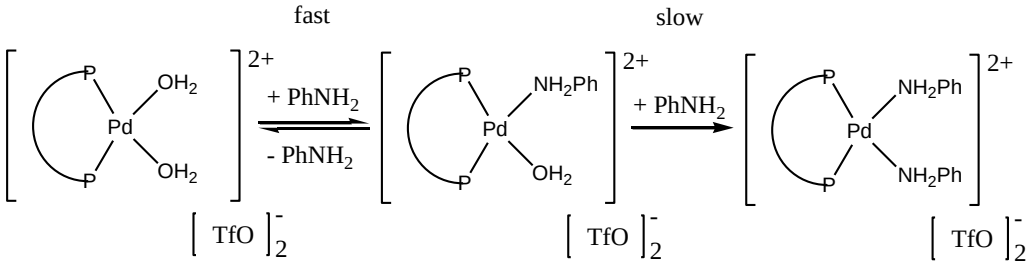

Figure 1.12: Scheme showing the addition of two amine groups to a palladium complex. The first addition is reversible whereas the second creates a stable diamine complex.[20]

The group then utilised reaction progress kinetic analysis as a probe into the catalytic cycle in order to determine critical factors that influence catalytic stability and turnover. They utilised *in situ* reaction calorimetry and NMR to show that they had an accurate following of the reaction progress. [20]

The initial experiments determined the role and reactivity of the catalyst over time. This was done by running two experiments where the concentrations of both substrates were changed, but the ["excess"] between the two concentrations was kept constant. A third reaction was then carried out. This was identical to the second experiment, but mimicking 54% conversion.[20] This meant that the product was also in the reaction from the start. This is useful as product inhibition, competitive activation and decomposition can cause changes in the effective concentration of the catalyst. The three experiments are detailed in table 1.1: [20]

exp	conditions	[alkene]	[amine]	[xs]	[product]
Exp 1	Initial	0.37	0.56	0.19	0
Exp 2	Initial	0.2	0.39	0.19	0
Exp3	54% conversion	0.2	0.39	0.19	0.17

Table 1.1: Reaction information on the palladium catalysed, aza-Michael addition reactions. Reactions were carried out to determine the possibility of product inhibition within the reaction. Data was reproduced from ref.[20]

The kinetic data for these reactions was then plotted to form a graphical rate equations of the rate as a function of the substrate (alkene) concentration. The plot is shown in figure 1.13:

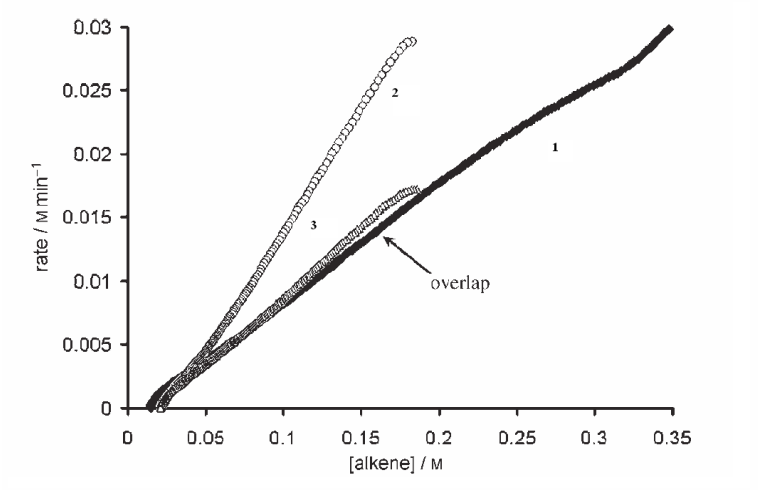

Figure 1.13: Graphical rate plot for the hydroamination of N-imides for the reactions shown in table 1.1. Plot shows determination of product inhibition. Reproduced from ref. [20]

As the experiments were performed under identical conditions, the three graphs should overlap one another if the reaction is occurring under steady state conditions (i.e. it is not affected by product inhibition). As 1 and 2 do not overlap, it shows that the driving force corresponding to the reactant concentrations is suppressed in the presence of product.

The obtained graphical rate equations were then divided by the total catalyst concentration and this gave a plot for turn over frequency (TOF) as a function of aniline concentration.

When this was plotted against the N-butenoyl imide concentration it showed that the reaction is first order in catalyst which rules out the likelihood of dimeric species formation within the reaction.

It was hypothesised that high aniline concentrations within the reaction resulted in a diamine complex. This was detrimental to the reaction as it inhibits the catalyst activity. The rate was then plotted against the aniline concentration and it shows a first order dependence in alkene concentration. Monitoring throughout a single reaction shows that there is an overall zero order in aniline concentration. The resulting proposed mechanism for the reaction is shown in figure 1.14:

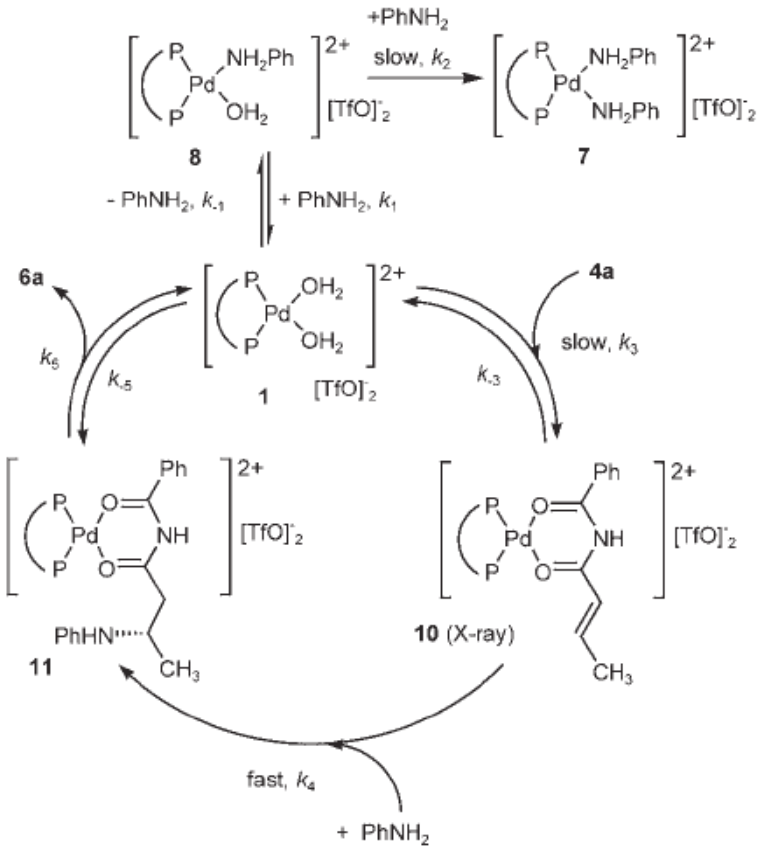

Figure 1.14: Reaction scheme proposed by Hii et al [22] for the palladium-BINAP catalysed addition of aniline to α,β-unsaturated N-imides. Reproduced from ref. [20]

Another reaction which has utilised this technique is the polypeptide catalysed epoxidation of chalcone. [23] It is shown, using reaction progress kinetic analysis, that the reaction proceeds via the reversible addition of chalcone to a poly(*L*)-leucine (PLL)-bound hydroperoxide, forming a transitory hydroperoxy enolate species, shown in figure 1.15.

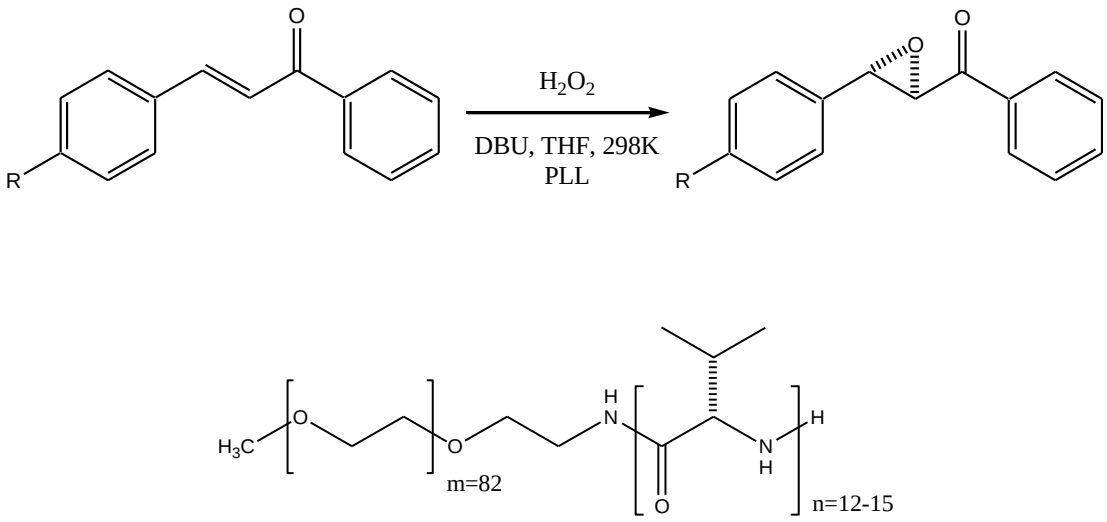

Figure 1.15: Scheme showing the polypeptide catalysed epoxidation of chalcone using a poly(L)-leucine (PLL)-bound hydroperoxide. [23]

The reaction was monitored by reaction calorimetry and the accuracy of this method was confirmed by periodic sampling and high-performance liquid chromatography (HPLC) analysis. The manipulation of the data obtained shows that at low conversion rates the rate appears to be suppressed. Whereas within the steady state conditions (above 10% conversion), a first order dependence of the rate on chalcone concentration is observed. This is shown graphically in figure 1.16:

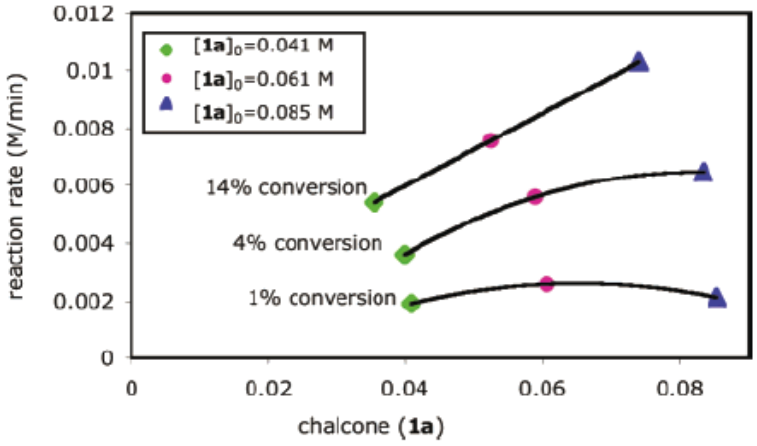

Figure 1.16: Graph showing the reaction rate for the polypeptide catalysed epoxidation of chalcone as a function of the chalcone concentration. Graph highlights that above 10% conversion, when the reaction reaches steady state, there is a first order dependency on the chalcone concentration. Graph reproduced from ref. [23]

Further investigations utilising different initial concentrations employing the same "excess" show that there is an overlay in each of the plots and this occurs at 10-15 % conversion. This shows that beyond this point the reaction proceeds under steady state conditions. This suggests that the initial rate behaviour, when there is a high concentration of chalcone, can possibly be attributed to an induction period before the establishment of the steady state as opposed to substrate inhibition which is suggested by Ottolina and co-workers [24]

Similarly, Rosner *et al* [25] have studied the amino alcohol-catalyzed asymmetric alkylation of benzaldehyde with diethylzinc and how product inhibition affects the reaction. This study is based on primary work carried out by Noyori and co-workers.[26] They show that the reaction proceeds via the formation of a monomeric aminoalkoxide catalyst species which exists in equilibrium with a non catalytically active dimer species. Based on these works and those outlined by Kagan *et al*, [27] Rosner *et al* [25] report the asymmetric alkylation of benzaldehyde with diethylzinc making use of (2*S*)-(-)-3-*exo*-(*N*-morpholino)isoborneol, ((-)-MIB) as a chiral reagent (figure 1.17). The reaction was followed with reaction calorimetry and substantiated by GC analysis.

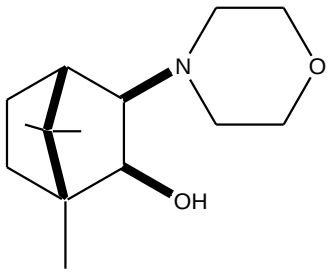

Figure 1.17: MIB ((2S)-(-)-3-exo-(N-morpholino)isoborneol, ((-)-MIB)). [25]

The work describes how, upon the injection of the benzaldehyde, the reaction calorimeter recorded a rise in heat to a maximum before a steady drop in the heat given out throughout the reaction. When the heat profile was converted to a rate measurement it was concluded that the steady decrease in heat after injection was as a result of the positive order kinetics in both substrates, figure1.18.

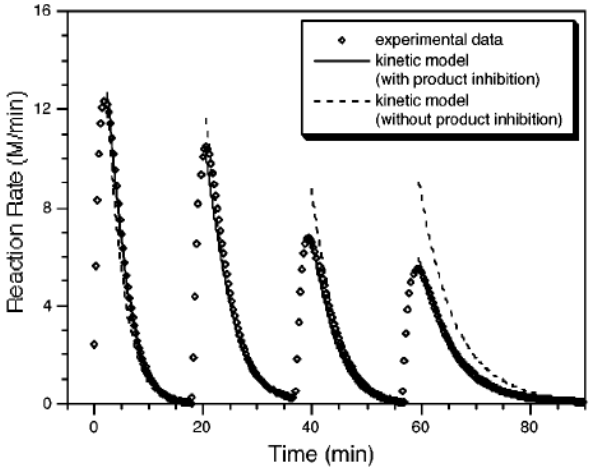

Figure 1.18: Graphical plot showing the rate of the reaction as a function of time for four injections of benzaldehyde the graph compares the experimental data to two kinetic models (with and without inhibition). This allows for the determination of product inhibition within the reaction. Graph reproduced from ref. [25]

Subsequent aliquots of benzaldehyde were injected and as is shown in figure 1.18, the overall conversion decreases over time. This is postulated to be as a result of product inhibition owing to the build up of a catalyst bound product throughout the reaction.

Effective studies into the 1,4-addition of organometallic reagents to *α-β* unsaturated compounds to promote C-C bond formation, in the presence of Rh/binap catalysts have been carried out by Kina *et al.* [28] They have presented a detailed study of the kinetics within the multi-step 1,4-addition of phenylboronic acid to *α-β* unsaturated ketones (methyl vinyl ketone). Within these reactions the dominant species is an inactive dimeric hydroxorhodium complex. The formation of the hydroxorhodium complex results in the observation of a negative nonlinear effect.

The reaction was monitored via reaction calorimetry and the kinetics were studied using ["excess"] relationships and graphical rate equations developed by Blackmond. [9] Two experiments with the same ["excess"] concentrations were run, which confirmed that the reaction proceeded under steady state conditions with constant catalyst concentrations. When the phenylboronic acid concentration was plotted against the rate, the resulting straight line implied first order kinetics, with zero order kinetics in the methyl vinyl ketone concentration. Verification of this was achieved by conducting the reaction with a different excess concentration.

The reaction does not show a proportional rise in rate with the addition of extra catalyst therefore plotting the square root of the rhodium concentration against the phenylboronic acid concentration highlights that there is a half order dependency in rhodium concentration. The studies have concluded that the catalytic cycle involves transmetallation of the phenyl group from the boron to the hydroxorhodium complex. This is thought to be the rate determining step for the reaction. The subsequent addition of the phenylrhodium bond to an enone leads to the formation of an oxo-π-allylrhodium intermediate which hydrolyses to give the 1,4 addition product. The homodimer species formed within the reaction is the catalytically inactive species as it is considerably more stable than the heterodimer species. This results in the observed negative non linear effect in the product enantioselectivity.

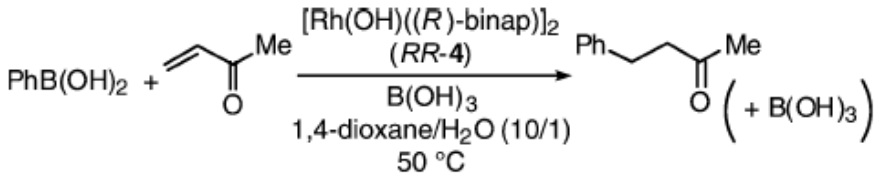

Figure 1.19: The rhodium catalysed 1,4-addition of phenylboronic acid to methyl vinyl ketone.[28]

Visentin *et al* [29] make use of a reaction calorimeter with an integrated infrared- attenuated, total reflection probe (FT-IR-ATR). They couple this with IR and gas uptake analysis to study the heterogeneously catalysed hydrogenation of nitrobenzene and ethyl-4-nitrobenzoate utilising a palladium on carbon catalyst with a 1 wt % loading. The utilisation of three orthogonal techniques allows for a more in-depth look at what is happening within the reaction.

The studies incorporated nitrobenzene as it is the simplest aromatic nitro molecule. It is also the most commonly employed standard reaction when testing and comparing activity for hydrogenation catalysts. The second reactant used was ethyl-4-nitrobenzoate as a result of its likelihood to form ethyl-4-hydroxylaminobenzoate as an intermediate species as shown in figure 1.20.

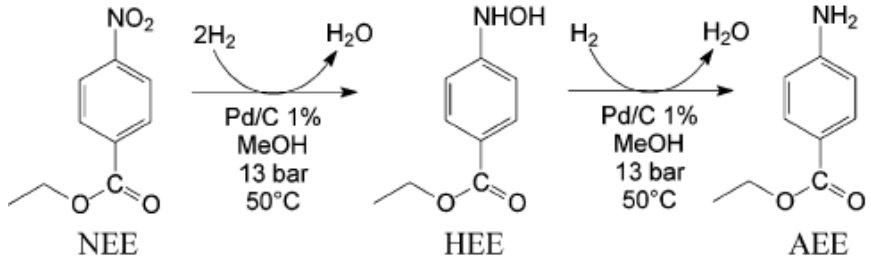

Figure 1.20: The consecutive hydrogenation of ethyl-4-nitrobenzoate to produce ethyl-4-aminobenzoate via an ethyl-4-hydroxylaminobenzoate intermediate. [29]

It was shown in the hydrogenation of nitrobenzene that there was an observed accumulation of <10% (based on total conversion observed) of the hydroxylamine intermediate. This was validated via the gas uptake analysis and the calorimetric data. These are not the expected

conditions for the formation of the intermediate species. Therefore it was postulated that the reaction proceeded directly to the aniline without any intermediate accumulation.

When the hydrogen uptake was analysed, the reaction was run at constant pressure and the H_2 uptake was measured from an intermediate reservoir. It was found that there was an almost linear gas uptake, which indicates that the rate of reaction is independent of substrate concentration. As this is the only reacting component changing reaction is zero order in substrate. The study also detailed the mass transfer and diffusion effects within the reaction.

Results were also shown for the hydrogenation of ethyl-4-nitrobenzene. This was also studied owing to its strong electron acceptor capabilities compared to nitrobenzene. It has also been postulated that the stabilisation of a hydroxylamine intermediate is encouraged in the presence of electron acceptor substituents.

The reaction was run along with two subsequent injections of ethyl-4-nitrobenzene. The behaviour for the first injection was different from that of the two subsequent injections. There is an observed increase in the reaction rate which is postulated to be as a consequence of the uncontrolled activation of the catalyst, figure 1.21. The two subsequent reactions follow a similar pathway to the nitrobenzene reactions. This may be as a result of the pre-treatment of the catalyst from the first reaction.

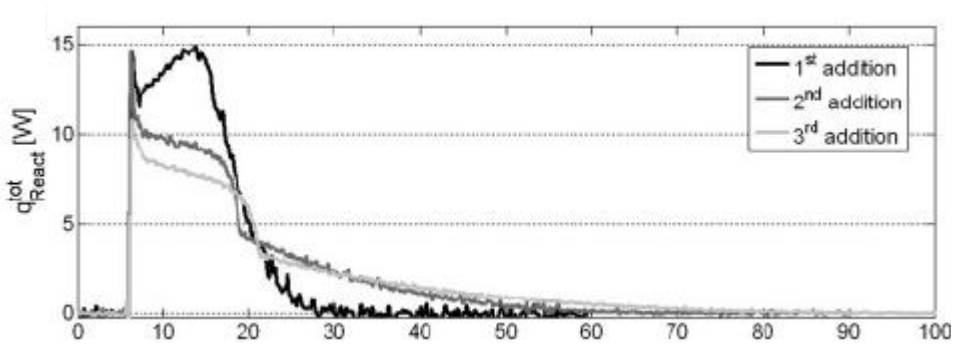

Figure 1.21: Heat flow for the three additions of ethyl-4-nitrobenzene showing the initial activation of the catalyst and then subsequent reactions proceeding without any need for activation. [29]

Through combining several techniques it was possible to elucidate the presence of an intermediate hydroxylamine species. This was highlighted clearly in the different behaviour of the calorimetric and gas-uptake signals.

1.11 Aims

As was shown by Visentin and co-workers [29] gas uptake signals can be utilised as an effective *in situ* method for data collection. The ability to implement open (constant pressure) and closed (constant volume) experiments allows for data to be collected under different conditions from the same apparatus and gives the ability to extrapolate different types of information.

Gas uptake analysis is a very useful tool as it allows for reactions involving gases, such as hydrogenations and hydroformylations to be studied in great depth and the kinetics of such reaction to be studied in more detail. The constant pressure and constant volume systems can be used as integral method and has the potential to be combined with other methods they can produce a comprehensive picture of what is happening throughout a reaction. This allows for a more in depth study on the effects of gases, varying pressures and varying concentrations on the overall reaction.

The primary objectives of this project is to utilise a set of probe reactions, on known reaction systems, to establish the capacity of gas uptake signals to be employed as an effective *in situ* method for the extraction of kinetic data from gas uptake analysis. The reactions to be initially studied have been subject to extensive research and the kinetics and catalytic cycles are well established.

This project utilises a homogeneous batch reactor with sufficient gas liquid mixing and the ability to take and record continuous, high pressure, *in situ* kinetic measurements. The reactor and its key parts are shown in figure 1.22:

Figure 1.22: Photograph of the reactor.

The key reactions which will be studied throughout this project are hydrogenation, carbonylation and hydroformylation reactions which utilise homogeneous rhodium or palladium catalysts in combination with various phosphine ligands. It is hoped that, via simple manipulation of the data collected, the RPKA methodology can be applied and graphical rate equations can be formulated. From this, key information can be extracted for these reactions, including orders in reactants and catalysts;

A schematic of the rig is provided in figure 1.23. This gives greater clarity when referring to parts within the discussion section.

1.) Cylinder attachment
2.) Pressure transducer 1 (P1)
3.) Mass flow controller
4.) Pressure release valve
5.) Valve to open/closed autoclave from other areas of the reactor

6.) Screw cap seal for the autoclave

7.) Pressure transducer 2 (P2) and thermocouple for controlling temperature

8.) Stirrer

9.) Heating jacket

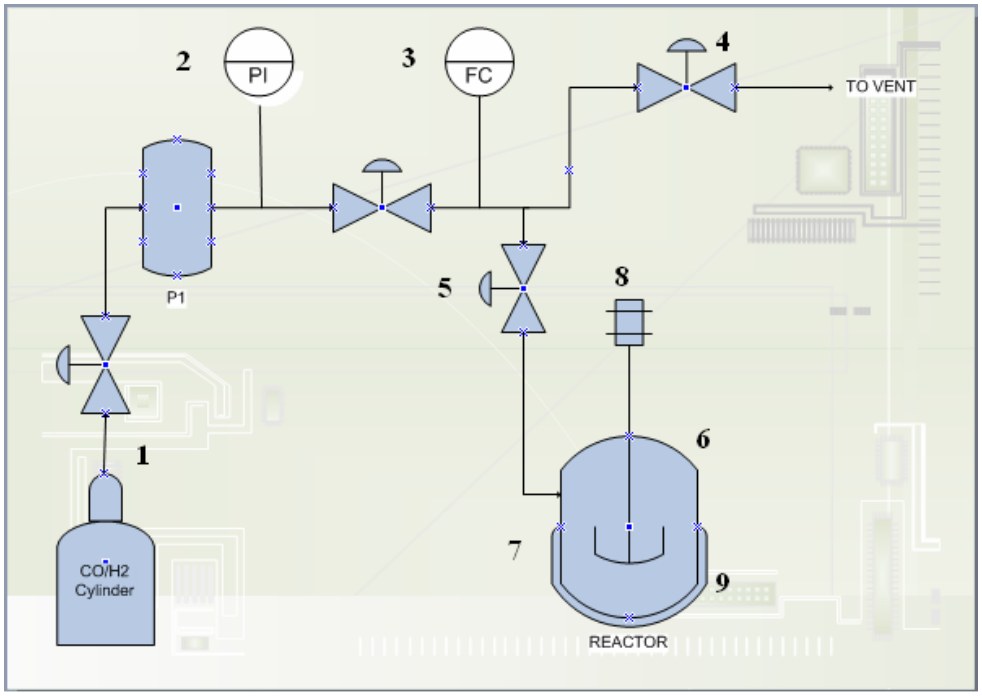

Figure 1.23: Shows a schematic flow diagram for the reactor highlighting key areas of the rig.

1.12 References

1 J. J. Berzelius, *Jahresber. Chem.*, 1836, **15**, 237.

2 J. A. Osborn, F. H. Jardine, J. F. Young, and G. Wilkinson, *J. Chem. Soc. A*, 1966, **12**, 1711.

3 *Pure and Applied Chemistry*, 1981, **53**, 753.

4 J. Flabe and H. Bahrmann, *J. Chem. Educ.*, 1984, **61**, 961.

5 R. V. Chaudhari, A. Seayad, and S. Jayasree, *Cat. Today*, 2001, **66**, 371.

6 D. J. Cole-Hamilton and R. P. Tooze, 'Catalyist Separation, Recovery and Recycling', ed. D. J. Cole-Hamilton and R. P. Tooze, Springer-Verlag, 2006.

7 J. Helpern, *Science*, 1982, **217**, 401.

8 'The Handbook of Homogeneous Hydrogenation', ed. J. G. d. Vries and C. E. Elsevier, Wiley VCH.

9 D. G. Blackmond, *Angew. Chem: Int. Ed.*, 2005, **44**, 4302.

10 L. Michaelis and M. L. Menten, *Biochemische Zeitschrift*, 1913, **49**, 333.

11 H. E. Avery, 'Basic Reaction Kinetics and Mechanisms', The MacMillan Press Ltd, 1974.

12 H. Lineweaver and D. Burk, *J. Am. Chem. Soc.*, 1934, **56**, 658.

13 T. Rosner, J. L. Bars, A. Pfaltz, and D. G. Blackmond, *J. Am. Chem. Soc.*, 2001, **123**, 1848.

14 D. G. Blackmond, C. R. McMillan, S. Ramdechul, A. Schorm, and J. M. Brown, *J. Am. Chem. Soc.*, 2001, **123**, 10103.

15 D. G. Blackmond, N. S. Hodnett, and G. C. Lloyd-Jones, *J. Am. Chem. Soc.*, 2006, **128**, 7450.

16 L. P. C. Neilson, C. P. Stevenson, D. G. Blackmond, and E. N. Jacobsen, *J. Am. Chem. Soc.*, 2004, **126**, 1360.

17 M. Klussmann, S. P. Mathew, H. Iwamura, D. H. W. Jr, A. Armstrong, and D. G. Blackmond, *Angew. Chem: Int. Ed.*, 2006, **45**, 7989.

18 D. G. Blackmond, *Angewandte Chemie: International Edition*, 2005, **44**, 4302.

19 J. S. Mathew, M. Klussmann, H. Iwamura, F. Valera, A. Futran, E. A. C. Emanuelsson, and D. G. Blackmond, *J. Org. Chem.*, 2006, **71**, 4711.

20 P. H. Phua, S. P. Mathew, A. J. P. White, J. G. d. Vries, D. G. Blackmond, and K. K. Hii, *Chemistry: A European Journal*, 2007, Advanced Article.

21 P. H. Phua, K. K. Hii, and J. G. d. Vries, *Adv. Synth. Catal*, 2006, **384**, 587.

22 P. H. Phua, S. P. Mathew, A. J. P. White, J. G. de Vries, D. G. Blackmond, and K. K. Hii, *Chemistry: A European Journal*, 2007.

23 S. P. Mathew, S. Gunathilagan, S. M. Roberts, and D. G. Blackmond, *Org. Lett.*, 2005, **7**, 4847.

24 G. Carrea, S. Colonna, A. D. Meek, G. Ottolina, and S. M. Roberts, *Chem. Commun.*, 2004, 1412.

25 T. Rosner, P. J. Sears, W. A. Nugent, and D. G. Blackmond, *Org. Lett.*, 2000, **2**, 2511.

26 M. Kitamura, S. Suga, H. Oka, and R. Noyori.

27 C. Puchot, O. Samuel, E. Dunach, S. Zhao, C. Agami, and H. B. Kagan, *J. Am. Chem. Soc.*, 1986, **108**, 2353.

28 A. Kina, H. Iwamura, and T. Hayashi, *J. Am. Chem. Soc.*, 2006, **128**, 3904.

29 F. Visentin, G. Puxty, O. M. Kut, and K. Hungerbuhler, *Ind. Eng. Chem. Res.*, 2006, **45**, 4544.

Chapter 2: The Rhodium Catalysed Hydrogenation of 1-Octene

As was described previously, reaction progress kinetic analysis allows for reactions to be looked at as a whole and therefore the same data can be collected using fewer experiments.[1] The majority of systems have used reaction calorimetry as a primary investigative tool whereas IR, UV and gas uptake analysis are used as complimentary methods. As such the limitations of gas uptake analysis have not been established. In order to determine if gas uptake analysis can be used as a viable primary investigative tool, a set of known reactions have been run to establish if constant volume and pressure measurements from batch reactors are comparable to the measurements taken using reaction calorimetry. One of the simplest reactions incorporating a single gas is the hydrogenation of an alkene.

2.1 Overview

The most common and convenient methods for hydrogenation in organic chemistry tend to involve Raney nickel or palladium on carbon catalysts owing to their convenient handling and ease of removal by filtration once the reaction is complete.[2-4] Despite the mild conditions in which reactions like these can be conducted, heterogeneous reactions are disadvantageous as a result of their lack of specificity.[2]

There are a multitude of soluble metal complexes available to catalytically reduce organic compounds, and, in general, homogeneously catalysing hydrogenations allows for a much greater selectivity when compared to heterogeneous catalysts.[2] Comprehensive studies into homogeneously catalysed hydrogenations have allowed for a greater understanding of relationships between ligands and metal centres and this has helped in the development of reaction mechanisms.[5] Different combinations and conditions alter properties such as the steric and electronic effects of the metal centres. Increased knowledge of these properties has also allowed for the tailoring of regio- and stereo-selectivity within reactions.

In homogeneously catalysed hydrogenations, rhodium, iridium and ruthenium are the more commonly used metal centres, but it is found that rhodium complexes are typically more reactive than their iridium and ruthenium derivatives.[2]

2.2 Wilkinson's Catalyst

Chlorotris(triphenylphosphine)rhodium(I) also known as Wilkinson's catalyst [$RhCl(PPh_3)_3$] is the most commonly utilised and extensively studied of all hydrogenation catalysts.[6-8] Benzene and toluene are commonly used as the solvent of choice for this reaction as the aromatic nuclei are inert. The addition of a polar solvent such as ethanol can significantly increase the rate, whereas introducing chlorinated hydrocarbons can significantly reduce the rate owing to the resulting oxidation of the catalyst to form trichlorortris(triphenylphosphine)rhodium(III) [$RhCl_3(PPh_3)_3$]. [2]

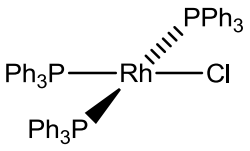

Figure 2.1: Wilkinson's catalyst.

The catalytic cycle for hydrogenation with Wilkinson's catalyst proceeds via the formation of the hydride followed by the coordination of the alkene. [2] This is shown in figure 2.2 for propene as the substrate.

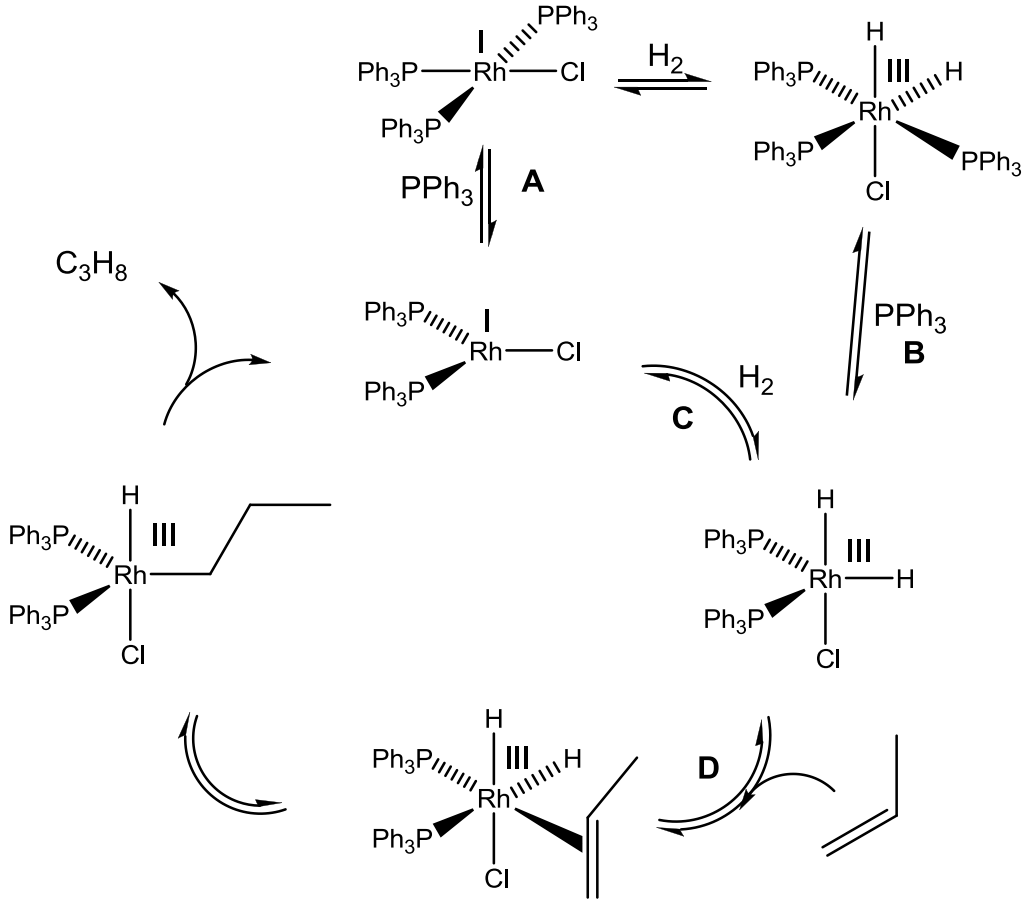

Figure 2.2: Schematic of Wilkinson's catalytic cycle for the hydrogenation of alkenes. [9]

Within this reaction, there are very minute concentrations of dimeric rhodium species formed such as $[RhCl(PPh_3)_2]_2$ and $[H_2RhCl(PPh_3)_2]_2$. These have no significant effect on the overall reaction as H_2 reacts with $[RhCl(PPh_3)_2]$ much more rapidly than dimer formation.[9]

Variations in the rate within this reaction tend to be associated with the alkene stereochemistry and how this effects the formation of the $[H_2RhClL_2(alkene)]$ intermediate.

Wilkinson's catalyst is particularly advantageous over other homogeneous catalysts as it hydrogenates alkenes specifically, even in the presence of other easily reducible groups such as $–NO_2$ or –C=O. An example of this is shown in figure 2.3. It also preferentially hydrogenates terminal alkenes as opposed to internal alkenes.

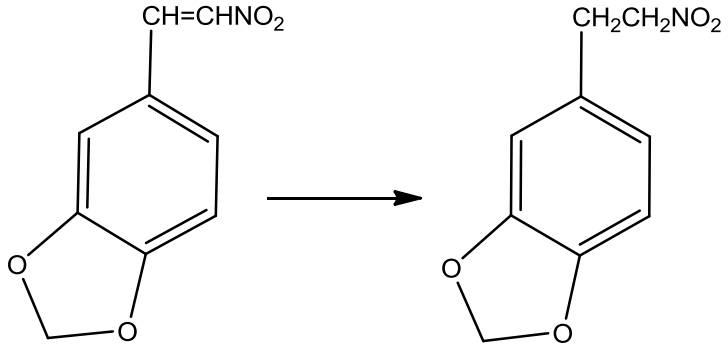

Figure 2.3: Shows preferential hydrogenation of alkene when it is conjugated with a nitro group. [9]

The aim of the work reported in this chapter was to investigate the applicability of gas uptake measurements for reaction progress kinetic analysis[1] in a simple well defined system and to determine whether the orders with respect to 1-octene and to hydrogen could be reliably obtained from just two experiments. Working at constant $[RhCl(PPh_3)_3]$, $[PPh_3]$ and temperature, the rate expression for this catalytic reaction should be:

$$\text{Rate} = k[\text{1-octene}]^n \, p_{H2}{}^m$$

2.3 Results

The aim of these experiments was to establish the potential for the orders with respect to individual reacting components to be established within minimal numbers of experiments. This can be done by creating pseudo zero order conditions on one substrate to measure the rate with respect to another. It was postulated that if, in the case of the hydrogenation of 1-octene, you ran an experiment under a constant H_2 pressure of 30 bar, the result would be pseudo zero order kinetics with respect to the partial pressure of hydrogen. Thereafter, if you ran the reaction under constant volume conditions, you can determine the order with respect to gas, as the order in substrate is already known.

2.3.1 Constant Pressure Reaction

By working at constant pressure the rate expression becomes:

$$\text{Rate} = k'[\text{1-octene}]^n \text{ where } k' = kp_{H2}$$

The hydrogenation of 1-octene (1ml, 0.00637 mol, and figure 2.4) was carried out at 40°C and 30 bar H_2 pressure in a constant pressure system. Maintaining the system at constant pressure by continuously feeding hydrogen from a reservoir and monitoring the pressure drop in the autoclave allowed for the determination of the order with respect to 1-octene. The resulting gas uptake plot is shown in figure 2.5

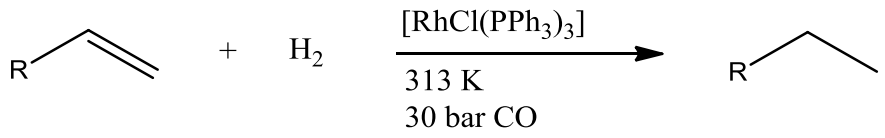

Figure 2.4: The hydrogenation of 1-octene.

The plot of $\ln(p_1-p)$ (p_1 is the pressure in the ballast vessel at time *t*; p is the final pressure at the end of the reaction) against time is a straight line, indicating that the reaction is first order in 1-octene concentration.

2.3.2 Constant Volume Reaction

The reaction was then re-run under constant volume conditions, to create a system where both the hydrogen concentration and the 1-octene concentration were changing simultaneously. The resulting gas uptake plot is shown in figure 2. The rate constant measured for the constant pressure system was 0.00469 bar/s and the rate for the constant volume system was found to be 0.00468 bar/s.

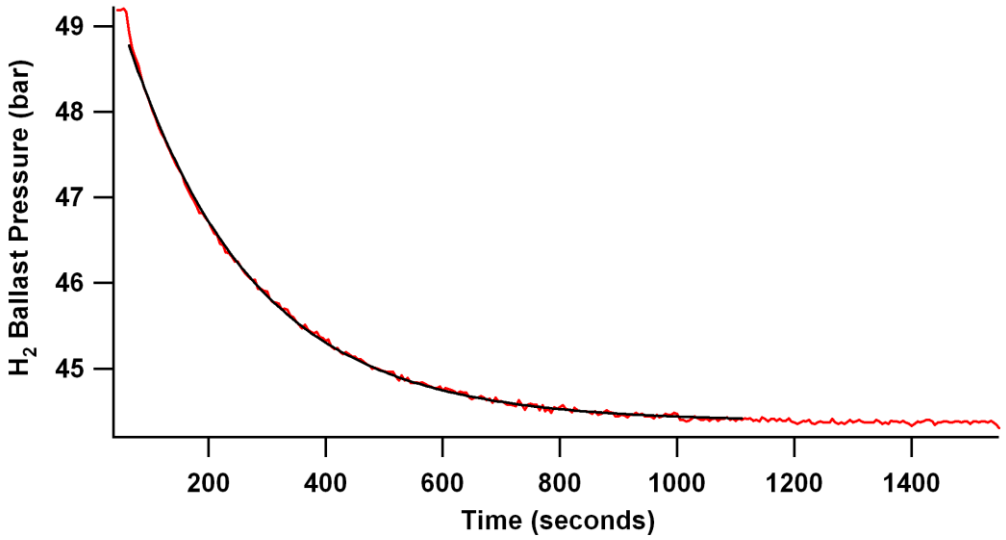

Figure 2.5: Plot of the gas uptake curve for the hydrogenation of 1-octene within an open, constant pressure system.

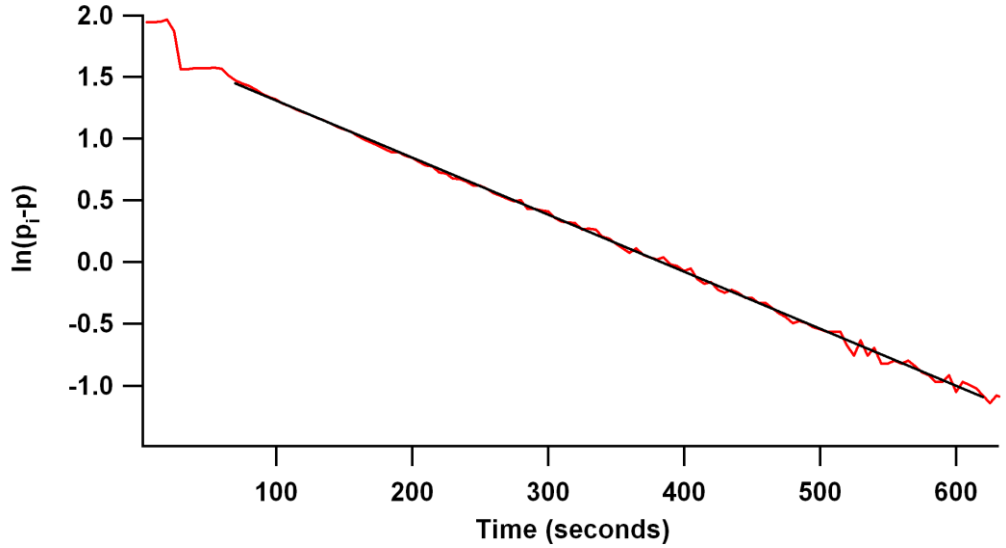

Figure 2.6: Plot of the natural log of the gas uptake for the hydrogenation of 1-octene in an open system as a function of time.

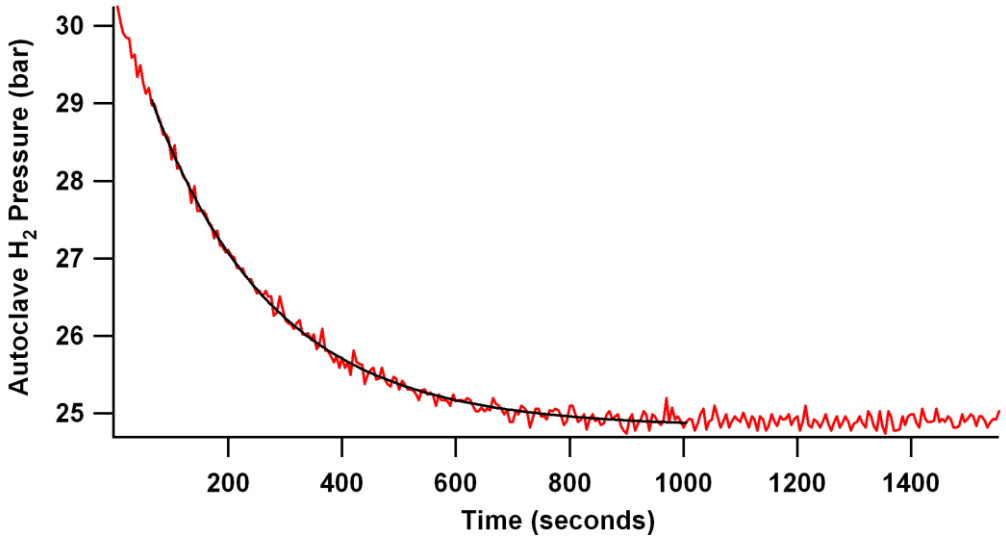

Figure 2.7: Plot of the gas uptake curve for the hydrogenation of 1-octene in a closed system.

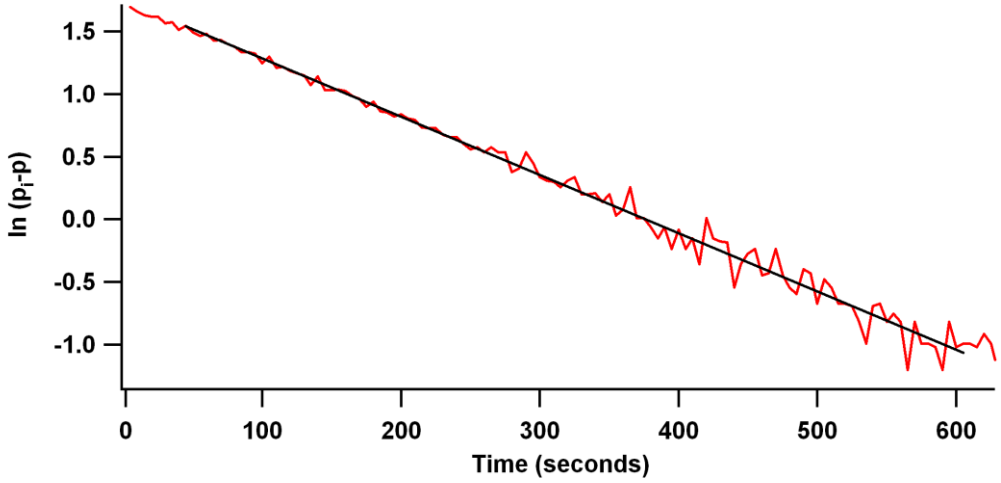

Figure 2.8: Plot of the natural log of the gas uptake for the hydrogenation of 1-octene in a closed system as a function of time.

The linearity of the plot of ln(p_1-p) (p_1 is the pressure in the reactor at time t, p is the final pressure at the end of the reaction) against time shows that the reaction has an overall order of 1 when run in a constant volume system. As the system was shown to be first order within a constant pressure system, the reaction is first order in 1-octene concentration. The reaction remains the same rate and order when the system is run under constant volume conditions suggesting that the reaction is 0 order with respect to the partial pressure of H_2

gas. Care must be taken in reading too much into this observation since the pressure drop during the reaction is only 5 bar from a starting pressure of 30 bar. If the reaction were first order in hydrogen, the rate would only decrease by 20% over the course of the reaction. This should be observed as an upward curvature from linearity of the $\log(p_1\text{-}p)$ vs t plot. We believe that a 20% drop in rate should be observable under these conditions, but a partial order in pH_2 might be masked.

This data was then processed to establish is if was possible to show the order with respect to each reacting component by calculation from the constant volume reaction. The substrate concentration was calculated from the gas uptake. The substrate concentration as a function of time is shown in figure 2.9.

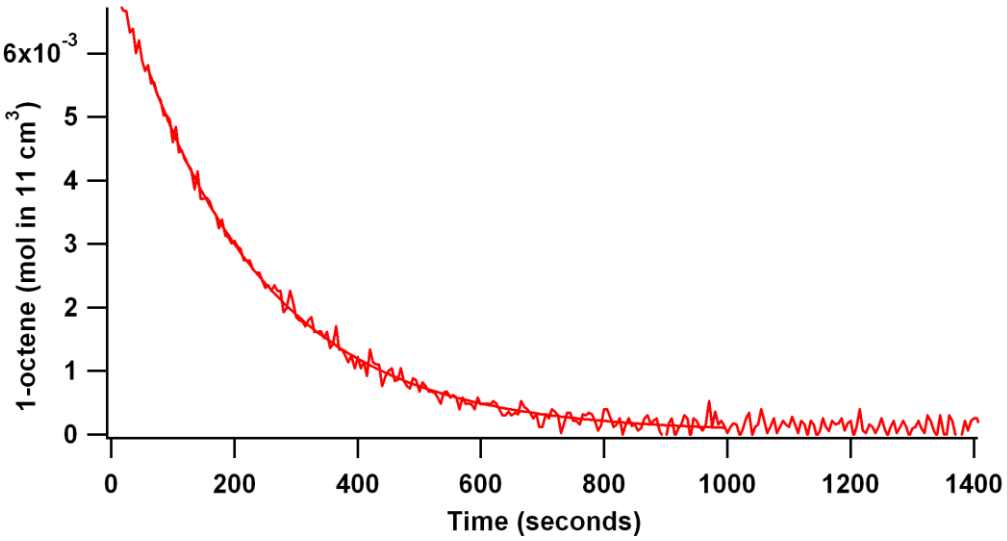

Figure 2.9: The substrate concentration as a function of time for the hydrogenation of 1-octene in a closed system.

Using these values for 1-octene concentration, the rate of reaction was then calculated for each point within the reaction. The rate was then plotted as a function of 1-octene concentration to give the overall order with respect to substrate. A straight line passing through the origin was obtained, suggesting again that the reaction is first order in 1-octene (figure 2.10).

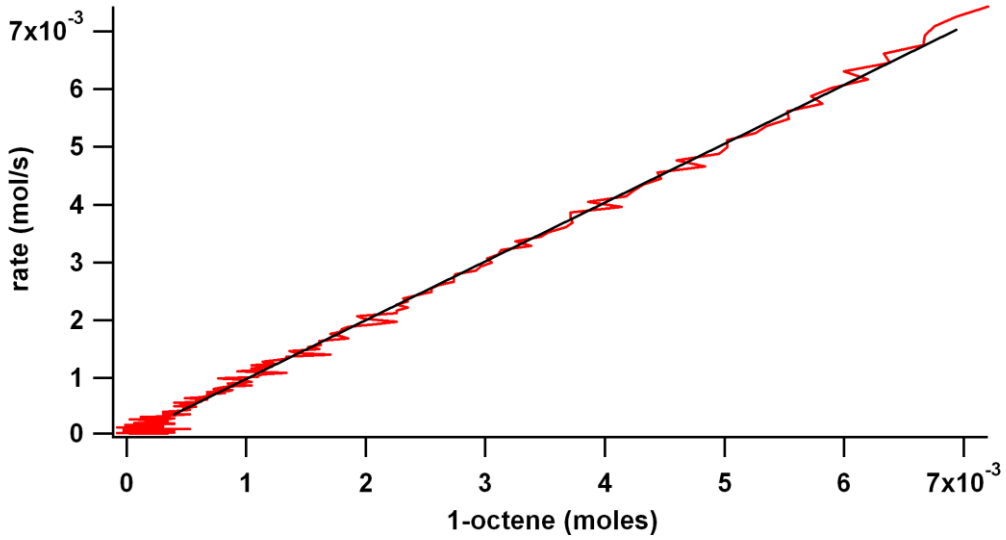

Figure 2.10: The rate as a function of substrate concentration for the hydrogenation of 1-octene in a closed system.

The rate was then divided by the substrate concentration and the natural log was taken and plotted as a function of the partial pressure of hydrogen to show the order with respect to hydrogen pressure. A straight line parallel to the x axis confirms that the reaction is zero order in pH_2.

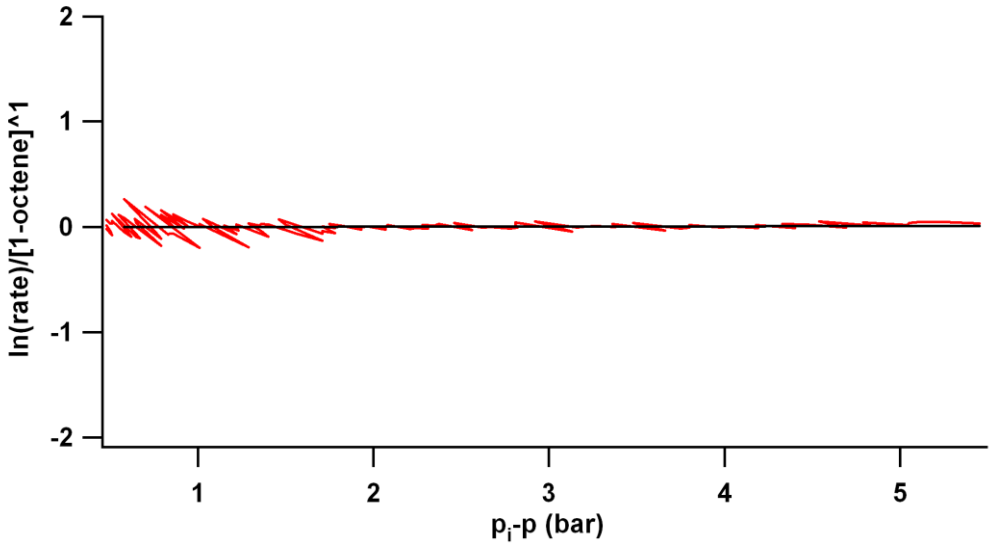

Figure 2.11: The natural log plot of the rate divided by substrate concentration as a function of the pressure drop, showing an overall order of zero with respect to the partial pressure of H_2.

2.4 Discussion

The hydrogenation of 1-octene was carried out at 40˚C and 30 bar of hydrogen pressure to establish the order with respect to both the 1-octene concentration and hydrogen pressure. The aim of this study was to establish if it was possible to establish these orders in two experiments. The constant pressure system successfully established that the reaction was first order in 1-octene concentration and therefore that the co-ordination of the alkene to the rhodium is the rate determining step for the reaction.

Within the constant volume reaction, where both reacting components were changing simultaneously, it was found that the reaction was first order overall, therefore it was postulated that the order with respect to the hydrogen pressure was 0. This would imply that the co-ordination of the hydrogen to the metal centre is fast. The manipulation of the closed system data showed that when the order of one reacting component was established, it was possible to use this to calculate the order with respect to the other reacting component.

There have been many studies of the kinetics of hydrogenation of alkenes using Wilkinson's catalyst. Generally these studies agree that the reaction is first order in alkene and zero order in hydrogen. The most noted of these being by Osborn *et al*. [8] They studied the overall rates of hydrogenation for several alkenes, measuring the dependence on temperature, pressure, substrate concentration and catalysts concentration. They showed that the rate determining step of the reaction was possibility is the attack of the olefin on the vacant site in the dihydrido complex to form a complex containing both the hydrogen atoms and the alkene attached to the metal centre. This confirms that oxidative addition of hydrogen is not rate determining.

The first order dependence of [alkene] could indicate two different possibilities. The actual catalytic cycle could involve alkene in the rate determining step so that alkene coordination (Step **C** in Figure 2.2) is rate determining. Alternatively, the amount of catalyst in the active cycle may be increased by increasing the alkene concentration (Step **A** or **B** in Figure 2.2). *In situ* NMR studies[10] have shown that the main species observed during hydrogenation reactions is $[RhH_2Cl(PPh_3)_3]$, a resting state outside the catalytic cycle, so that the first order dependence on alkene probably arises from Equilibrium **B** (Figure 2.2) increasing the

amount of active complex and hence the rate as [alkene] increases. However, studies using *para*-hydrogen, which can lead to enhancements of NMR signals, especially of dihydrido complexes of >1000x, have shown that it is possible to observe small amounts of $[RhH_2(alkene)(PPh_3)_3]$, indicating that this must be the complex just before the rate determining step and hence that H migration onto alkene is rate determining.[10] Our kinetic results are entirely consistent with this conclusion.

2.5 References

[1] D. G. Blackmond, *Angew. Chem: Int. Ed.*, 2005, **44**, 4302.

[2] R. S. Dickson, 'Homogeneous Catalysis with Compounds of Rhodium and Iridium', D. Reidel Publishing Company, 1985.

[3] B. R. James, 'Homogeneous Hydrogenation', Jonh Wiley, New York, 1973.

[4] F. J. McQuillin, 'Homogeneous Hydrogenation in Organic Chemistry', D. Reidel, Dordrecht, Holland, 1968.

[5] C. D. Frohling and C. W. Kohlpaintner, 'Applied Homogeneous Catalysis with Organometallic Compounds', ed. B. Cornils and W. A. Herrmann, Wiley-VCH, 1996.

[6] J. F. Young, J. A. Osborn, F. H. Jardine, and G. Wilkinson, *Chem. Commun.*, 1965, 131.

[7] F. H. Jardine, *Progress in Inorganic Chemistry*, 1981, **28**, 63.

[8] J. A. Osborn, F. H. Jardine, J. F. Young, and G. Wilkinson, *J. Chem. Soc. A*, 1966, **12**, 1711.

[9] R. S. Dickson, 'Homogeneous Catalysis with Compounds if Rhodium and Iridium', D. Reidel Publishing Company, 1985.

[10] S. B. Duckett, C. L. Newell, and R. Eisenberg, *J. Am. Chem. Soc.*, 1994, **116**, 10548.

Chapter 3: The Rhodium Catalysed Hydroformylation of 1-octene

3.1: Overview

One of the most reliable starting points for gas uptake reactions which involve more than one gas reactant would be alkene hydroformylation. This reaction was a particularly advantageous starting point as the hydroformylation of alkenes has been widely studied in both academia and industry over the past 30 years.

3.2 Background

Hydroformylation is the simultaneous addition of carbon monoxide (CO) and hydrogen (H_2) to a substrate. The first set of catalysts utilised in this area were cobalt based and did not contain phosphine ligands. [1] As a result of the low activity of cobalt, the reaction conditions were harsh, but the system was widely applied in lower, higher and internal alkene hydroformylation, producing mainly linear aldehyde products. [2] Cobalt phosphine systems incorporating ligands such as tributylphosphine improved selectivity of these cobalt catalysts. [3] In search for a milder alternative reaction, rhodium was considered as a catalyst, but initial studies found rhodium reactions to be slow, as a result of the formation of rhodium hydride species, which require high hydrogen pressures. [4]

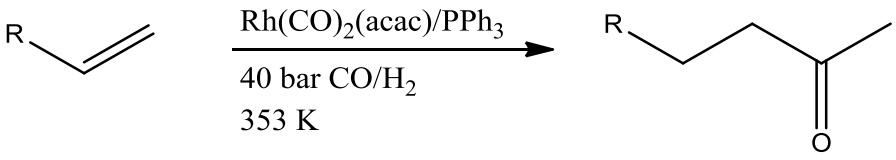

Figure 3.1: Hydroformylation of an alkene

The first reported use of phosphines with rhodium was by Shell [5-7] This led the way for many industries to use phosphine ligands with rhodium catalysts.[8, 9] The major breakthrough with phosphines with rhodium catalysts came with the work of Wilkinson, when he showed that arylphosphines could be very active ligands for catalysis even under mild conditions.[10]

This second generation process used triphenylphosphine and was first used by Celanese in 1974.[11] Thereafter, it was utilised by Union Carbide Corporation in 1976 and Mitsubishi Chemical Corporation in 1978, again using triphenylphosphine (tpp). [2] The major benefits of these catalysts are the milder conditions required; the increased utilisation of feedstock and the better selectivity towards linear aldehydes.[1, 2, 12] This reaction is now the largest scale homogeneous reaction utilised in the chemical industry, producing over 8M tonnes of aldehyde products annually.

3.3 Reaction

The most famous rhodium catalyst precursor for hydroformylation is still $[RhH(PPh_3)_3CO]$, first reported in 1963 by Vaska [13] The discovery of its activity is credited to Wilkinson and co-workers. This catalyst is commonly formed by the addition of hydrogen and carbon monoxide to Wilkinson's catalyst $[RhCl(PPh_3)_3]$. [14-16] The Rh-PPh_3 chemistry has been reviewed many times [1, 17-22] and as such makes this catalyst system of particular interest in our investigation. There has been considerable debate as to "the rate determining step" within this reaction. Most textbooks have commonly reported that it is the oxidative addition of hydrogen, [1, 17, 18, 20-24] but van Leeuwen *et al* [25 26] have presented evidence to the contrary. As this system is of such importance and the mechanism is so well established, this chemistry was thought to be a reliable starting point for establishing the possibility of our reactor system for measuring the kinetics of a reaction system.

3.4 Mechanism

The mechanism for the rhodium/tpp catalysed hydroformylation reaction was originally proposed by making slight modifications to the Heck-Breslow Cycle, [1] and is equivalent to the commonly known dissociative mechanism reported by Wilkinson, shown in figure 3.2. [14-16] The starting complex $[RhH(PPh_3)_3CO]$ (1) converts to (2*ae*/2*ee*) when CO is introduced. The hydrogen remains in the apical position, which means the CO coordination occurs in either the axial-equatorial positions or in the equatorial-equatorial positions, *ae* and *ee* respectively. The dissociation of an equatorial ligand or carbonyl allows for the formation of the *cis* and *trans* isomers of the square planar complex (3), which then

associates the alkene into the equatorial plane to form (4) in either ee or ae form. Previous studies have suggested that the formation of the four-coordinate complex (3) is as a result of the dissociation of a phosphine from either of species (1) or (2). [1]

Complex (4) then undergoes migratory insertion into the Rh-H bond to give a square planar alkyl complex (5) in either the *cis* or *trans* form. This species then reacts with CO to produce a trigonal bipyramidal complex (6) It has been shown that at low temperatures (<70 ˚C) and at higher pressures (>10 bar CO) the CO coordination becomes irreversible and as such the regioselectivity of the final product is determined. Complex (6) then undergoes the second migratory insertion of the carbonyl to form the *cis* and *trans* acyl intermediate species (7).

This species then reacts with H_2, via oxidative addition and reductive elimination, to give the aldehyde product and regenerates the square planar intermediate species (3), hence completing the cycle. This reaction mechanism is thought to be typical of catalytic conditions (70-120 ˚C, 10-30 bar, rhodium concentrations of ~10^{-3} and a hundred fold excess of phosphine).

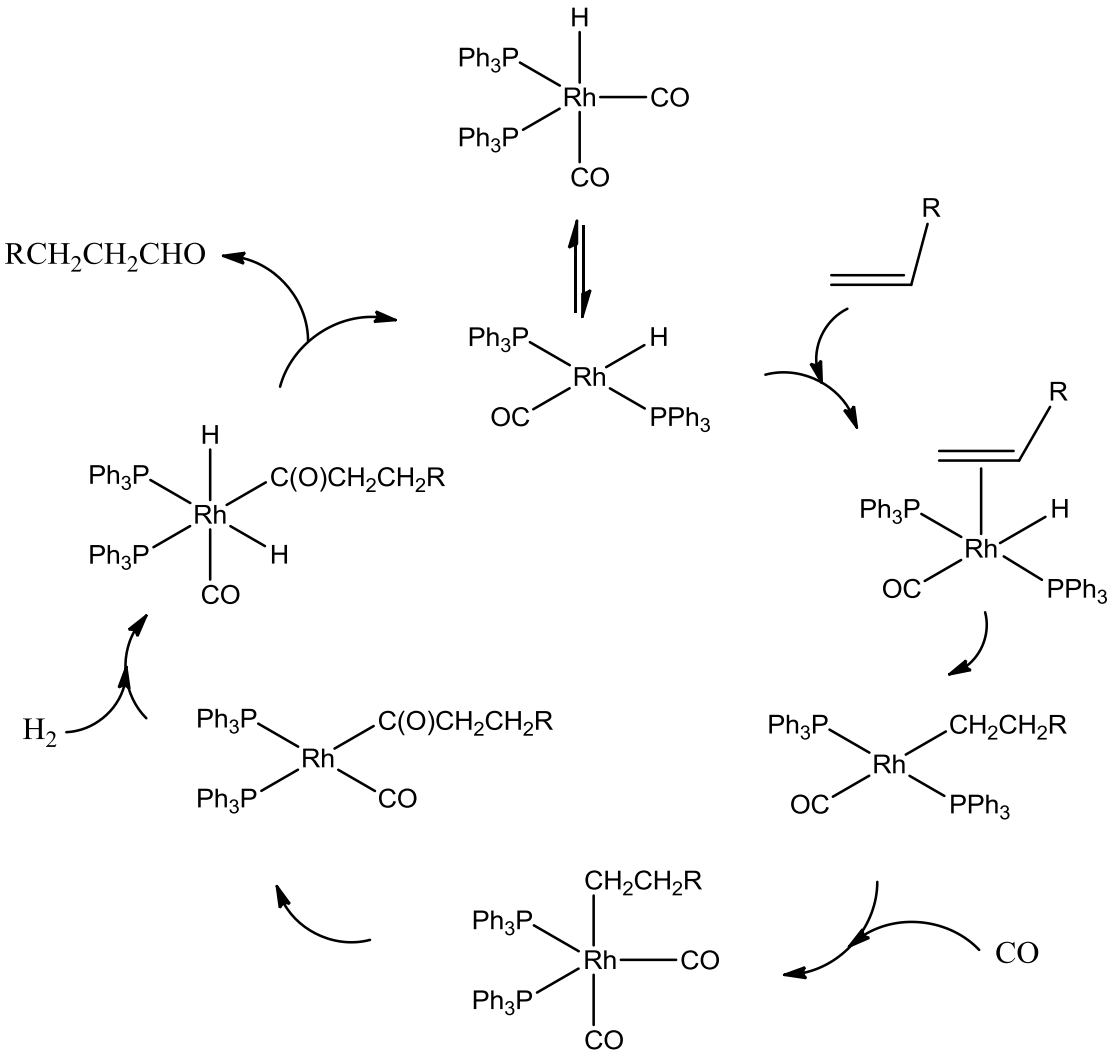

Figure 3.2: The dissociative mechanism for the hydroformylation of 1-octene[1]

3.5 Kinetic Studies

Despite the well-established mechanism for this reaction, and the importance of the system industrially, there have been very few kinetic studies published, and those that have been published have often been contradictory. The kinetics of rhodium carbonyl catalysed hydroformylation was first studied in the sixties by Wilkinson. Wilkinson [27] showed that increased CO pressures and PPh_3 concentrations had an inhibitory effect on the rate of reaction for 1-hexene, whereas increased substrate and rhodium concentrations lead to higher catalytic rates. It was also found that an increase in H_2 concentration has an increase

on the rate, but this is thought to be an artefact brought on by the removal of inactive di-rhodium species at higher pressures.

Contrary to this, *van* Leeuwen *et al* [25] [28] argue that the reaction is first order in alkene concentration and rhodium concentration, zero order in hydrogen with a negative order in ligand concentration (albeit phosphine or CO). This is thought to be the case for "standard conditions".

The most detailed study was carried out for propene by Cavalieri d'Oro *et al* [29, 30] who found the following rate expression. The reaction conditions were: 90-110 ˚C, p(CO) = 1-25 bar, $p(H_2)$ = 1-45 bar, $[PPh_3]$ = 0.05-5 mol dm^{-3}, [Rh] = $(0.5\text{-}7).10^{-3}$ mol dm^{-3}, PPh_3/Rh = 300:1 to 7:1, $[propene]_{t=0}$ = 2-7 mol d^{-3}.

$$V=k[C_3H_6]^{0.6}[PPh_3]^{-0.7}[CO]^{-0.1}[Rh]^{1}[H_2]^{0} \qquad (3.1)$$

The order of less than 1 in propene may be an indication of saturation kinetics. This could be shown if the reaction showed first order kinetics at low propene concentrations and tended towards zero order at higher propene concentrations. It has also been reported that for 1-hexene and 1-octene, a first order behaviour has been observed when using Rh-PPh_3 catalysts. [26, 31] It has also been reported at higher 1-hexene concentrations that a negative order in substrate is observed. [32] A negative (inverse) order in pCO has been described by Moser. [33] Studies from both Wilkinson [14] and Strohmeier [31] have shown results consistent with a negative order in pCO and a zero order dependence on pH_2.

3.6 Results

3.6.1 Determination of the overall order for the reaction

The initial reaction was the hydroformylation of 1-octene (0.5ml, 3.15 mmol) in a constant pressure system. The motivation for this was to establish an approximation of the order with respect to the 1-octene concentration. This was achievable as the only reacting component for which the concentration is changing within this reaction is the 1-octene. Figure 3.3

shows the resulting uptake plot. This reaction was measured by maintaining a constant pressure within the reaction vessel by feeding in gas from a reservoir attached to the system, which is regulated using a mass flow controller. The resulting drop in pressure within the reservoir was measured using a pressure transducer. (P1, denoted as point 2 on figure 1.19).

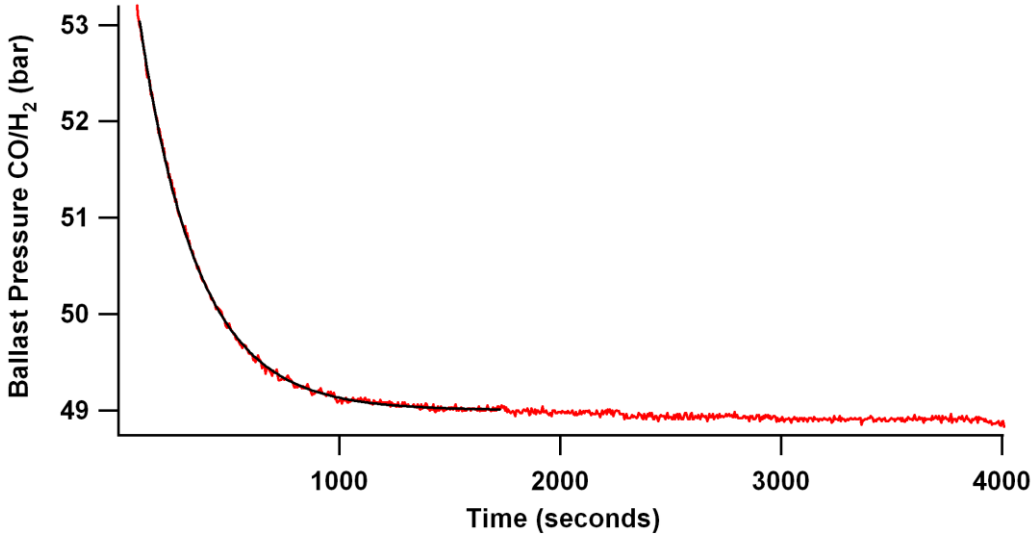

Figure 3.3: The gas uptake (1:1 synthesis gas) as a function of time for the hydroformylation of 1-octene.

This graph was then fitted with an exponential curve fit, using a curve fitting software program (Igor). This fit is shown in figure 3.4. The curve fit (black) shows good correlation with the uptake (red). The data was then processed and converted to allow for plotting the natural log of the pressure drop as a function of time (figure 3.5) to confirm that the reaction appears first order with respect to 1-octene concentration.

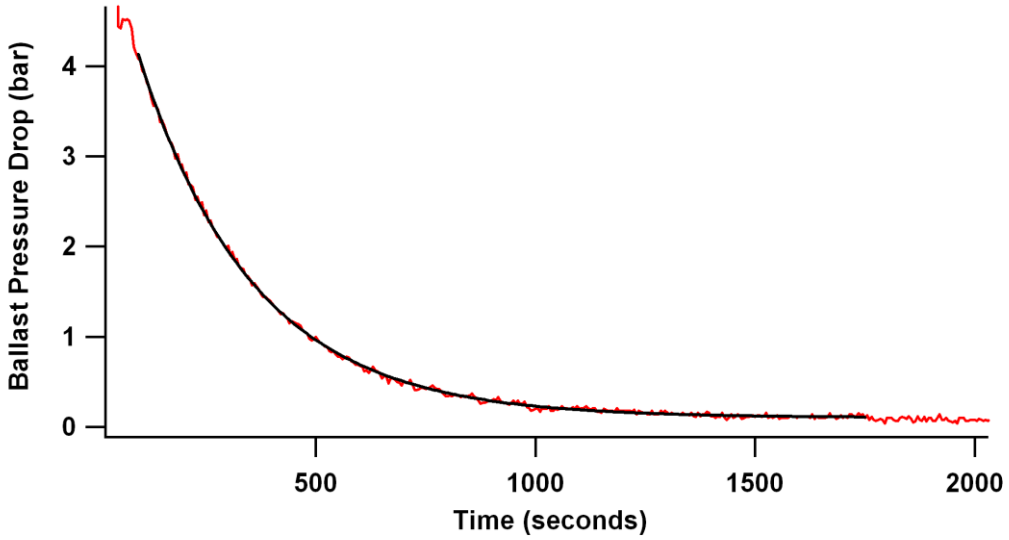

Figure 3.4: The exponential curve fit applied to the pressure drop data recorded as in figure 3.3.

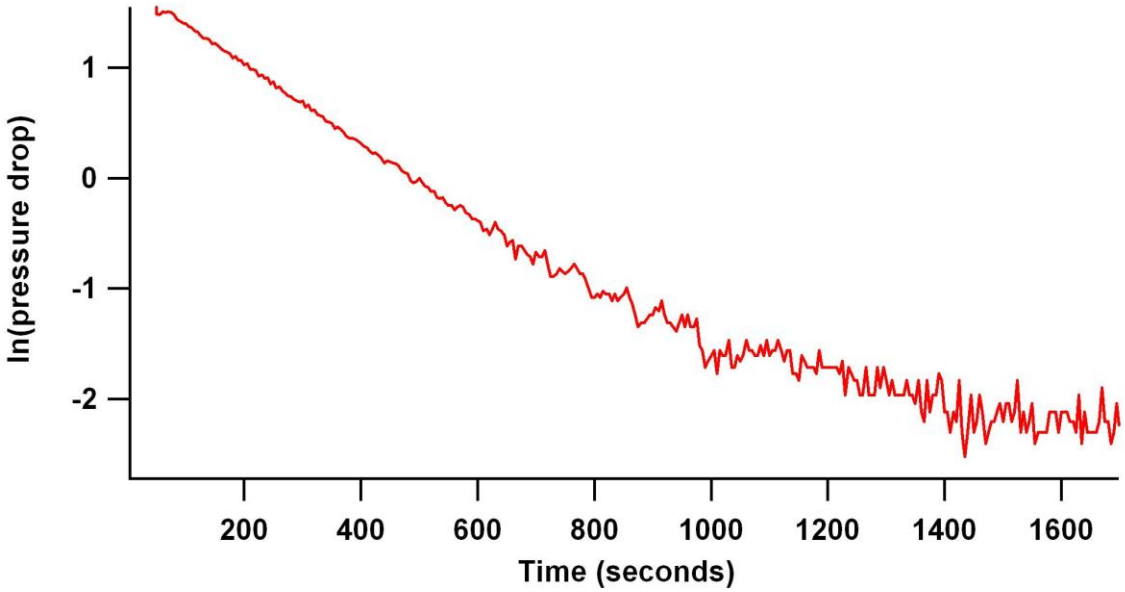

Figure 3.5: The natural log plot of the gas uptake as a function of time.

The area shown in figure 3.5 is the area denoted by the curve fit shown in figure 3.4 (black fit). It can be seen that the reaction is first order in substrate, until it reaches approximately 1000 seconds. It deviates from this thereafter, and when it is correlated to figure 3.3, it shows that by this point greater than 95% conversion has already occurred so there is substantial noise.

Having ascertained that the reaction appears first order with respect to 1-octene concentration, the same reaction was then run in a constant volume system. This would allow for the determination of the overall order for the reaction, as all three of the variable components within the reaction are changing simultaneously. The catalyst and ligand concentrations remain constant assuming both are stable. It is known from the reaction stoichiometry that 1 mole of CO is consumed for every 1 mole of H_2; therefore, as the feed gas is a 1:1 synthesis gas mix, the concentration of each gas can be calculated at any point throughout the reaction.

Furthermore, as the volume of gas required to convert 1 ml of substrate is known, it is possible to calculate the substrate concentration at any point in the reaction, assuming no side reactions are occurring within the reaction. The resulting graph is shown in figure 3.6. The graph is fitted with an exponential curve fit (black).

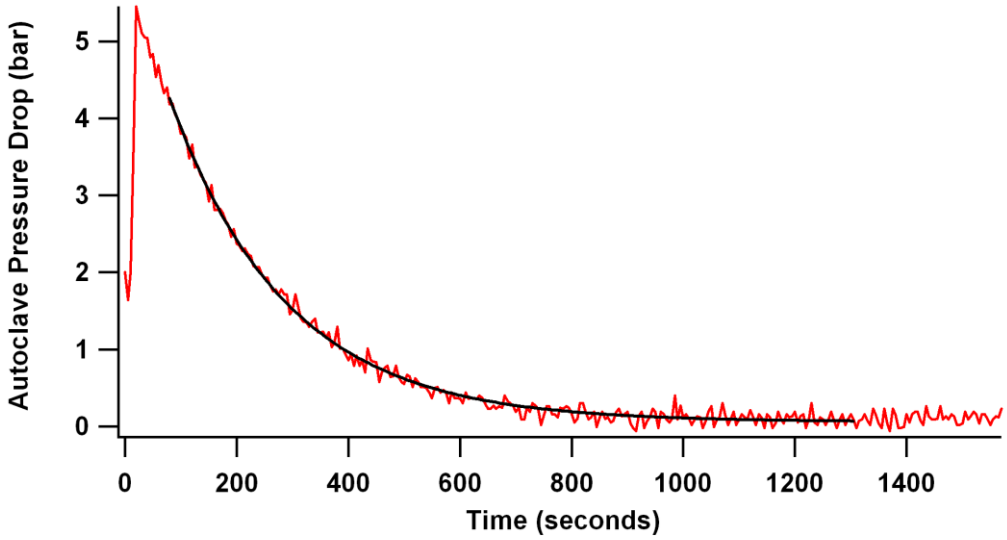

Figure 3.6: A graph showing the gas uptake for the hydroformylation of 1-octene in a constant volume system (red).

It can be noted in this graph that there is a first order dependency, brought on by 1-octene concentration. This can be shown more clearly in the natural log plot. (Figure 3.7) The log plot gets noisy once again when the reaction is almost at completion.

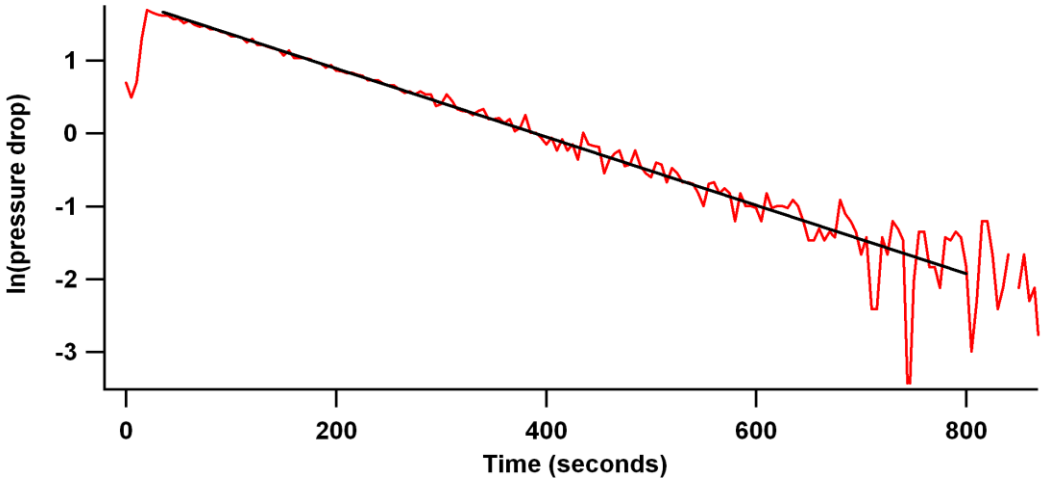

Figure 3.7: The natural log plot of pressure as a function of time within a constant volume system.

3.6.2 Determination of the order with respect to pH_2

Once the order in 1-octene concentration was established, the next step was to look at each of the gases in turn, to determine what extent the partial pressures of each of the gases played on the overall rate of reaction. In order to determine the overall order with respect to each gas, a series of reactions was set up where the concentration of one of the gases was varied whilst the other was kept constant.

As the baseline reaction was run at 40 bar with 1:1 syngas, the consistent pressure throughout this study was 20 bar of either CO or H_2, whilst the other gas was varied between 10 and 30 bar. To ensure consistency, each of the reactions was run at a set pressure of 50 bar, and made up to this pressure with nitrogen when necessary. For each uptake, the initial rate for the reaction was calculated. The results of these experiments are shown in table 3.1.

H_2 Pressure (bar)	CO Pressure (bar)	Nitrogen Pressure (bar)	Rate mol/s
10	20	20	0.0169
15	20	15	0.0176
18	20	12	0.0179
20	20	10	0.018
25	20	5	0.0187
30	20	0	0.0189

Table 3.1: Details of variable H_2 pressure experiments

The natural log of both the rate and the hydrogen pressure were calculated and used to construct a double logarithmic plot. The gradient of the line of best fit was then used to determine the order with respect to the hydrogen pressure. This gave an overall order in hydrogen between 10 and 30 bar of 0.1.

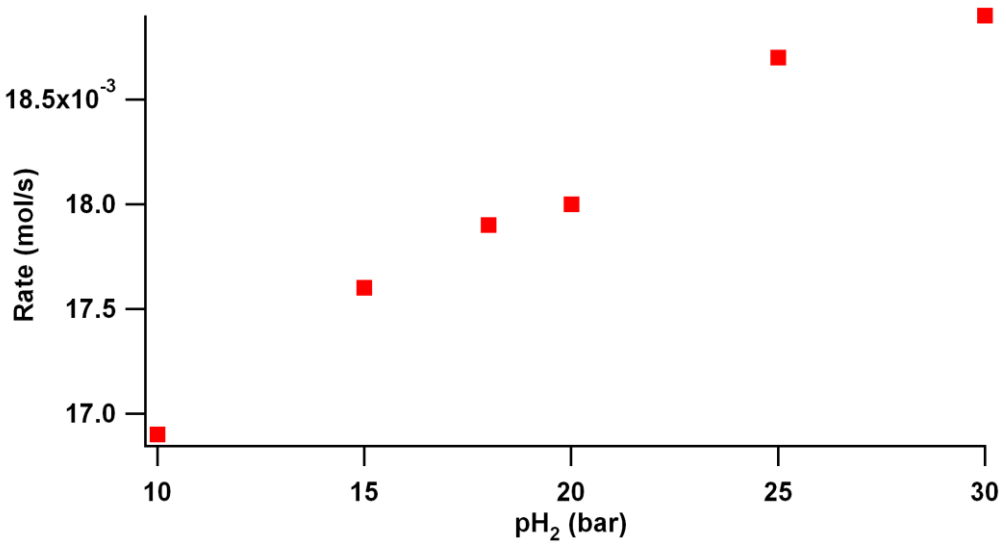

Figure 3.8: The measured rate constant as a function of the partial pressure of hydrogen, varied between 10 and 30 bar.

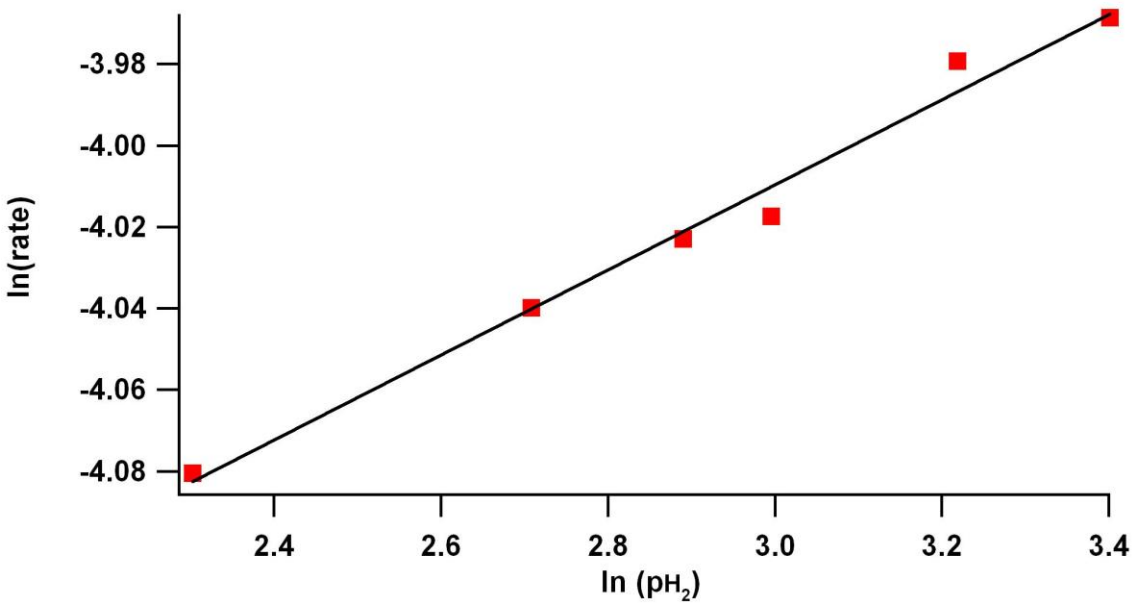

Figure 3.9: Double reciprocal plot of the rate vs. the partial pressure of hydrogen, varied between 10 and 30 bar.

3.6.3 Determination of the order with respect to pCO

Once the order in pH_2 was established, the series of experiments was re run, this time changing the CO pressures, whilst maintaining the H_2 pressure. Again when required nitrogen made the pressure up to 50 bar. The initial rate constants were again measured and are shown for each condition in table 3.2.

H_2 Pressure (bar)	**CO Pressure (bar)**	**Nitrogen Pressure (bar)**	**Rate mol/s**
20	10	20	0.0262
20	15	15	0.0222
20	20	10	0.0194
20	25	5	0.0182
20	30	0	0.0164

Table 3.2: Details of variable CO pressure experiments.

These results are shown graphically in figure 3.10. It can be easily seen that the increase in CO pressure has a negative effect on the rate of reaction.

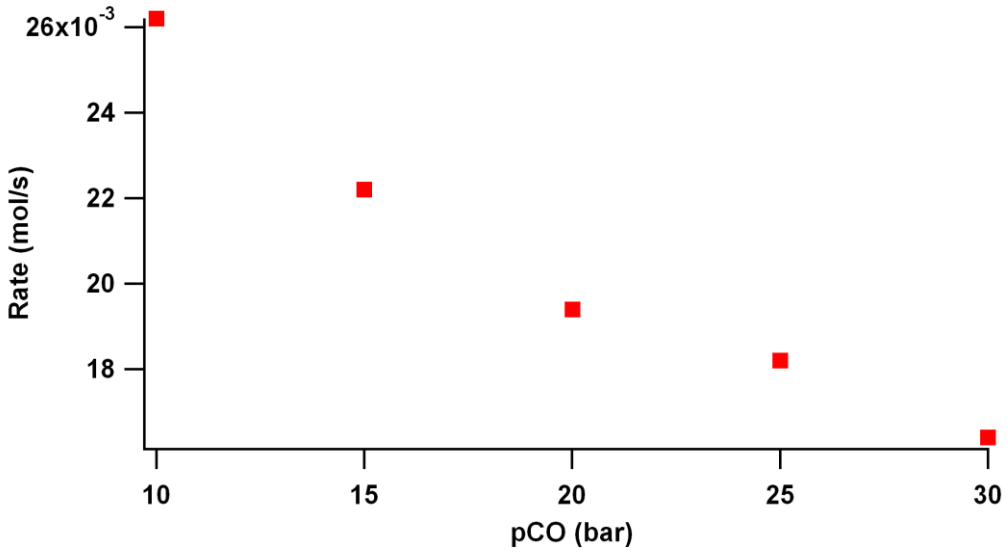

Figure 3.10: Graph plotting the rate against the partial pressure of carbon monoxide, varied between 10 and 30 bar.

The natural log of both the rate and the carbon monoxide pressure were calculated and used to construct a double logarithmic plot. This gradient of the line of best fit was then used to determine the order with respect to the carbon monoxide pressure. This gave an overall order in carbon monoxide between 10 and 30 bar of –0.4.

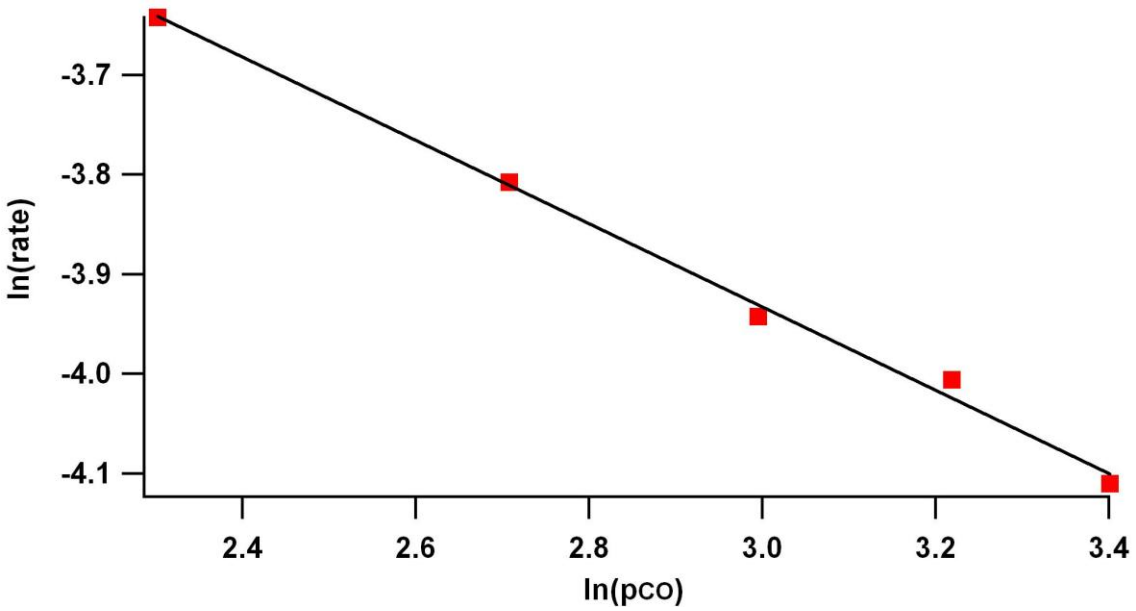

Figure 3.11: Double reciprocal plot of the rate vs. the partial pressure of carbon monoxide, varied between 10 and 30 bar. The fit gives an order with respect to carbon monoxide pressure of -0.4.

3.7 Discussion

3.7.1 Simplifications and Considerations

In order to minimise the complexity of this study, it was decided to only vary those components, which would be of particular impact to using the reactor setup. In order to achieve this, standardised catalyst conditions were chosen to optimise the rate of reaction. The remaining components were kept constant throughout the study so their contributions could be omitted from the overall rate equation.

All reactions were run at a temperature of 80˚C, for consistency and to reduce the overall time it took for the reaction to run to completion. The choice of alkene throughout this experiment was purified 1-octene (1 cm^3) and the stirring speed for the reactor was maintained at 1000 rpm (which was checked regularly using a tachometer). The catalyst was formed *in-situ* from [Rh(acac)$(CO)_2$] (12.9 mg, 0.05 mmol) and PPh_3 (1.1 mg, 0.288 mmol) The solvent was toluene (10 cm^3). After 30 minutes preforming under synthesis gas (15 bar)

at 80^{o}C, the 1-octene was injected into the reactor and the pressure adjusted to the desired operating pressure. In experiments containing other then 1:1 CO:H_2, the autoclave was charged with the appropriate mixture, but 1:1 synthesis gas was fed from the ballast vessel.

A series of experiments was undertaken to ensure the volumes of each of the sections of the reactor were known (see Chapter 6,). From these volumes, it was possible to calculate the expected gas uptake per cm^3 of substrate used, based on its molecular weight and density. The expected pressure drop within the ballast vessel for reaction of 1 cm^3 (0.0063 moles) of octene when feeding gas at constant pressure is 4.2 bar for each gas (CO and H_2).

The reaction was also run using the maximum stirring speed possible on the reactor (1000 rpm) in order to minimise mass transport effects. Chaudhari *et al* [32] previously carried out an experiment showing that, within their study of the hydroformylation of 1-hexene. They found that at agitation speeds >400 rpm, there was no longer any effect of mass transport limitation. Despite this their reactions were run at 900-rpm agitation speed to ensure their studies were always within the kinetic regime. Therefore 1000 rpm should provide sufficient gas liquid mixing within the autoclave to ensure that there are no mass transport limitations on the system.

It was not felt necessary to vary the rhodium concentration as it has been commonly shown in the literature that the hydroformylation of alkenes using this catalyst system has a first order dependence in rhodium concentration above a critical concentration. It was therefore decided to choose and fix a catalyst concentration, above the critical concentration point, where the reaction becomes first order in catalyst concentration, when the reaction switches from the associative mechanism (which has previously been shown to predominate at very low catalyst concentrations) to the dissociative mechanism which is the commonly accepted mechanism for this reaction.

The Rh:P ratio was fixed at 1:10. This ratio optimises between the decrease in rate brought on by increasing the phosphine concentration and the lowering of competing side reactions, inhibiting the formation of the inactive dimeric rhodium species and increasing the selectivity towards the linear product. The linear product is formed more favourably in these conditions as a result of the interactions of the substrate with the bulky phenyl groups on the

phosphine ligands. This meant that the areas focused on within this study were the alkene concentration and the partial pressures of hydrogen and carbon monoxide.

Toluene was chosen as the solvent for this study as the catalyst precursor is suitably soluble within it. It is non-chlorinated, which is essential to prevent the solvent reacting with the hydride intermediate species formed within the reaction. Furthermore, toluene cannot be hydrogenated within the reaction and it is non protic and therefore does not interfere with the reaction itself.

3.7.2 Order in reacting components

Several conflicting orders with respect to each of the reacting component concentrations, have been reported, leading to a variety of explanations and mechanisms. These variations are often brought about as a result of studies focussing on different reaction conditions and drawing conclusions from a variety of spectroscopic methods using initial rate expressions.

It was found that, when the substrate concentration was followed as a function of gas uptake and assuming a 1:1 conversion, the reaction has an overall order of 1 with respect to 1-octene concentration. Furthermore, the order with respect to the partial pressure of H_2 is 0.1 and the partial pressure of CO has an overall order of -0.4.

These observations agree with studies by van Leeuwen *et al*, [28] who have shown that this reaction is first order in substrate concentration and zero order with respect to H_2 concentration and as such, the rate determining step within this reaction is not the commonly accepted oxidative addition of H_2 reaction step, but the coordination of the alkene.

This conflicts with previous studies by Wilkinson *et al*,[14, 27] who have shown that the rate with respect to alkene concentration reaches an asymptotic value as the catalyst to substrate ratio increases. Deshpande *et al* [32]showed that an increase in alkene concentration (albeit 1-hexene) initially had a positive effect on the rate of reaction before reaching a maxima and then changing to a negative effect as the concentration increases towards an inhibition range.

They postulate that the initial increase in rate arises as a result of an inhibition of the inactive dimer formation brought on by the introduction of the alkene into the reaction system. However it has been found that beyond certain concentrations (in excess of $4x10^{-4}$ mol/cm^{-3}) there was a decrease in the rate as a function of 1-hexene concentration. This would not be the case for the reactant conditions used within these experiments.

Furthermore they found the reaction to be first order in H_2 and as such postulate that the oxidative addition of the hydrogen to the acyl intermediate species is the rate-determining step for this catalytic cycle.

There is a general consensus that increasing the concentration of CO has a negative effect on the rate of the reaction, despite this, the extent to which this occurs varies dramatically from study to study. Wilkinson *et al* [14, 27]have stated that they observed that the CO concentration had a much more significant impact on the overall rate of reaction in comparison to the H_2 concentration. However, when they were present in a 1:1 ratio, the order for each gas cancel each other out. Despite this Wilkinson *et al* [14, 27]have determined that the rate determining step for the reaction in the oxidative addition of hydrogen.

Contradictory to this, as discussed previously, Cavalieri d'Oro *et al* [30] derived the order with respect to CO concentration to be -0.1; this implies that the CO concentration does not have a significant impact on the overall rate of reaction. They also found the reaction to be zero order in H_2 concentration, implying that neither gas is involved in the rate-determining step for this reaction. Deshpande *et al* [32] showed a complex order with respect to CO pressure, these studies were over pressures in the range of 0-15 atm and showed that initially the increase in CO pressure increases the rate of reaction, but once excess CO pressures are present, it has a negative effect with respect to the reaction rate. This initial positive effect would not be seen in our study as all of the CO concentrations used were always in excess.

If the reaction is first order in pH_2, negative order in CO and shows saturation kinetics in 1-octene, the most likely explanation is that the rate determining step is oxidative addition of hydrogen, but that there is an equilibrium between $[RhH(CO)_2(PPh_3)_2]_2$ and $[RhH(CO)(PPh_3)_2(alkene)]$, shown in figure 3.13.

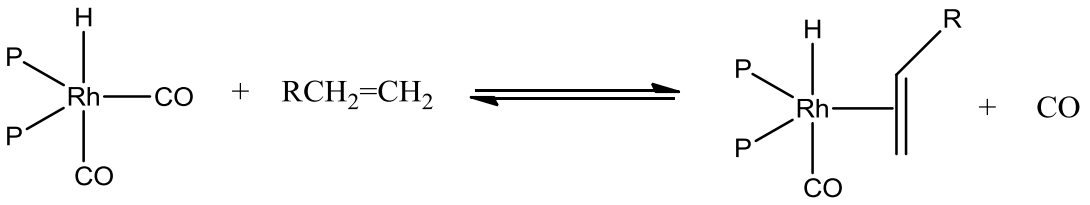

Figure 3.13: The equilibrium step between [RhH(CO)$_2$(PPh$_3$)$_2$] and [RhH(CO)(PPh$_3$)$_2$(alkene)].

[RhH(CO)$_2$(PPh$_3$)$_2$] is a resting state outside the catalytic cycle and has been observed to be present under the reaction conditions using *in situ* spectroscopy by both van Leeuwen and Brown. The concentration of catalyst in the catalytic cycle depends upon the position of this equilibrium. When the alkene concentration is low, this equilibrium will not lie completely to the right. The amount of [RhH(CO)(PPh$_3$)$_2$(alkene)] will be proportional to the alkene concentration and so the reaction will appear first order in alkene.

The reaction will appear negative order in CO because increasing CO moves the equilibrium to the left, decreasing the amount of catalyst in the cycle. Once the alkene concentration is high enough to push the equilibrium entirely to the right, the reaction will appear zero order in alkene but still first order in H_2. For this explanation, a further equilibrium, in which the alkene in [RhH(CO)(PPh$_3$)$_2$(alkene)]. is replaced by PPh$_3$, explains the negative order in PPh$_3$ because this again lowers the concentration of rhodium species in the catalytic cycle.

However, this is not the only explanation for the reaction to be first order in hydrogen. A second equilibrium is possible, this time between [RhH(CO)(PPh$_3$)$_3$] and [Rh(CO)(PPh$_3$)$_6$] as shown in figure 3.14.

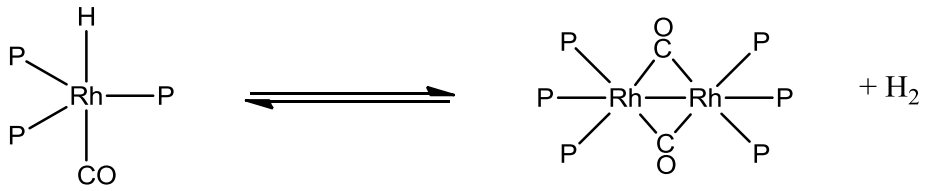

Figure 3.14: The formation of the catalytically inactive dimer species.

Here saturation kinetics would be observed in hydrogen, although at low pH_2, the reaction would appear to be second order in hydrogen. Inhibition by CO and PPh_3 would still be observed and the reaction might also show saturation kinetics in alkene. In our studies we observe little dependence on CO or on hydrogen, but first order kinetics in alkene. One explanation is that the equilibrium between $[RhH(CO)_2(PPh_3)_2]$ and $[RhH(CO)(PPh_3)_2(alkene)]$ lies completely to the alkene side but that coordination of alkene to $[RhH(CO)(PPh_3)_2]$ is slow and rate determining.

A possible alternative is that the equilibrium between $[RhH(CO)_2(PPh_3)_2]$ and $[RhH(CO)(PPh_3)_2(alkene)]$ does not lie fully to the alkene side. This would give a first order dependence on alkene and a -1 order in CO. If, however, the coordination of CO to $[RhH(alkyl)(CO)(PPh_3)_2]$ were rate determining, the overall order in CO would be zero. A very high alkene concentration would render the reaction zero order in CO if alkene coordination were rate determining, but first order in CO if CO coordination were rate determining.

As has been extensively discussed, this negative effect is as a result of the formation of the $(RCO)Rh(CO)_2(PPh_3)_2$ and/or $(RCO)Rh(CO)_3(PPh_3)$ complexes, both of which are un-reactive towards hydrogen. The formation of both of these complexes occurs in equilibrium with the $(RCO)Rh(CO)(PPh_3)_2$ complex and as such it is a reversible process. The increased presence of CO also hinders the dissociation of the CO/L that produces the square planar complex, to which the alkene coordinates and as such inhibits the process.

Furthermore, increasing the partial pressure of CO has been previously shown to reduce the predominance of the linear aldehyde product. This change in selectivity has been explained by an equilibria in which, PPh_3 is replaced by CO. The bisphosphine cycle is believed to lead predominantly to the linear product, whilst the monophosphine cycle gives much less linear product.

3.8 Conclusions

Constant volume and constant pressure experiments have been used to elucidate the orders with respect to the individual reacting components within the rhodium catalysed hydroformylation of 1-octene. Experiments have shown that, under the conditions used, there is a first order dependency on 1-octene concentration, a 0.1 order in hydrogen concentration and a -0.4 order in carbon monoxide concentration. The most likely explanation for these orders is that the rate-determining step for this reaction is the 1-octene coordination step.

3.9 References

1 C. D. Frohling and C. W. Kohlpaintner, 'Applied Homogeneous Catalysis with Organometallic Compounds', ed. B. Cornils and W. A. Herrmann, Wiley-VCH, 1996.

2 'Rhodium Catalysed Hydroformylation', ed. P. W. N. M. v. Leeuwen and C. Claver, Kluwer Academic Publishers, 2000.

3 K. Weissermal and J. Arpe, 'Industrial Organic Chemistry', Verlag-Chemie, 1978.

4 J. L. Vidal and W. E. Walker, *J. Inorg. Chem*, 1981, **20**, 249.

5 L. H. Slaugh and R. D. Mullineaux, 1966.

6 L. H. Slaugh and R. D. Mullineaux, USA, 1966.

7 L. H. Slaugh and R. D. Mullineaux, *J. Organomet. Chem.*, 1968, **13**, 469.

8 E. Billig, A. G. Abatjoglou, and D. R. Bryant, 1986.

9 E. Billig, A. G. Abatjoglou, and D. R. Bryant, 1986.

10 J. F. Young, J. A. Osborn, F. H. Jardine, and G. Wilkinson, *Chem. Commun.*, 1965, 131.

11 Anon, in 'Celanse Corp. Annual Business Report', 1974.

12 R. S. Dickson, 'Homogeneous Catalysis with Compounds of Rhodium and Iridium', D. Reidel Publishing Company, 1985.

13 S. S. Bath and L. Vaska, *J. Am. Chem. Soc.*, 1963, **85**, 3500.

14 D. Evans, J. A. Osborn, and G. Wilkinson, *J. Chem. Soc. A*, 1969, 3133.

15 C. K. Brown and G. Wilkinson, *Tetrahedron Lett.*, 1969, 1725.

16 C. K. Brown and G. Wilkinson, *J. Chem. Soc. A*, 1970, 2753.

17 R. L. Pruett, *Adv. Organomet. Chem.*, 1979, **17**, 1.

18 B. Cornils, 'New Synthesis with Carbon Monoxide', ed. J. Falbe, Springer, 1980.

19 P. Pino, F. Piacenti, and M. Bianchi, 'Organic Synthesis via Metal Carbonyls', ed. I. Wender and P. Pino, Wiley, 1977.

20 P. W. N. M. v. Leeuwen and G. V. Koten, 'Catalysis, An Integrated Approach', ed. R. A. van Santen, P. W. N. M. v. Leeuwen, J. A. Moulijn, and B. A. Averill, Elsevier Science Publishers, 1999.

21 C. A. Tolman and J. W. Faller, 'Homogeneous Catalysis with Metal Phosphine Complexes', ed. L. H. Pignolet, Plenum Press, 1983.

22 'Homogeneous Catalysis', ed. Hegedus, W. Cotton, Masters, G. W. Parshall, and S. D. Ittel, Wiley.

23 A. M. Trzreciak and J. Ziolkowski, *J. Coord. Chem. Rev.*, 1999, **190**, 883.

24 P. Pino, *J. Organomet. Chem.*, 1980, **200**, 223.

25 P. W. N. M. v. Leeuwen and G. van Koten, *Studies Surf. Sci. Catal.*, 1993, **79**, 199.

26 A. van Rooy, J. N. H. de Bruijn, C. F. Roobeek, P. C. J. Kamer, and P. W. N. M. v. Leeuwen, *J. Organomet. Chem.*, 1996, **507**, 69.

27 D. Evans, G. Yagupsky, and G. Wilkinson, *J. Chem. Soc. A*, 1968, 2660.

28 P. W. N. M. v. Leeuwen, 'Rhodium Catalysed Hydroformylation', Kluwer Academic Publishers, 2000.

29 G. Gregorio, G. Montrasi, M. Tampieri, P. Cavalieri d'Oro, G. Pagani, and A. Andreeta, *Chim. Ind.*, 1980, **62**, 389.

30 P. Cavalieri d'Oro, L. Raimondi, G. Pagani, G. Montrasi, G. Gregorio, and A. Andreeta, *Chim. Ind.*, 1980, **62**, 572.

31 W. Strohmeier and M. Michel, *Z. Phys. Chem.*, 1981, **124**, 23.

32 R. M. Deshpande and R. V. Chaudhari, *Ind. Eng. Chem. Res.*, 1988, **27**, 1996.

[33] W. R. Moser, C. J. Papite, D. A. Brannon, R. A. Duwell, and S. J. Weininger, *J. Mol. Cat.*, 1987, **41**, 271.

Chapter 4: The Palladium Catalysed Methoxycarbonylation of Vinyl Acetate Monomer

4.1 Overview

Methoxycarbonylation can be used as a direct route for the synthesis is esters. These reactions are of potential industrial interest as a result of the low cost and ready availability of the required feed stocks coupled with the low generation of waste. [1]

The aim of the next set of reactions was to try to study the kinetics of a more complex system. The secondary aim was to develop a greater understanding of this reaction and to build on the findings concerning the methoxycarbonylation of vinyl acetate detailed by Rucklidge. [2]

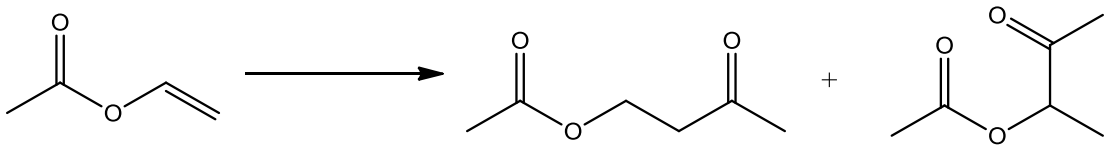

Figure 4.1: The methoxycarbonylation of vinyl acetate.

4.2 Palladium Catalysed Methoxycarbonylation

Initial studies suggested that palladium systems for the methoxycarbonylation of ethene show a selectivity dependence on the nature of the phosphine ligand used. It was thought that monodentate phosphines gave selectivity towards methyl propanoate whereas bidentate phosphines tended to show selectivity towards polyketone (co-polymer) formation. [3, 4]

The rationalisation behind the original idea was that monodentate phosphines can facilitate a *cis-trans* isomerisation during the reaction, once the system has formed an

acyl intermediate species. This was thought to occur in order to reduce steric interactions between the two bulky phosphine ligands and to inhibit the unfavourable coordination of the Pd-P bond *trans* to the Pd-C bond. This would ultimately result in the vacant site within the reaction forming *trans* to the acyl group, which inhibits any chain growth coming from migratory insertion. The addition of methanol then results in the methanolysis of the acyl intermediate resulting in the formation of methyl propanoate.

In the case of bidentate phosphines, the preference to *cis*-chelation results in the vacant site being *cis* coordinated and this allows for chain growth via the multiple migratory insertions of both CO and ethene into the coordinated acyl intermediate, which results in the production of polyketone. This however has been since shown not to hold true in studies by Cole-Hamilton *et al*.[5]

It has been shown that methoxycarbonylation can proceed via two possible reaction pathways. Firstly, the carbomethoxy mechanism, figure 4.2, which involves the initial formation of a methoxycarbonyl complex via migratory insertion of CO into a Pd-OMe bond, or by nucleophillic attack of the methanol on the coordinated CO. This is followed by the coordination and insertion of ethene and methanolysis to give the desired products. [6] Examples where this mechanism has been shown to operate include the carbonylation of propyne to form methylmethacrylate using Pd complexes of PPh_2py, [7] the copolymerisation of CO and ethene [4] and it is also possible in the formation of methylpropanoate (MeP) and methyl methacrylate (MMa) with rhodium complexes containing β-ketophosphine and related ligands. [8]

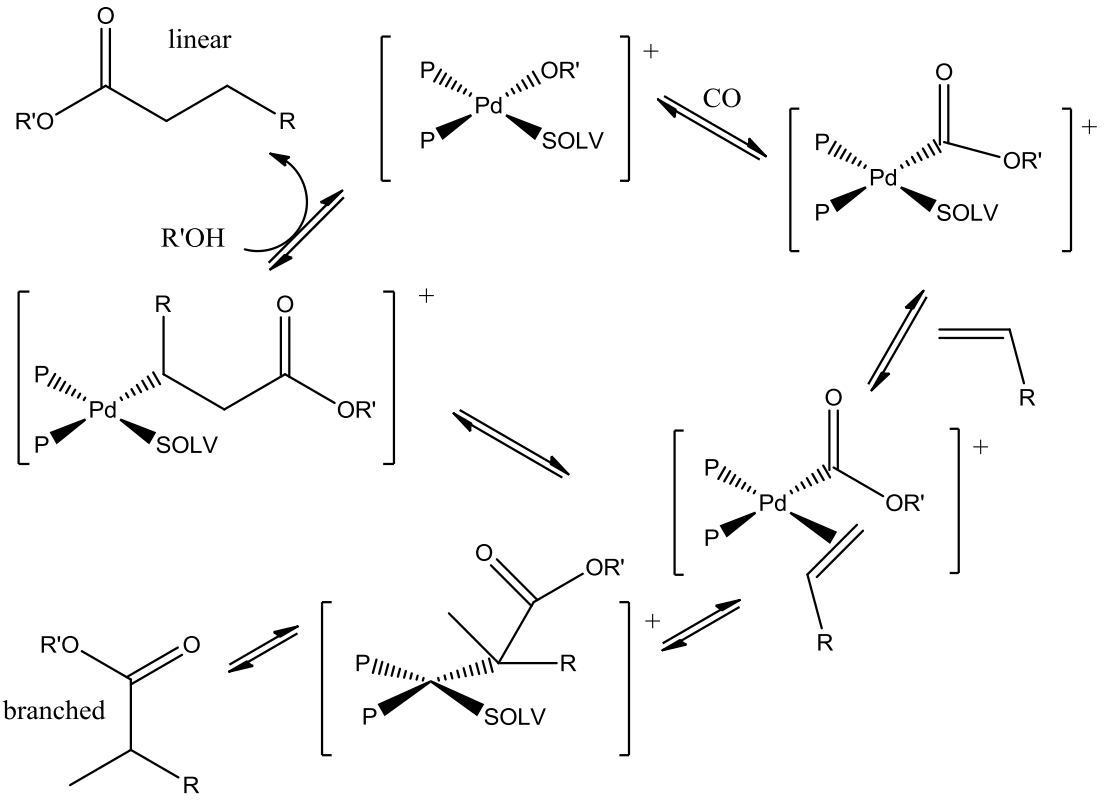

Figure 4.2: Carbomethoxy mechanism for the palladium catalysed alkoxycarbonylation of alkenes.

The other possible reaction pathway is the hydride mechanism, shown in figure 4.3, within which, a metal hydride complex is formed via the protonation of the palladium centre. The sequential coordination and insertion of ethene and then carbon monoxide leads to the formation of an acyl complex, which then undergoes nucleophilic attack by methanol to produce MeP.[6, 9, 10] This mechanism has been shown to occur in the copolymerisation of CO and ethene, the methoxycarbonylation of ethane with Pd/PPh_3 complexes [11] as well as in the synthesis of 3-pentanone using rhodium complexes of triethylphosphine. [12]

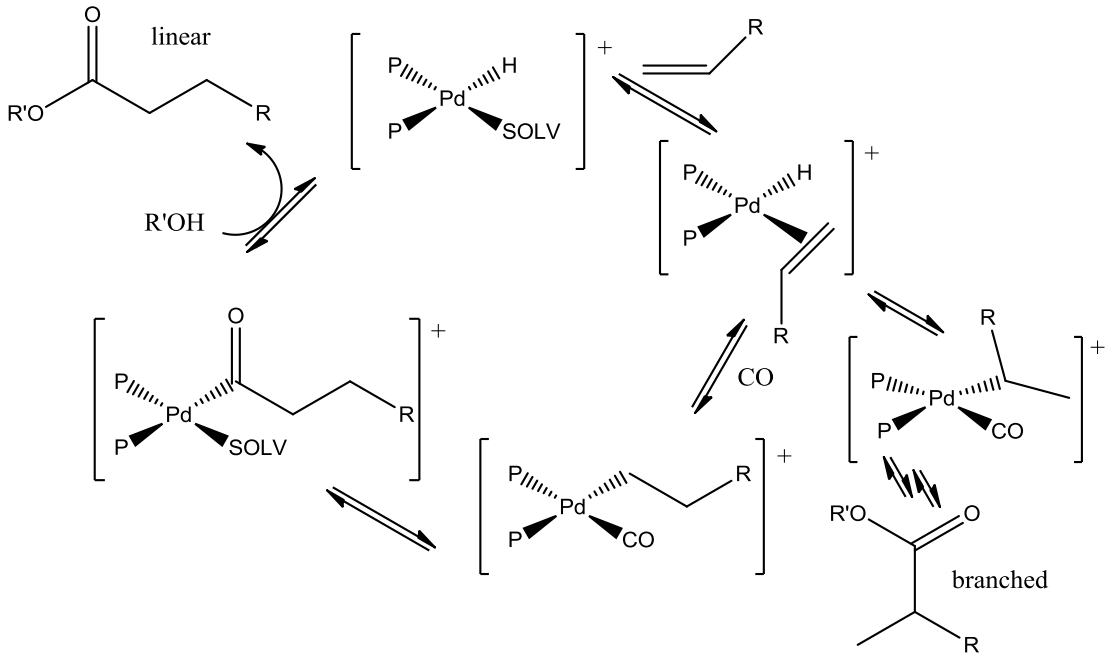

Figure 4.3: Hydride mechanism for the alkoxycarbonylation of alkenes.

4.3 BDTBPMB in Catalysis

A phosphine ligand which has been shown to be an effective ligand in carbonylation reactions is 1,2-bis(di-*tert*-butylphosphinomethyl)benzene, (BDTBPMB). This ligand shown in fig, 4.4 was first described by Shaw [13] and later explored by Spencer, [14] who incorporated this ligand in the first example of a stable *cis*-dihydride platinum (II) complex, although very little characterisation was carried out on this ligand prior to studies by Eastham.[6, 15]

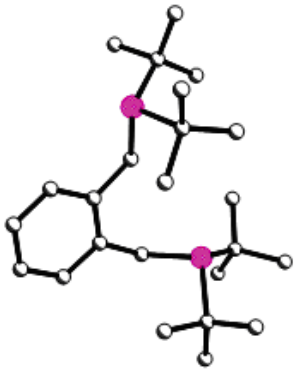

Figure 4.4: Crystal structure of BDTBPMB, phosphorus atoms are shown in pink

The ligand has a very large steric bulk owing to the presence of the benzene ring and four *tert*-butyl phosphine groups. The phenyl ring backbone increases the rigidity of the ligand which in turn increases its activity. The presence of 2 *tert*-butyl groups per phosphorus atom gives the ligand high electron donating properties.

The large bite angle of the ligand (103.9˚) and its ability to form a 7-membered ring allows for the easy chelation to a palladium or platinum centre, as the bulky *tert*-butyl groups are far enough apart, i.e. the P-metal-P bond angle can be large and the stereochemistry and rigidity of the $CH_2C_6H_4CH_2$ framework promotes chelation and inhibits bridging of two metal atoms, although such a bridging geometry has also been described on rhodium. [16]

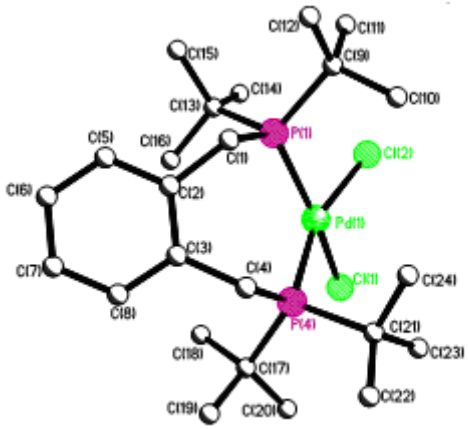

Figure 4.5: Crystal structure of BDTBPMB when coordinated to a palladium dichloride metal centre (shown in green). The distance between the 2 phosphorus atoms (shown in pink) is shown clearly allowing for the formation of the 7-membered chelate ring.

When BDTBPMB is used in catalysis, it has been shown to give exceptional activity and selectivity and stability towards methyl propanoate production. Eastham *et al* [6] reported that addition of BDTBPMB to $Pd_2(dba)_3$ results in the formation of $L_2Pd(dba)$. Adding methanesulfonic acid results in the formation of the hydride species which is the catalytically active species and gives methyl propanoate and a rate of 50,000 mol prod, per mole of catalyst per hour, selectivities of 99.98% at 80 ˚C and a combined CO and ethene pressure of 10 bar. This reaction is of particular importance as it is the first step of a two-stage process for producing methyl methacrylate from ethene.

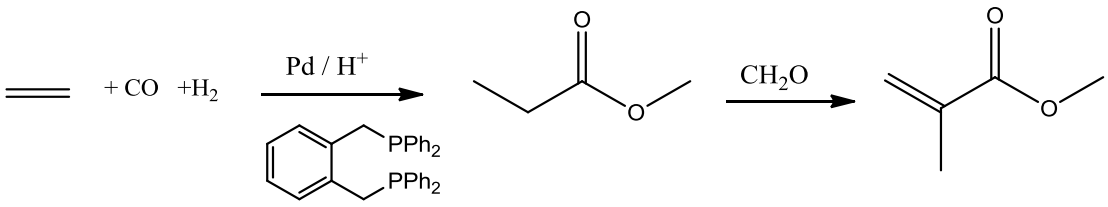

Figure: 4.6: The two stage formation of methyl methacrylate from ethene.

In comparison, other systems show lower activities and selectivities. Drent [17] shows that when 1,3-bis(ditertbutylphosphino)propane is used it gives turnover values of 15,000 and linear selectivities of 98%. [18] This study also shows that when PPh_3 systems are used in continuous flow, the turnovers are 1800 indicating very low catalyst stability.

Eastham [15] shows that altering the functionalisation of the 3-6 positions on the aryl bridge results in no noteworthy effect and this is thought to be as a result of little change in the distance between the bridging aryl groups and the palladium centre. Despite this, slight modifications of the substituents on the phosphorus groups show a marked decrease in activity. For example *tert*-butyl groups give a turnover frequency, (TOF) of 12000 h^{-1} with a selectivity of 99.9% whereas, isopropyl groups give activities of 200 h^{-1} and selectivities of 20% this shows a drop in activity by a factor of 60.[15] This study also determines that the parallel pocket angle as opposed to the bite angle [19] affects reaction activities and selectivities.

The full spectroscopic characterisation of all the intermediates in this reaction by Eastham and co-workers [6] indicates that this reaction proceeds via a hydride mechanism, where the palladium species is protonated to form the catalytically active palladium hydride. The carbonyl group is displaced by a *solvo* group, which in turn is displaced by ethene to produce an ethyl-palladium species. The tandem coordination and migratory insertion of the CO proceeds to form the acyl intermediate species before methanolysis produces methyl propanoate and regenerates the palladium hydride species. Deuterium labelling studies confirmed the reaction proceeds via the hydride mechanism. [20]

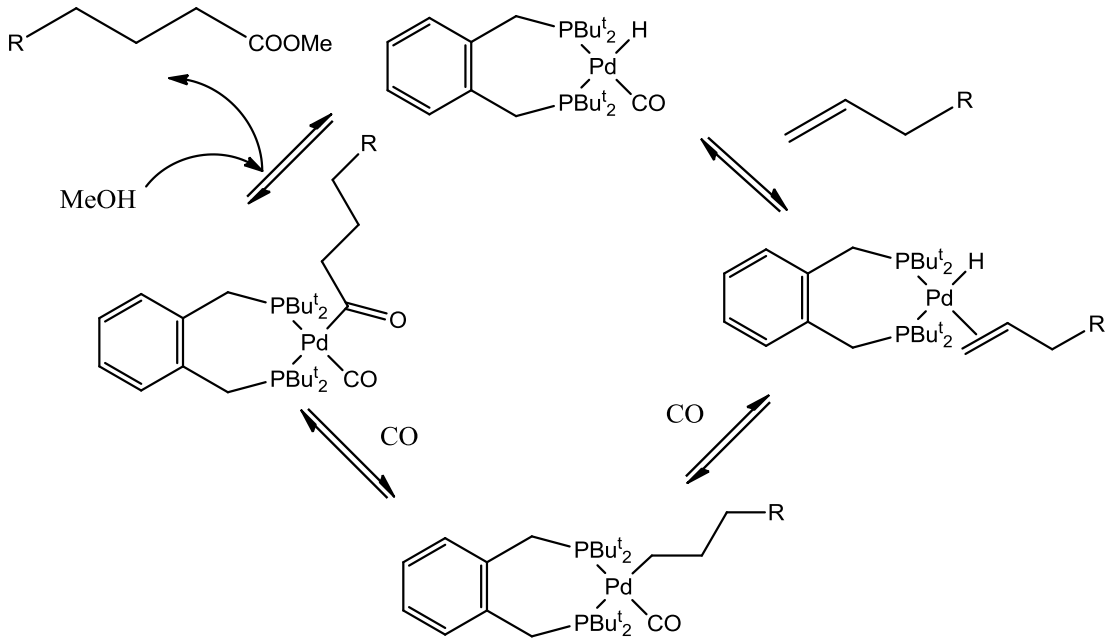

Figure 4.7: The palladium catalysed methoxycarbonylation of an alkene following the hydride mechanism.

The mechanistic pathway of this reaction was then compared with that of the platinum analogue. [21] The platinum analogue shows activities four orders of magnitude slower than its palladium counterpart. NMR studies were undertaken to ascertain if there was an inherent limitation associated with the 3rd row transition metals.

This was found not to be the case, whereas the Pt complex showed differences in behaviour – including the reversibility of the alkyl migration step, which can account for the low activity shown by Pt in this reaction – both the Pt and Pd interact with ethene to create a β-agostic interaction with the metal centre. The Pt complex forms a stable carbonyl-ethyl complex and the products from the migratory insertion step are not observed in NMR spectra at lower temperatures.

In the presence of excess CO, the Pt reaction proceeds via an ethyl intermediate to the carbonyl-ethyl complex and then to the carbonyl-acyl complex before reproducing the hydride complex. When the reaction contains limited CO, the hydride complex is a reaction sink that can be formed preferentially via the reversible coordination of the ethene to reproduce the hydride complex. (hydride↔ethyl↔acyl)

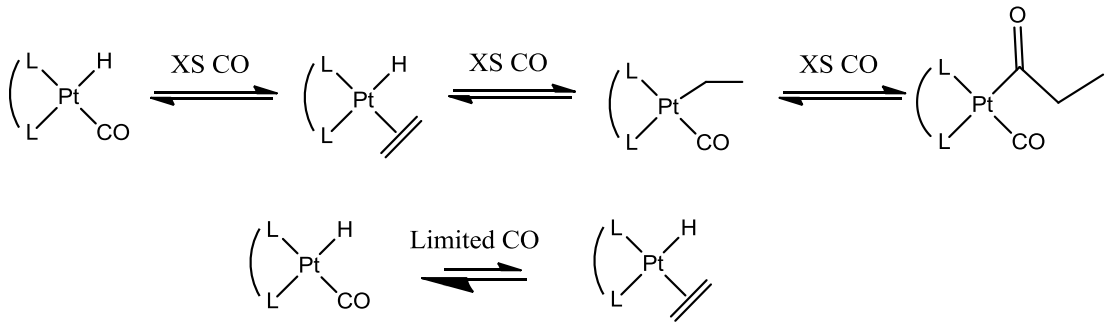

Figure 4.8: The reaction pathways with and without excess CO for the Pt catalysed methoxycarbonylation of ethene.

The Pt complex's affinity for CO results in the *solvo* complexes for the Pd mechanism being replaced by the carbonyl adducts for the Pt mechanism. This results in each of the steps within the Pt cycle being reversible. The carbonyl-hydride complex formed via the protonation of the initial complex formed *in-situ* is much less reactive to ethene than the solvated-hydride species formed by the Pd analogue, therefore it is postulated that this step is rate determining for the Pt mechanism. Although methanolysis is also slow.[22]

4.4 Cobalt Catalysed Methoxycarbonylation of Octene

The methoxycarbonylation of alkenes has previously been of particular interest as a possible alternative to hydroformylations.[23] These reactions have been shown to be successful using both cobalt and palladium catalysts. The main use of the products formed from these reactions include detergent range alcohols and plasticisers from higher C_n alkenes [24, 25] Another common use of the methoxycarbonylation of alkenes is the production adipate esters for use in the production of nylon 6, 6' from buta-1,3-diene. This reaction has been developed on a pilot plant scale by BASF and uses a two-step pyridine/Co-catalysed double methoxycarbonylation.[26] There is some evidence to show that the methoxycarbonylation of buta-1,3-diene proceeds via the methoxycarbonyl mechanism. [27] Cobalt catalysed carbonylation has been studied as a potential alternative to hydroformylations and Ugo *et al* [23] and the references therein illustrate this in greater detail.

In the case of the cobalt catalysed methoxycarbonylation of 1-octene, Jacob *et al* [28] reported the promotional effects of water and nitrogen-containing bases on this reaction. $[Co_4(CO)_{12}]$ was used as the catalyst precursor owing to its increased stability over the $[Co_2(CO)_8]$ variant as high CO pressures allow for the ready conversion to the latter complex. The reactions were performed at 140 bar of CO and at 160 ˚C.

It was shown that nitrogen-containing bases contradict the usual inverse activity/selectivity relationships of homogeneously catalysed reactions and act as catalytic promoters within Co catalysed methoxycarbonylation. [28] These additives have been previously shown to increase both activity and selectivity towards linear products. [25, 29] It has been claimed that nitrogen containing bases act as "second level" rate accelerators, as they assist in the direct methanolysis of the acylcobalt carbonyl intermediate, shown in reaction scheme 2. [28]

$$[RCH_2CH_2COCo(CO)_4]$$

$$\xrightarrow{py} [RCH_2CH_2Copy]^+ [Co(CO)_4]^- \qquad (3.1)$$

$$\xrightarrow{MeOH} RCH_2CH_2CO_2Me + [pyH]^+ [Co(CO)_4]^-$$

The same study also shows that low concentrations of water (0.1-0.5 ml) can have an effect on catalytic activity for this system, increasing the conversion from 34% - 83% over a 90 min reaction. Water is thought to enhance the $HCo(CO)_4$ concentrations required for the hydride mechanistic pathway to proceed. [28]

4.5 Palladium Catalysed Methoxycarbonylation of Octene

Whereas the homogeneous hydroformylation of alkenes to produce terminal oxygenates is of great importance industrially in the production of plasticisers, soaps and detergents. [30, 31] It has been found that α.ω-dicarboxylic acids and their esters are important chemicals in the synthesis of polyesters and polyamides such as nylon 6.6. [32] Industrially these compounds are made by the oxidation of cyclic alkanes. The

carbonylation of alkenes to carboxylic acid esters is also important as it allows for the production of ethoxylates. It can also be used to produce alcohols via hydrogenation of the carboxylic acid esters. These are particularly key reactions when the desired terminal products can be produced from internal alkenes.

Bis-adamantyl derived phosphines have been shown to carbonylate internal alkenes with an 80% linear selectivity.[33] Whereas 1,2-bis(di-*tert*-butylphosphino)propane shows a very low activity for this reaction, [33] palladium complexes containing 1,2-bis(di-*tert*-butylphosphinomethyl)benzene have been shown to give linear selectivities up to 97% for 1-octene at 30 bar and 100 ˚C [34] and 2-butene gave a 97% linear selectivity towards methyl pentanoate at 65 bar and 100 ˚C. [35] Thereafter it was reported that this same system gives linear selectivities up to >99.9% under milder conditions than previously reported for the methoxycarbonylation of both terminal and internal alkenes.[10]

Preliminary mechanistic studies have shown that there are two pathways from 1-octene to methyl nonanoate; initially the product is formed via the direct methoxycarbonylation of 1-octene, but alkene isomerisation competes with this carbonylation so much of the product is formed from the internal alkenes by tandem isomerisation carbonylation. It appears that carbonylation can only occur on the terminal atom, despite the fact that the terminal alkene is the least thermodynamically stable. Gas uptake plots [10] show two first order regimes present within the reaction (Figure 4.9), corresponding to the two stages within the reaction described previously. It can be noted that the pseudo first order rate constant for the second step is ~ 44% of that for the first step despite the presence of only ~ 5% of 1-octene within the system once the isomerisation equilibrium is reached.

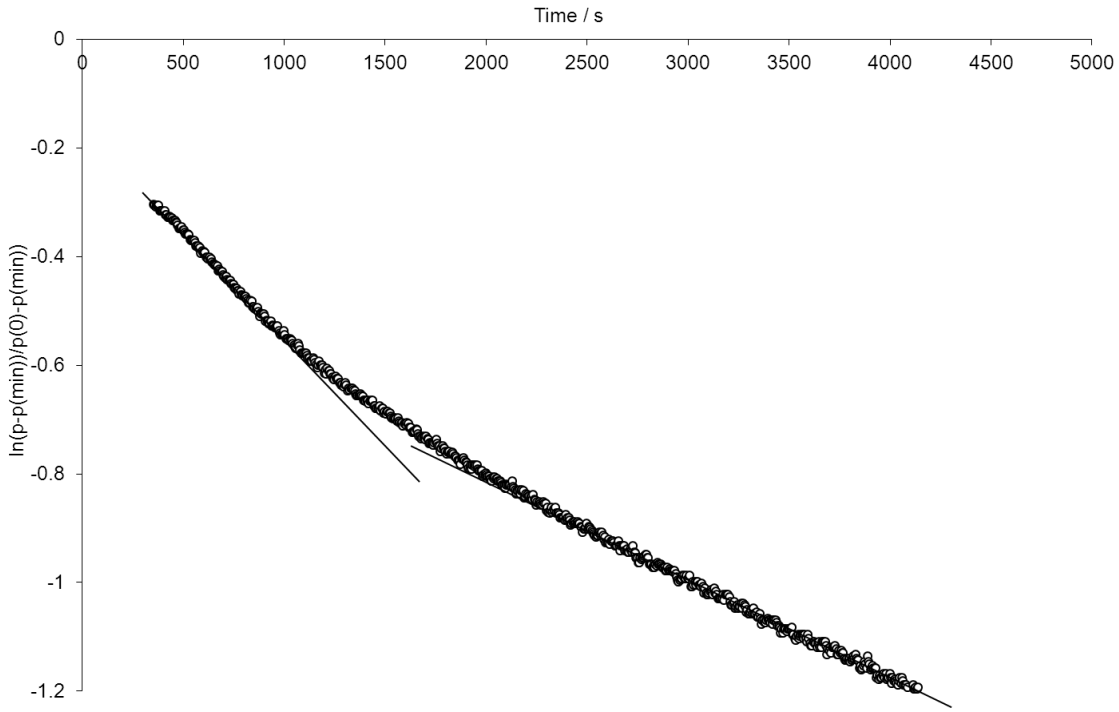

Figure 4.9: The natural log of the pressure drop as a function of time showing that the system has biphasic kinetics. [10]

Deuterium labelling studies have shown that the product distribution can account for the biphasic kinetics present within the reaction. Whereas all D_0-D_{15} isomers are formed during methoxycarbonylation of 1- octene in CH_3OD, D_1 methyl nonanoate is present in much larger quantities than expected for a simple distribution pattern (Figure 4.10). This can be rationalised by the direct carbonylation of the 1-octene resulting in the D_1-methyl nonanoate being produced, while the tandem reactions result in the presence of the other D substituted products.

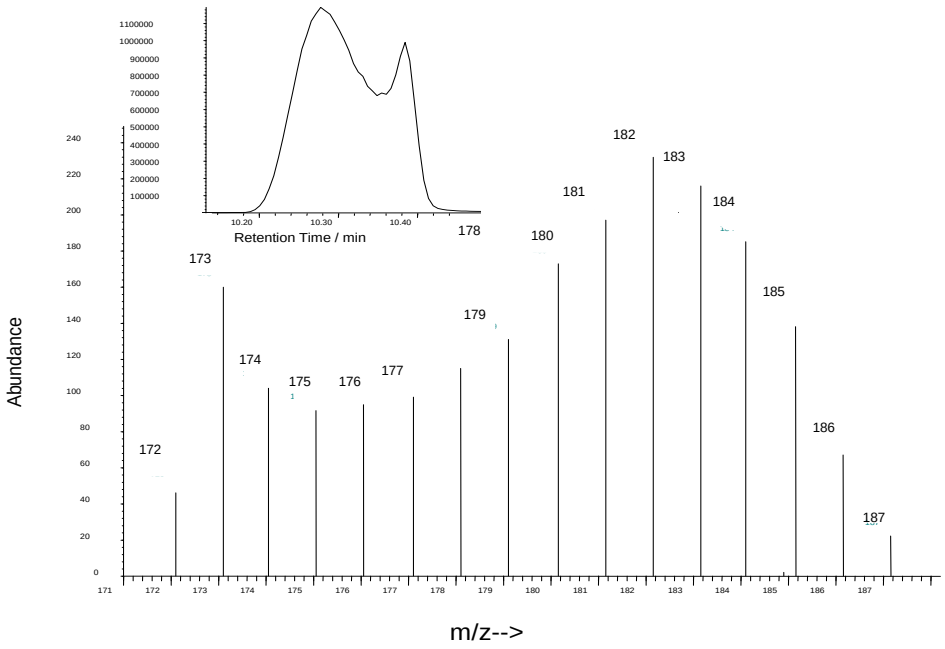

Figure 4.10: The deuterium labelling study of the methoxycarbonylation of 1-octene which shows the presence of biphasic kinetics. [10]

When the same reaction is carried out in a CH_3OD: toluene ratio of 1:4, the same products appear but the D_1 methyl nonanoate no longer predominates. This observation suggests that the methanolysis reaction must be slowed down relative to isomerisation, which, in turn, implies that the methanolysis of the acyl complex – which is formed via the migratory insertion of CO to the coordinated alkene – is the rate determining step within the reaction. The presence of D_0 methyl nonanoate implies that the hydride mechanism described previously [20] is operating within this system since the carbomethoxy route cannot form this product if only d^i methanol is present.

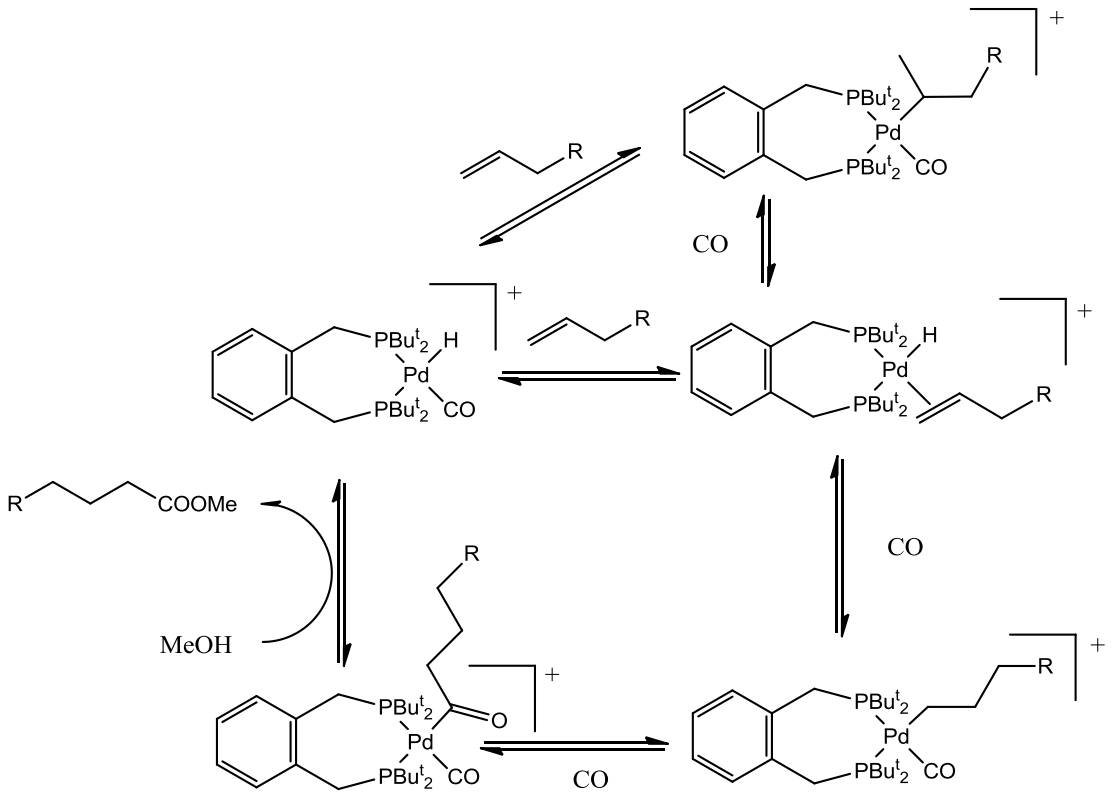

Figure 4.11: Proposed reaction mechanism for the methoxycarbonylation of 1-octene. [10]

4.6 Methoxycarbonylation of Vinyl Acetate

Vinyl acetate is produced from ethene and acetic acid via the Wacker process. It was first produced homogeneously from ethene and acetic acid using mercury sulphate catalysts. By 1965 it was formed exclusively in the gas phase over zinc salts of the corresponding carboxylic acids (i.e. zinc acetate) over active charcoal. The production of esters and polymers from lactic acid are of a great importance within the solvents and plastics industry. This is particularly interesting from a petrochemical perspective as lactic acid can, in principle, be synthesised via the methoxycarbonylation of vinyl acetate monomer (VAM) followed by hydrolysis of the methyl ester.

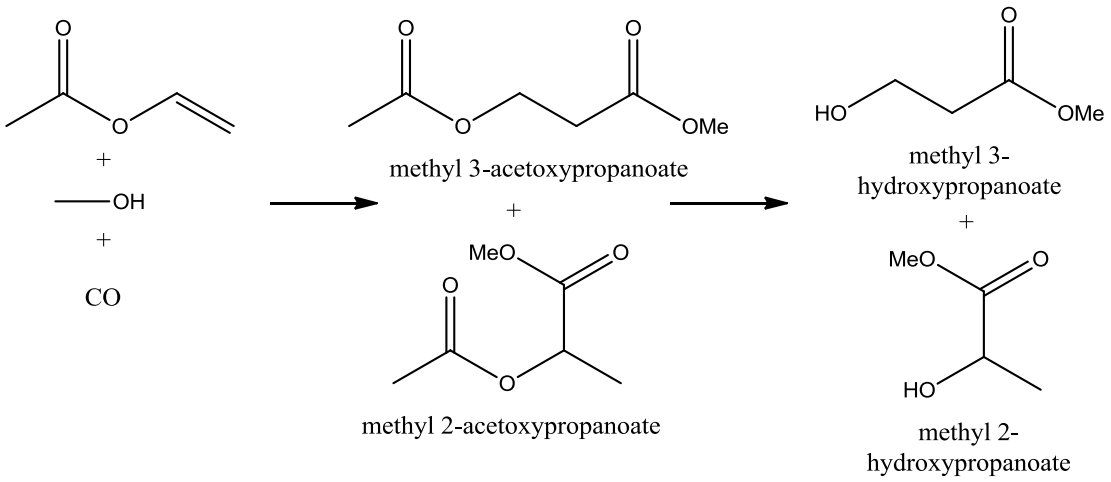

Figure 4.12: Alkoxycarbonylation of vinyl acetate to form the acetoxypropanoate intermediate species which can them be converted to the hydroxypropanoates.

The carbonylation can occur at either the site alpha or beta to the acetoxy group which would result in the production of the branched or linear isomers respectively. These intermediates can then undergo removal of the acetoxy groups to produce hydroxypropanoic acids.

It is widely known that as a result of political and consumer pressures, industry is looking for means to manufacture products and undertake processes which are environmentally friendly and where possible non-toxic. It is also desirable to produce materials, which can effectively decompose into non-toxic components, owing to issues with landfill and the increasing desire for biodegradable waste. This is particularly crucial when it comes to the production of disposable products such as fast-food boxes and carrier bags. It is thought that using lactate esters is a viable means to produce these as they can be polymerised to form polylactic acid, (PLA) and when the monomers of these products are predominantly in the S form, the resulting polymer shows similar properties to polystyrene and polyethylene whilst also being biodegradable.[2, 36, 37]

Previous studies have shown that lactic acid, the precursor for polylactic acid, can be produced via the fermentation of glucose from corn or starch.[38] These acids can then undergo a reaction to produce the cyclic dimer species known as lactide. These lactide can be purified by vacuum distillation, before being heated to allow for ring opening

polymerisation, usually in the presence of an initiator and a catalyst. PLA can be used in many applications, which have previously been covered using traditional hydrocarbon based polymers.

Ethyl lactate has been identified as a green solvent, and is so benign that the FDA approved its use in food products many years ago. Furthermore, this effective alternative solvent is non-toxic, biodegradable and has a low volatility. Despite these qualities the widespread use of ethyl lactate has been hindered by cost (~$1.60-$2.00 lb^{-1}).[2]

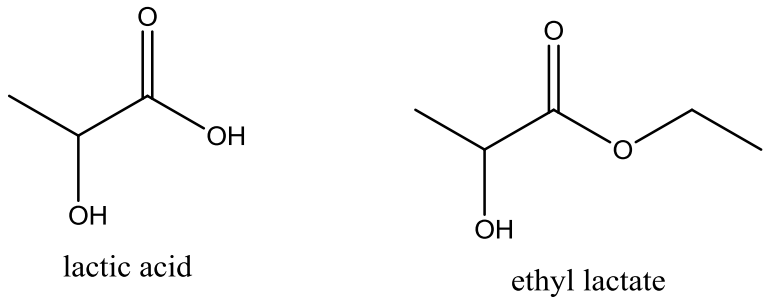

Figure 4.13: Lactic acid monomer and ethyl lactate.

In recent years, there have been numerous studies which detail the formation of acid and ester oxygenates from unsaturated molecules.[10, 20, 39] The majority of these studies involve palladium metal centres and unsaturated substrates such as ethene and styrene. These substrates are of particular importance as a result of the demand for methyl propanoate, which is a key intermediate in the formation of methyl methacrylate. Furthermore the methoxycarbonylation of styrene allows for the formation of intermediates, which are important in the synthesis of non-steroidal anti-inflammatory drugs such as ibuprofen. [40-42]

4.7 Palladium Catalysed Methoxycarbonylation of Vinyl Acetate

Previous studies by Drent [43] have shown that the methoxycarbonylation of vinyl acetate using palladium acetate and 1,3-bis(di-*tert*-butylphosphino)propane can be achieved at 75˚C and 40 bar, CO pressure. This reaction was shown to produce 200 moles of ester per gram of palladium per hour and have a branched to linear ratio of 2:1.

Further investigations by Kudo,[44] also showed that $PdCl_2/PPh_3$ with a catalytic amount of 2,6-lutidine methoxycarbonylates vinyl acetate at 120 ˚C and 200 bar CO pressure. In this reaction there are high quantities of methyl acetate formed as a result of the competing methanolysis of vinyl acetate. The study reported rate data under a variety of different conditions and in turn proposed the mechanism for the methoxycarbonylation of vinyl acetate is as shown in figure 4.14.

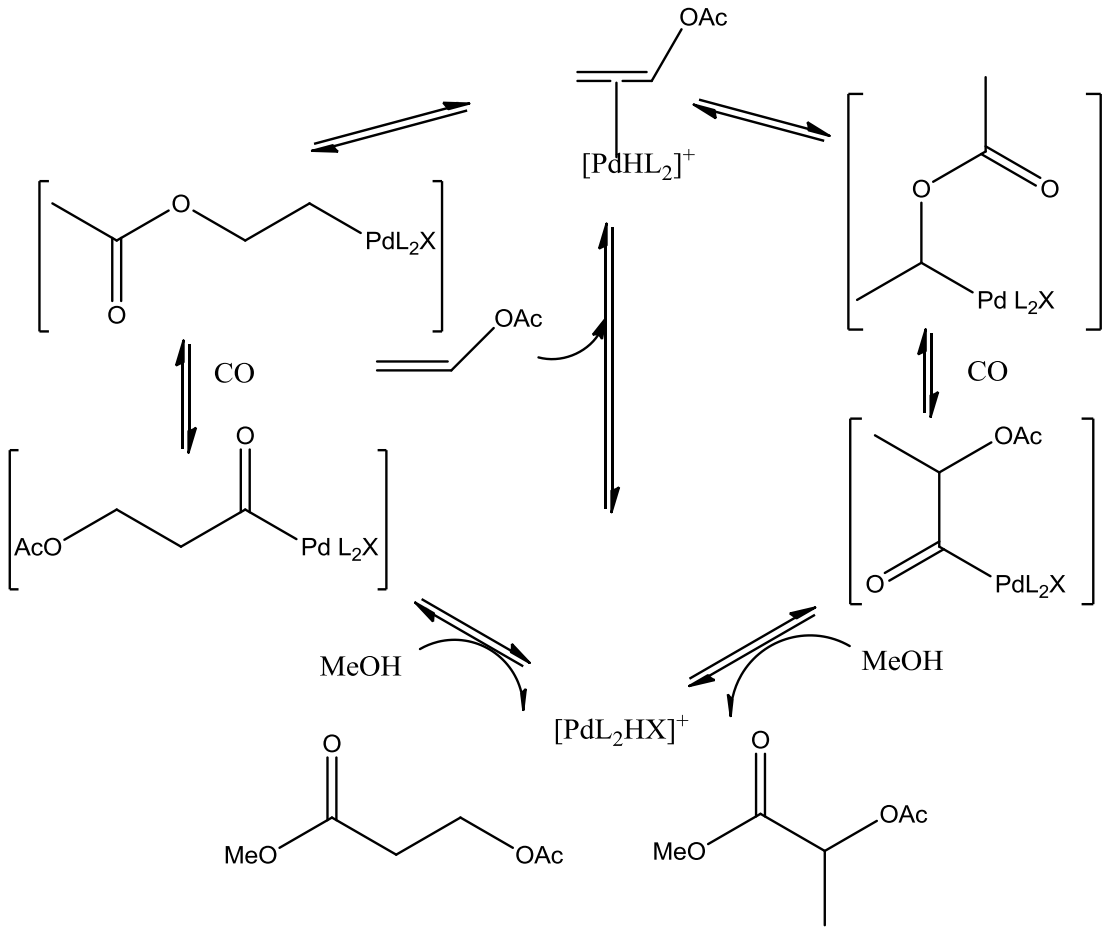

Figure 4.14: Proposed mechanism for the methoxycarbonylation of vinyl acetate. X = solvent, CO, Vinyl acetate of MeOH.

4.8 BDTBPMB in the Methoxycarbonylation of Vinyl Acetate

Rucklidge *et al* reported [36] and patented [45] the first examples of the methoxycarbonylation of vinyl acetate with palladium complexes of BDTBPMB and showed that this catalyst system produced the desired ester products. Tanaka and co-workers [39] published similar work that used both free and polymer bound methanesulphonic acid to form the catalytically active species and found that, although the polymer bound acid increased the overall rate of reaction, it decreased the b:l ratio.

Rucklidge *et al.* [46] showed that the methoxycarbonylation of vinyl acetate can be catalysed under mild conditions and that the competing methanolysis side reaction can be completely avoided. Studying the effects of both acids and bases on the reaction, established the primary causes of the methanolysis. As vinyl acetate is an ester it is likely to be susceptible to nucleophillic attack from either a base or an anion. Furthermore with methanol, it is possible to cause a transesterification reaction to form methyl acetate and vinyl alcohol. This vinyl alcohol can tautomerise to form ethanal, which can then be attacked by methanol to give 1,1-dimethoxyethane, making, the overall reaction irreversible. This is shown in figure 4.15.

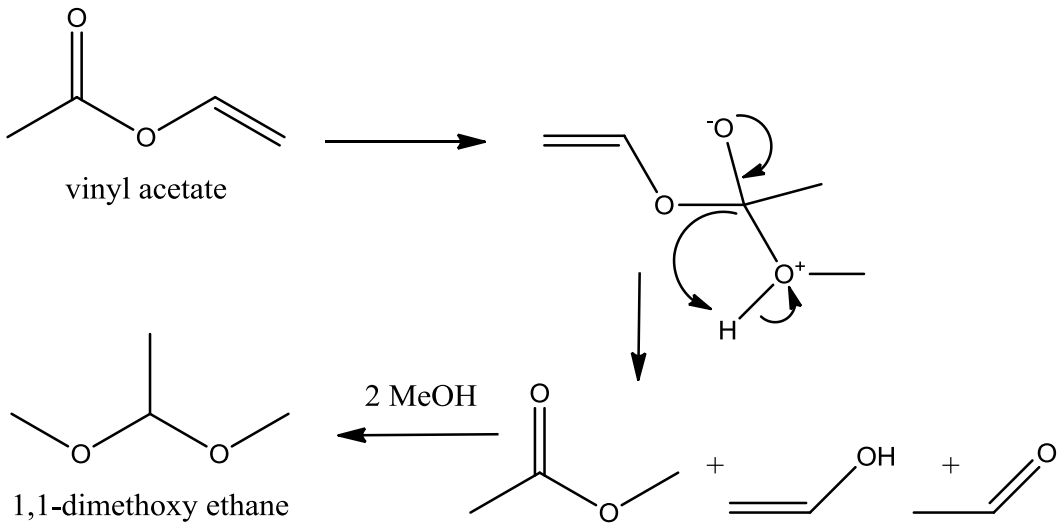

Figure 4.15: MeOH attack of vinyl acetate to produce MeOAc and 1,1-dimethoxyethane. [2]

It was thought that the presence of any acid, base or phosphine could catalyse the attack by methanol so studies were carried out to identify which components enhanced the side reaction.

4.9 Acid Base Causing Reaction

The studies showed that the methanolysis was acid catalysed and that when the phosphine is present in sufficiently high concentrations (in excess over the acid, the degradation is essentially eliminated. It was also found that when the methyl 2-

acetoxy propanoate was left in the presence of acid at room temperatures, it too reacted to produce methyl acetate. When the reaction was run at 80˚C and 30 bar of CO pressure a quantitative yield and 100 % ester selectivity was observed. The b:l ratio was found to be 1.2:1. The best b:l reported was 3.6:1 when the reaction was run at 25 ˚ C and 30 bar of CO pressure, but this only resulted in a 35 % conversion after 3 hours. This was still higher than all the other ligands tested in this study and amongst the best results reported for vinyl acetate carbonylation.

4.10 Varying Components Within the Reaction

4.10.1 Ligand Concentration

The methoxycarbonylation of vinyl acetate was carried out as previously detailed by Rucklidge. [2] In order to determine the effect of each of the components within the reaction, the ligand concentration, temperature, CO pressure and acid concentration were varied, in order to establish the optimum conditions for the reaction. In the case of the ligand concentration the ligand to acid ratio was maintained at 1:1 to ensure there was no free acid present.

4.10.2 Temperature

The reactions were carried out at 25, 40, 60, 80 and 100 degrees Celsius as previously reported by Rucklidge. [2] All reactions showed 100% selectivity towards ester formation, and as expected the conversion of vinyl acetate increased with temperature. It was shown that the branched to linear ratio improved when the temperature was lowered which suggests that the pathway towards the branched product has a lower activation energy than that of the linear product. This shows overall that running the reaction at lower temperatures, despite increasing the reaction time is advantageous as it allows for greater selectivity towards the branched product.

4.10.3 CO Pressure

When the CO pressure was varied it was found that increasing the pressure resulted in a decrease in the branched to linear ratio. The preference towards the branched product is thought to be as a result of the carbonyl oxygen in the palladium acyl species chelating to form a ring. (Figure 4.16) If the branched isomer is formed, the resulting ring would be 5-membered, whereas if the linear product was formed a 6-membered ring would be formed. The increased preference towards branched regioselectivity is as a result of the 5-membered ring being more stable. For this chelate ring to form there has to be a vacant site for coordination of the carbonyl oxygen atom. As the pressure increases, there would be a greater competition between CO coordination and chelate ring formation this is reflected in the decrease in the branched to linear ratios at higher CO pressures.

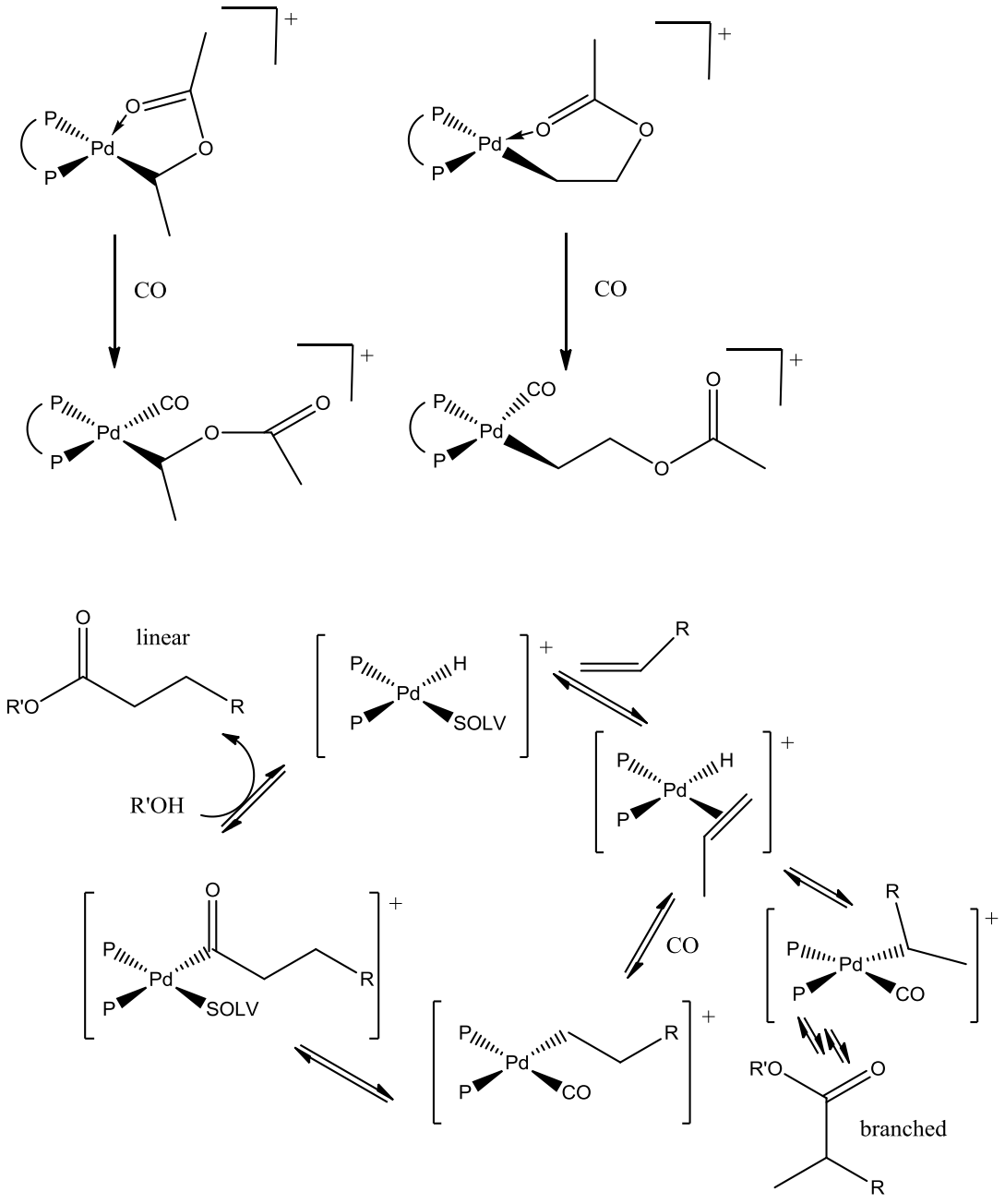

Figure 4.16: Disruption of the stabilising chelate as a result of increased CO pressure.

4.10.4 Effect of Changing the Acid Concentration

As it has been shown that the methanolysis to form methyl acetate is acid catalysed, the effect of acid concentration was studied in greater detail. It was shown that the maximum selectivity to ester products was obtained when the Pd:MSA ratio was 1:10 (Pd:P = 1:5) and thereafter the selectivity decreased rapidly. This reduction was brought about by competing methanolysis forming methyl acetate, which becomes rapid once free acid is present in the system. It was also shown that an increase in the [MSA] resulted in an increase in the b:l ratio.

4.11 Results

The aim of these experiments was to determine the orders with respect to the individual reacting components of the reaction. Thereafter the orders were to be used to help establish the potential rate determining steps within the reaction mechanism. The constant pressure experiments allowed for pseudo zero order conditions in CO. These experiments were initially run in high methanol to create pseudo zero order conditions in methanol. This would allow for the determination of the order with respect to the vinyl acetate concentration. The methanol concentration was then lowered in increments to establish the order with respect to methanol for this reaction. Once the order with respect to vinyl acetate and methanol were discovered, the reaction was then run whilst varying the partial pressure of CO to determine the order with respect to CO.

4.11.1 Initial Experiments

The methoxycarbonylation of vinyl acetate (1 ml, 0.01085 mol) was carried out at 80°C and 30 bar CO pressure in a constant pressure system. Maintaining the system at constant pressure and having methanol present in a high enough excess to impose pseudo zero order conditions allowed for the determination of the order with respect to vinyl acetate. The resulting gas uptake plot is shown in figure 4.17

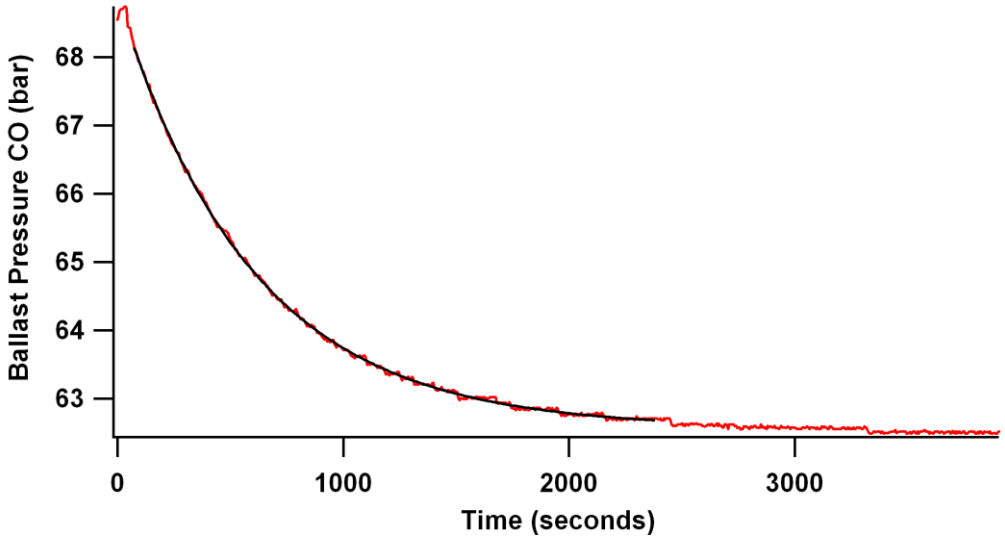

Figure 4.17: The gas uptake plot for the methoxycarbonylation of vinyl acetate under constant pressure conditions.

This graph, shown with an exponential curve fit, was then presented as a logarithmic plot of the CO pressure consumption as a function of time. To confirm the order with respect to vinyl acetate was 1.

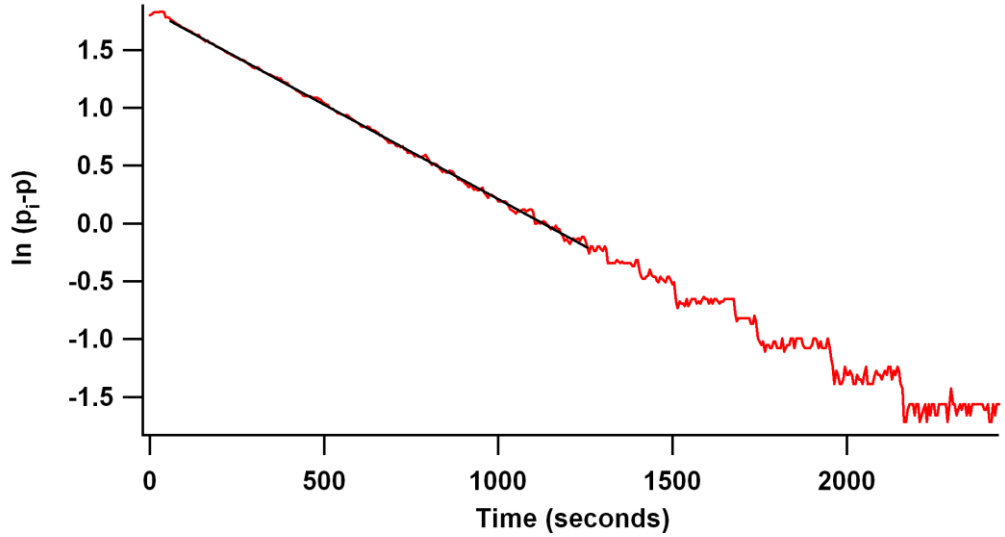

Figure 4.18: Plot of the natural log of the residual gas as a function of time. The graph is fitted with a linear fit to show the reaction is first order in vinyl acetate.

To confirm that the vinyl acetate showed first order behaviour, we ran another three experiments at constant pressure and the vinyl acetate concentration was varied

between 0.0054 and 0.0217 moles, (0.5 and 2 ml). The volume was kept constant by the addition of toluene to make a total of 2 ml. These reactions were again run at 80˚C and 30 bar of CO pressures with 10ml (0.1234 moles) of methanol. Table 4.1 shows the results from these experiments and figure 4.16 gives the graphical representation of these. The double logarithmic plot of these values shows that the reactions are approximately first order in vinyl acetate concentration measuring at 0.85.

Vinyl Acetate (ml)	Toluene (ml)	Initial Rate (mol/s)
0.6	1.4	-0.0079
1	1	-0.0114
1.5	0.5	-0.0166
2	0	-0.0223

Table 4.1: The variation in vinyl acetate concentration to determine the order with respect to vinyl acetate for the methoxycarbonylation of vinyl acetate.

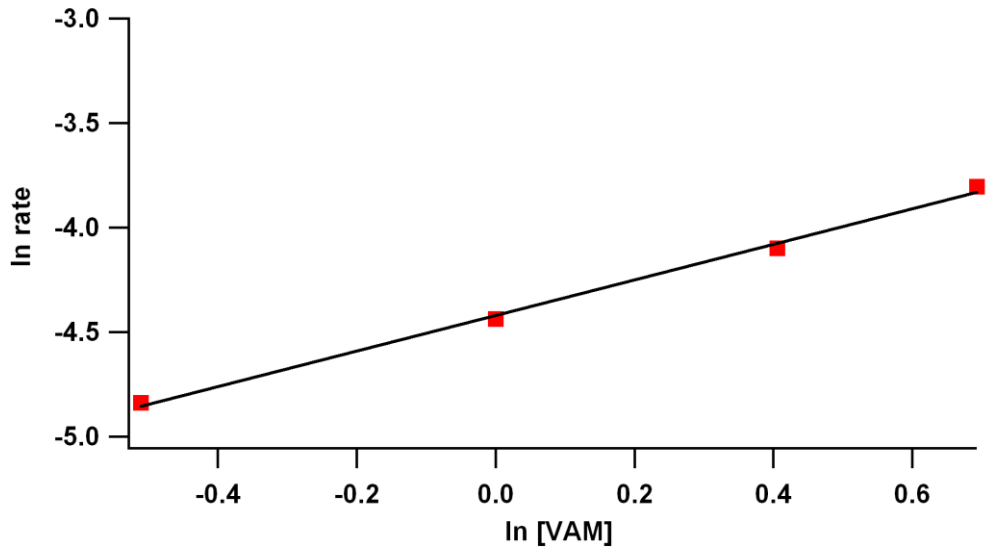

Figure 4.19: Double log plot of the change in initial rate as a function of vinyl acetate concentration.

To further confirm that the reaction was first order in vinyl acetate, the rate of reaction was plotted against the vinyl acetate concentration for the reactions run in 10 ml and 2

ml of methanol. The first was checked as it demonstrates pseudo zero order kinetics in methanol and as such only the vinyl acetate concentration was changing. In the reaction containing only 2 ml of methanol, both the vinyl acetate and methanol concentrations are changing simultaneously. This was added to determine if the order in vinyl acetate changes when the methanol concentration is lowered.

It was found that the reaction is first order in vinyl acetate for both reactions and these plots are shown in figure 4.20 and figure 4.21 respectively.

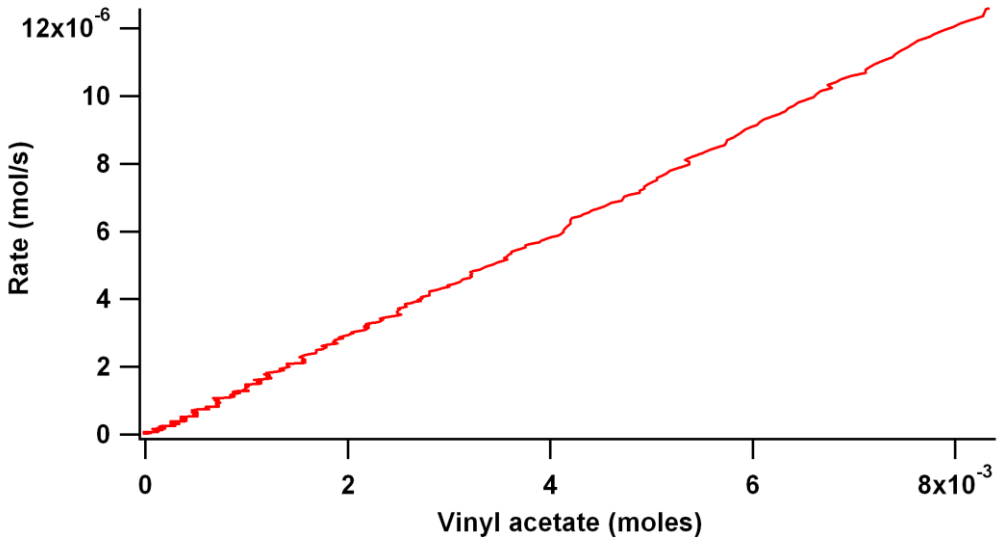

Figure 4.20: The rate as a function of vinyl acetate concentration for the methoxycarbonylation of vinyl acetate in 10 ml of methanol.

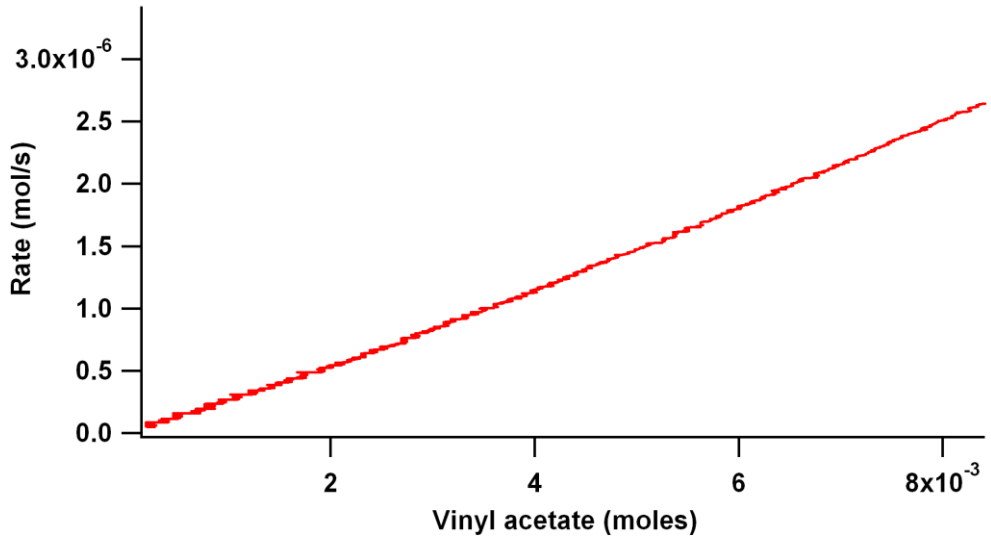

Figure 4.21: The rate as a function of vinyl acetate concentration for the methoxycarbonylation of vinyl acetate in 2 ml of methanol.

4.11.2 Order in Methanol

In order to establish the order with respect to methanol, a series of experiments was run where the other reacting components were kept constant and the methanol concentration was varied between 2 ml and 10 ml. In order to ensure that the reactions were run at a constant volume, the methanol was made up to a maximum of 10ml using toluene. The resulting initial rate constants for these reactions are shown in table 4.2 and shown graphically in figure 4.22.

Methanol (ml)	Toluene (ml)	Initial Rate (mol/s)
10	0	0.0114
8	2	0.00668
6	4	0.00446
4	6	0.00284
2	8	0.00177

Table 4.2: The variation in methanol concentration to determine the order with respect to methanol for the methoxycarbonylation of vinyl acetate.

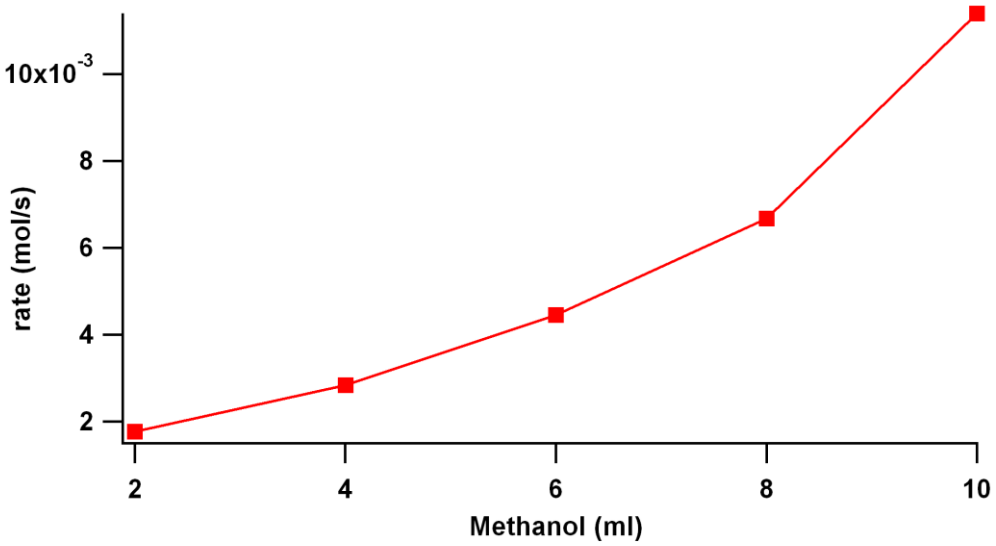

Figure 4.22: Graph showing the change in initial rate as a function of the methanol concentration within the reaction.

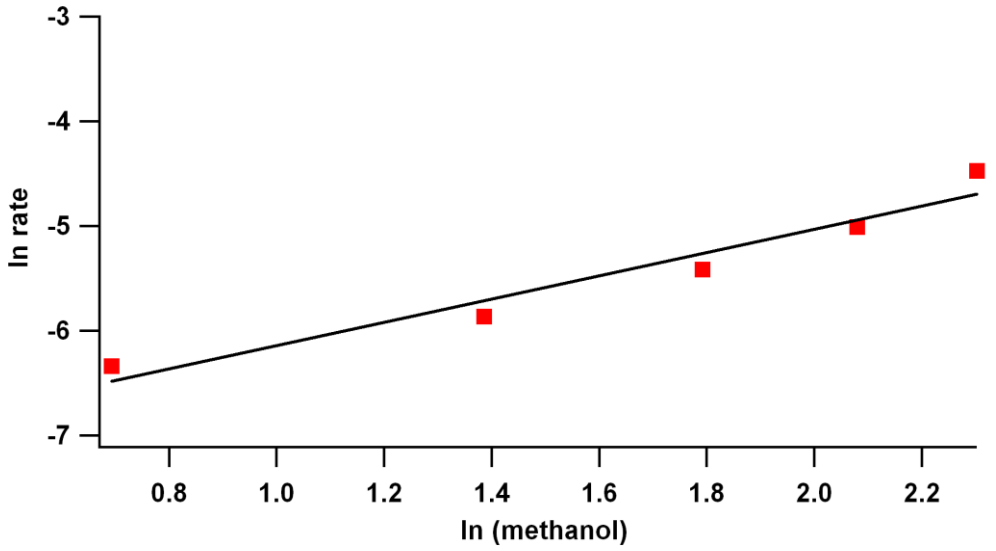

Figure 4.23: Shows the double log plot of the initial rate of reaction against the methanol concentration in the reaction.

The double logarithmic plot of the initial rate against the methanol concentration was taken in order to determine the order with respect to methanol concentration. This plot is shown in figure 4.23. The reaction was found to have an order of 1.1 with respect to

methanol concentration. However, the fit does appear curved, suggesting that the order potentially changes at different methanol concentrations. To confirm this theory, the rate was divided by the vinyl acetate concentration and plotted as a function of the methanol concentration for the reactions containing 10 ml and 2 ml of methanol respectively. The reaction with 10 ml of methanol, figure 4.24, was shown to have pseudo zero order conditions in methanol.

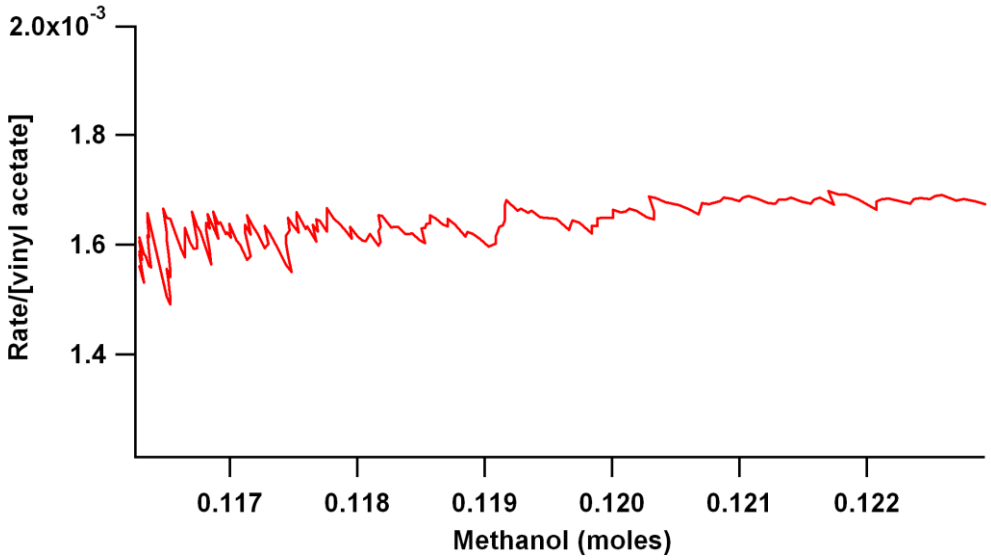

Figure 4.24: The rate divided by the vinyl acetate concentration as a function of methanol concentration for the methoxycarbonylation of vinyl acetate in 10 ml of methanol.

It was found however that when the reaction was run under lower methanol concentrations the reaction, shown in figure 4.25, was no longer observed to be zero order with respect to methanol.

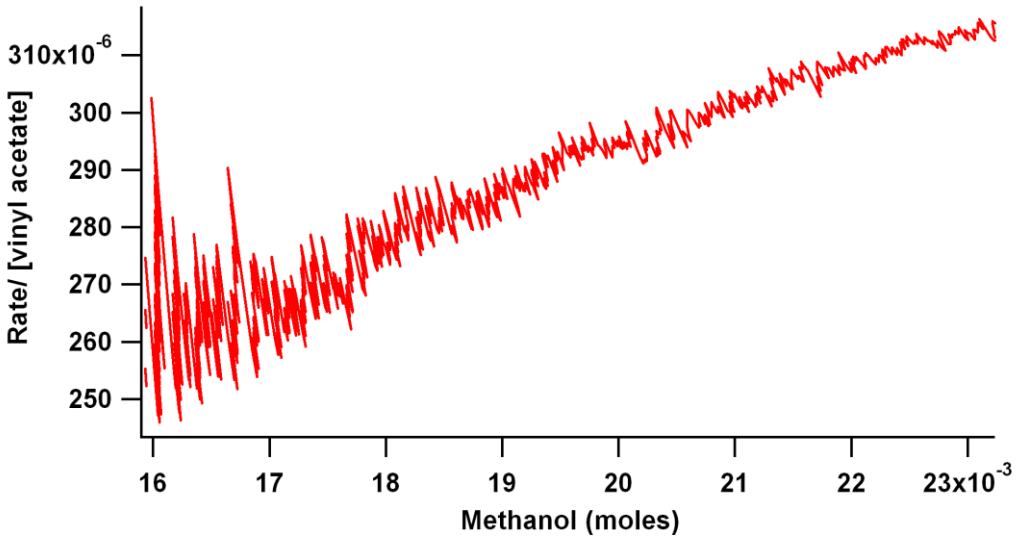

Figure 4.25: The rate divided by the vinyl acetate concentration as a function of methanol concentration for the methoxycarbonylation of vinyl acetate in 2 ml of methanol.

It can be seen in figure 4.25 that the order tends toward first order at lower methanol concentrations. This correlates with the observed positive order dependence in methanol as seen by the initial rate measurements.

4.11.3 Order in CO pressure

The order in CO pressure was then investigated using a series of experiments where the other reacting components were kept constant whilst the CO pressure was varied between 10 and 30 bar. Table 4.3 details the results of these experiments and figure 4.26, gives a graphical representation. Once again the double logarithmic plot of the rate against the partial pressure of CO was plotted and the gradient of the trend line showed that there was a negative order with respect to CO pressure, figure 4.27. The order is -1.1, but with only three points, there could be significant error.

CO (bar)	Methanol (ml)	Initial Rate (mol/s)
10	10	0.0390
20	10	0.0185
30	10	0.0114

Table 4.3: The variation in pCO to determine the order with respect to carbon monoxide for the methoxycarbonylation of vinyl acetate.

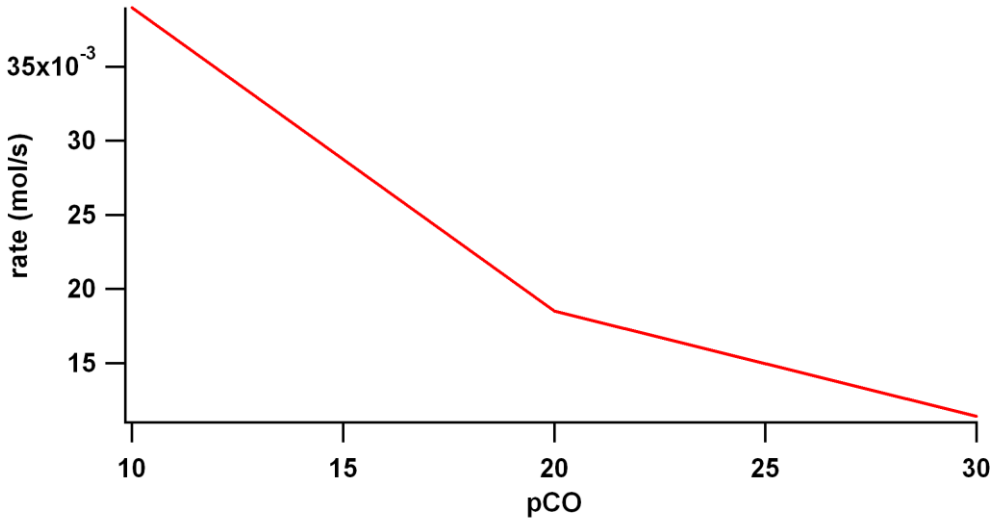

Figure 4.26: Change in initial rate as a function of CO pressure.

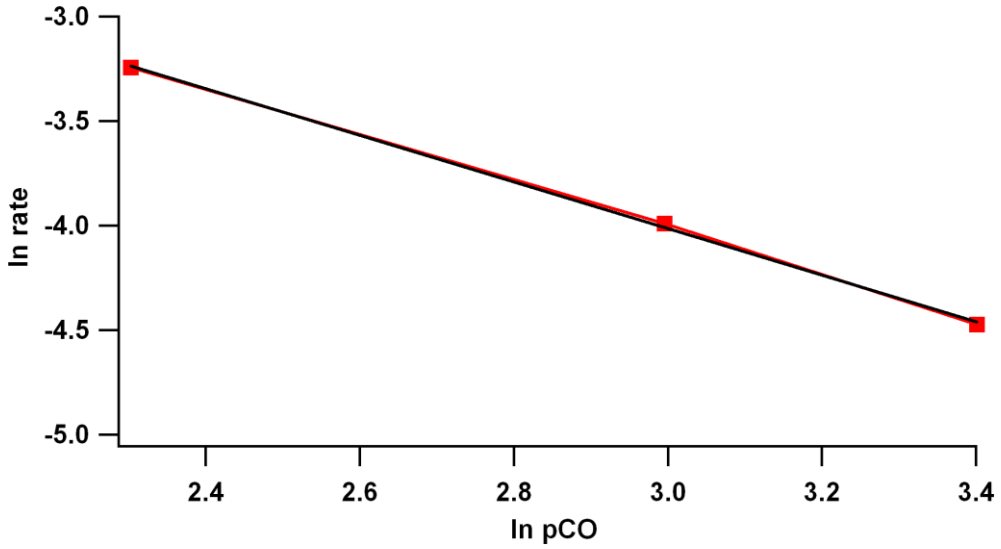

Figure 4.27: Double reciprocal plot of the change in initial rate as a function of CO pressure.

4.12 Discussion

Previous studies have established that the methoxycarbonylation of vinyl acetate proceeds via the hydride mechanism, in a similar way as linear alkenes and α,β-unsaturated carboxylic acids. The hydride mechanism starts by the methanesulphonic acid protonating the palladium/phosphine complex to form the catalytically active hydride species. Figure 4.28, shows the species formed in the presence of carbon monoxide.

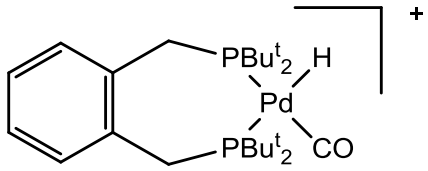

Figure 4.28: Catalytically active hydride species in the methoxycarbonylation of vinyl acetate.

The coordinated CO can then be displaced by vinyl acetate and the hydride migrates to produce a palladium alkyl complex. The double bond within the vinyl acetate forms

a β-agostic interaction with the palladium metal centre. This series of displacements is hindered in the presence of increased CO pressures, resulting in the removal of palladium from the catalytic cycle. There is an equilibrium between coordinated vinyl acetate and coordinated CO and this will result in the observed negative order in CO pressure. This mechanism is shown in figure 4.29.

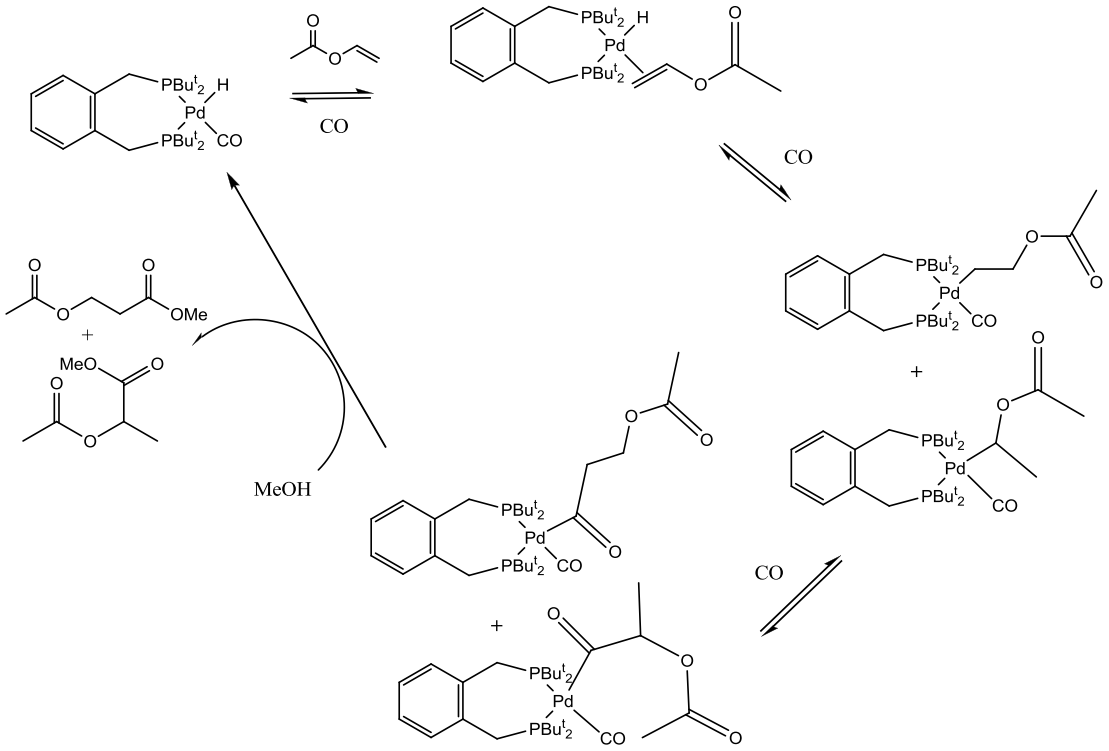

Figure 4.29: The hydride mechanism for the methoxycarbonylation of vinyl acetate.

A simplified version of the mechanism in Figure 4.29 is shown in Figure 4.30, concentrating only on the formation of the branched product.

As has been shown for previous reactions involving this catalyst, the rate-determining step within this reaction is the methanolysis of the acyl species, which produces the methyl acetoxypropanoate ester products and regenerates the hydride species. In the methoxycarbonylation of 1-octene, it was found that this hydride mechanism had a tandem isomerisation step. When the reaction was run in neat methanol, it was noted that the predominant portion of the product was formed via the direct methanolysis of

the 1-octene, but that significant competitive isomerisation to internal alkenes occurred. Later the reaction the tandem isomerisation – carbonylation of these internal alkenes occurred but still gave the terminal ester, albeit at a lower reaction rate.

It was found, however, that when the methanol concentration was lowered, the rate of the direct methanolysis reaction was suppressed so that almost all the alkene isomerised prior to carbonylation. These observations suggest that methanol is involved in the rate-determining step when 1-octene is the substrate. The observed order in methanol concentration, when using vinyl acetate as substrate was found to be 1, which suggests that methanolysis is rate determining in this reaction also.

The step in which vinyl acetate is introduced into the coordination sphere of the metal involves expulsion of CO (Figure 4.30). The first order dependence on [vinyl acetate] and the negative order in CO would then be entirely consistent with this step being effectively a pre-equilibrium within the catalytic cycle.

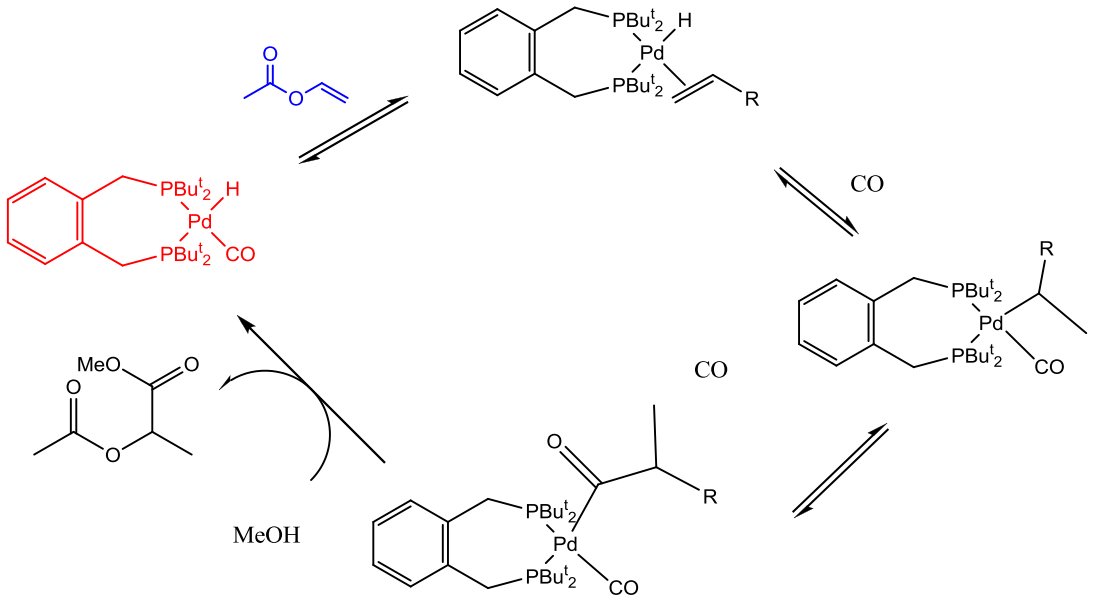

Figure 4.30: Mechanism for the formation of methyl 2-acetoxypropanoate from vinyl acetate showing the rate determining step shown in blue and the catalytic resting state or pre-equilibrium in red, R = OAc.

4.13 Conclusions

The palladium catalysed methoxycarbonylation of vinyl acetate was carried out under constant pressure conditions to determine the orders with respect to the individual reacting components within the reaction. The use of equimolar amount of acid minimised the competitive side reaction within the reaction and allow for better elucidation of the orders in methanol, carbon monoxide and vinyl acetate monomer. It was found that the reaction was first order with respect to vinyl acetate and methanol and a -1 order with respect to carbon monoxide concentration. These orders suggest that methanolysis is rate determining, but that there is a core-equilibrium between a carbonyl complex and one containing coordinated vinyl acetate. This gives the reaction an overall order of 1 as observed in the figure 4.17.

4.14 References

[1] G. Kiss, *Chem. Rev.*, 2001, **101**, 3435.

[2] A. J. Rucklidge, 'Production of Alkyl Lactate by the Alkoxycarbonylation of Vinyl Acetate', PhD, University of St Andrews, St Andrews, 2004.

[3] E. Drent, J. A. M. Vanbroekhoven, and M. J. Doyle, *J. Organomet. Chem.*, 1991, **417**, 235.

[4] E. Drent and P. H. M. Budzelaar, *Chem. Rev.*, 1996, **96**, 663.

[5] G. Smith, N. R. Vautravers, and D. J. Cole-Hamilton, *J. Chem. Soc., Dalton Trans.*, 2009, 827.

[6] G. R. Eastham, B. T. Heaton, J. A. Iggo, R. P. Tooze, R. Whyman, and S. Zacchini, *Chem. Commun.*, 2000, 609.

[7] E. Drent, P. Arnoldy, and P. H. M. Budzelaar, *J. Organomet. Chem.*, 1994, **475**, 57.

[8] R. A. M. Robertson and D. J. Cole-Hamilton, *Chem. Soc. Rev.*, 2002, **225**, 67.

[9] W. Clegg, G. R. Eastham, M. R. J. Elsegood, B. T. Heaton, J. A. Iggo, R. P. Tooze, R. Whyman, and S. Zacchini, *J. Chem. Soc., Dalton Trans.*, 2002, 3300.

[10] C. Jimenez-Rodriguez, D. F. Foster, G. R. Eastham, and D. J. Cole-Hamilton, *Chem. Commun.*, 2004, 1720.

[11] R. P. Tooze, K. Whiston, A. P. Malyan, M. J. Taylor, and N. W. Wilson, *J. Chem. Soc., Dalton Trans.*, 2000, 3441.

[12] R. A. Robertson, A. D. Poole, M. J. Payne, and D. J. Cole-Hamilton, *Chem. Commun.*, 2001, 47.

[13] C. J. Moulton and B. L. Shaw, *Chem. Commun.*, 1976, 365.

[14] L. E. Crascall and J.L.Spencer, *J. Chem. Soc., Dalton Trans.*, 1992, 3445.

[15] W. Clegg, G. R. Eastham, M. R. J. Elsegood, R. P. Tooze, X. L. Wang, and K. Whiston, *Chem. Commun.*, 1999, 1877.

[16] C. Jimenez-Rodriguez, P. J. Pogorzelec, G. R. Eastham, A. M. Z. Slawin, and D. J. Cole-Hamilton, *J. Chem. Soc., Dalton Trans.*, 2007, 4160.

[17] E. Drent and E. Kragtwijk, 1991.

[18] W. G. Reman, G. B. J. De Boer, S. A. J. Van Langen, and A. Nahuuijsen, 1989.

[19] Y. Koide, S. G. Bott, and A. R. Barron, *Organometallics*, 1996, **15**, 2213.

[20] G. R. Eastham, R. P. Tooze, M. Kilner, D. F. Foster, and D. J. Cole-Hamilton, *J. Chem. Soc., Dalton Trans.*, 2002, 1613.

[21] J. Wolowska, G. R. Eastham, B. T. Heaton, J. A. Iggo, C. Jacob, and R. Whyman, *Chem. Commun.*, 2002, 2784.

[22] G. N. Il'inich, V. N. Zudin, A. V. Nosov, V. A. Rogov, and V. A. Likholobov, *J. Mol. Cat. A. Chem.*, 1995, **101**, 221.

[23] G. F. Pregaglia, A. Andreeta, G. F. Ferrari, and R. Ugo, *J. Organomet. Chem.*, 1971, **30**, 387.

[24] P. Pino, F. Piacenti, and M. Bianchi, 'Organic Synthesis via Metal Carbonyls', ed. I. Wender and P. Pino, Wiley, 1977.

[25] P. Hoffmann, K. Kosswig, and W. Schafer, *Ind. Eng. Chem. Prod. Res. Dev.*, 1982, **19**, 330.

[26] B. Cornils and W. A. Herrmann, 'Applied Homogeneous Catalysis with Organometallic Compounds', ed. W. A. Herrmann, Wiley-VCH.

[27] D. Melstein and J. L. Huckaby, *J. Am. Chem. Soc.*, 1982, **104**, 6150.

[28] C. Jacob, B. T. Heaton, J. A. Iggo, and R. Whyman, *J. Mol. Cat. A.*, 2003, **204**, 149.
[29] P. Hoffmann and W. H. E. Mueller, *Hydrocarbon Processing Int. Ed.*, 1980, **60**, 151.
[30] 'Rhodium Catalysed Hydroformylation', ed. P. W. N. M. v. Leeuwen and C. Claver, Kluwer Academic Publishers, 2000.
[31] C. D. Frohling and C. W. Kohlpaintner, 'Applied Homogeneous Catalysis with Organometallic Compounds', ed. B. Cornils and W. A. Herrmann, Wiley-VCH, 1996.
[32] C. Jimenez-Rodriguez, G. R. Eastham, and D. J. Cole-Hamilton, *Inorg. Chem. Commun.*, 2005, **8**, 878.
[33] R. I. Pugh, E. Drent, and P. G. Pringle, *Chem. Commun.*, 2001, 1476.
[34] G. R. Eastham, R. P. Tooze, X. L. Wang, and K. Whiston, in 'Process for the Carbonylation of Ethylene and Catalyst System for Use Therein', UK, 1996.
[35] E. Drent and W. W. Jager, USA, 2001.
[36] A. J. Rucklidge, G. E. Morris, and D. J. Cole-Hamilton, *Chem. Commun.*, 2005, 1176.
[37] A. J. Rucklidge, G. E. Morris, A. M. Z. Slawin, and D. J. Cole-Hamilton, *Helvetica Chimica Acta*, 2006, **89**, 1783.
[38] G. Taylor, *Chem. Ind.*, 2002, 6.
[39] H. Ooka, T. Inoue, S. Itsuno, and M. Tanaka, *Chem. Commun.*, 2005, 1173.
[40] A. A. Nunez-Magro, L. M. Robb, P. J. Pogorzelec, A. M. Z. Slawin, G. R. Eastham, and D. J. Cole-Hamilton, *Chem. Sci.*, 2010, **1**, 723.
[41] E. Drent and D. H. L. Pello, 1995.
[42] K. Itoh, M. Miura, and M. Nomura, *Tetrahedron Lett.*, 1992, **33**, 5367.
[43] E. Drent, 1992.
[44] K. Kudo, Y. Oida, K. Mitsuhashi, S. Mori, K. Komatsu, and N. Sugita, *Bull. Chem. Soc. Jpn.*, 1996, **69**, 1337.
[45] A. J. Rucklidge, G. R. Eastham, and D. J. Cole-Hamilton, 2004.
[46] A. J. Rucklidge, G. E. Morris, and D. J. Cole-Hamilton, *Chem. Commun.*, 2005, 1176.

Chapter 5: The Palladium Catalysed Methoxycarbonylation of Alkynes

5.1 Background

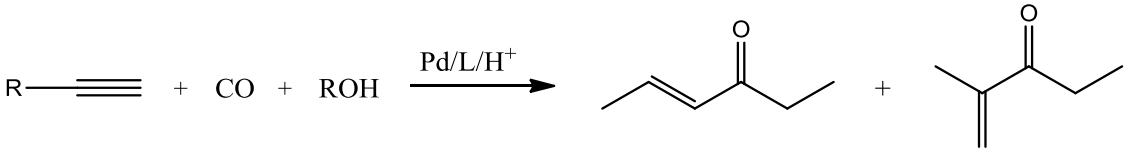

Fig 5.1: Alkoxycarbonylation of alkynes.

In the alkoxycarbonylation of alkynes, there have been several reports of both high activities and marked regioselectivites to branched products, (Fig 5.1). Drent *et al* [1-5] and Dervisi *et al* [6, 7] have studied the synthesis of methyl methacrylate from propyne in a one step process. Another major area in this work involves the preparation of important precursors such as methyl atropates (R, Ar=Ph) [4, 8-18] and methyl naphthylpropanoates (R, Ar=naphth).[19] These are of particular importance owing to their facile transformation, *via* asymmetric hydrogenation, into anti-inflammatory drugs such as Ibuprofen and Naproxen (Fig 5.2).

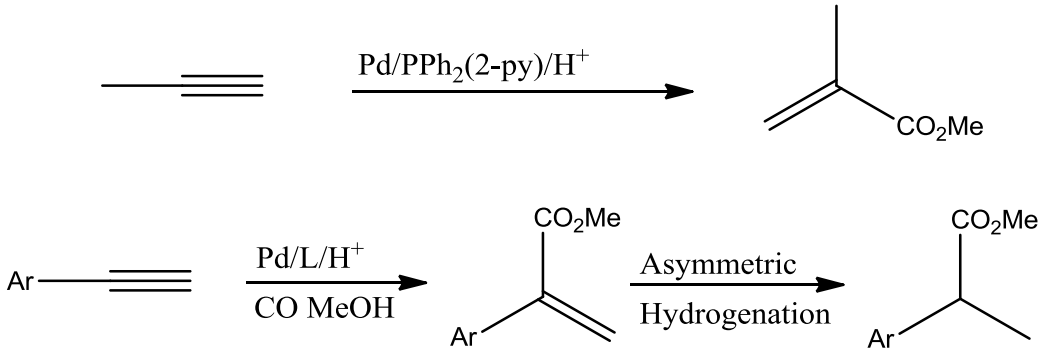

Ar = Ph/naphth

Fig 5.2: Examples of methoxycarbonylation of alkynes.

Furthermore the possibility of producing several variants of furan-2(5H)-ones, presents multiple uses in the areas of anti-bacterial, anti-fungal and anti-inflammatory pharmaceuticals industries. These products have been shown to be synthesised via the cyclic carbonylation of propargyl alcohols. [20-22]

Notwithstanding the necessity for these branched derivatives throughout industry, the linear regioisomer products, such as β-substituted methyl acrylates or methyl cinnamates (in the case of R=Ar), are also highly desirable. Despite this requirement, there are very few catalysts that have been reported which have shown even a partial preference towards the linear regioisomeric product. [4, 15] As a result of the lack of sufficient active and selective catalyst for this sort of reaction, these important molecules are predominantly prepared utilising Heck reactions.[23-25] This reaction is an effective, well studied and established route in the synthesis of such molecules.

The drawback of the Heck reaction for industrial application is the use of halo-arene starting materials and at least one equivalent of base. This hydrohalide salt of the base then has to be removed as waste after the reaction. It is therefore, highly advantageous to discover new active and highly regioselective catalyst systems which can successfully generate the linear regioisomeric products via a *waste-free* process.

5.1.1 Alkyne synthesis

Alkynes are formed in various different ways, dependant upon the desired product. The most common commercially available alkyne, acetylene is produced via the dehydrogenation of natural gas. Longer chain alkynes are often formed from the dehydrohalogenation of vinyl halide, geminal dihalides or vicinal dihalides. [26]

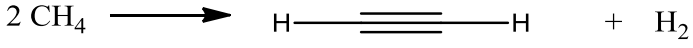

Figure 5.3: The synthesis of acetylene from methane.

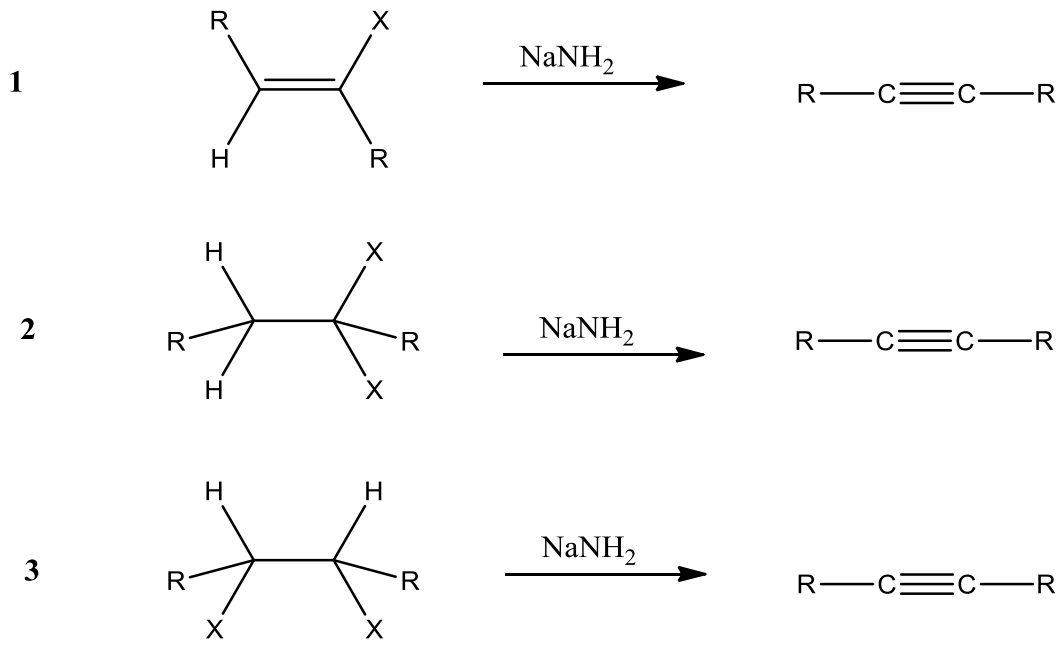

*Figure 5.4: The synthesis of alkynes via the dehydrohalogenation of vinyl halides (**1**), the dehydrohalogenation of geminal dihalides (**2**) or the dehydrohalogenation of vicinal dihalides (**3**).*

Other methods for producing speciality alkynes include the dehydrohalogenation of vicinal alkyl dihalides or vinyl halides,[27] the Frisch-Buttenberg-Weichell rearrangement of vinyl bromides [28] (1), the Corey-Fuchs reaction [29] using aldehydes (2) and the Seyferth-Gilbert homologation of ketones [30, 31] (3)

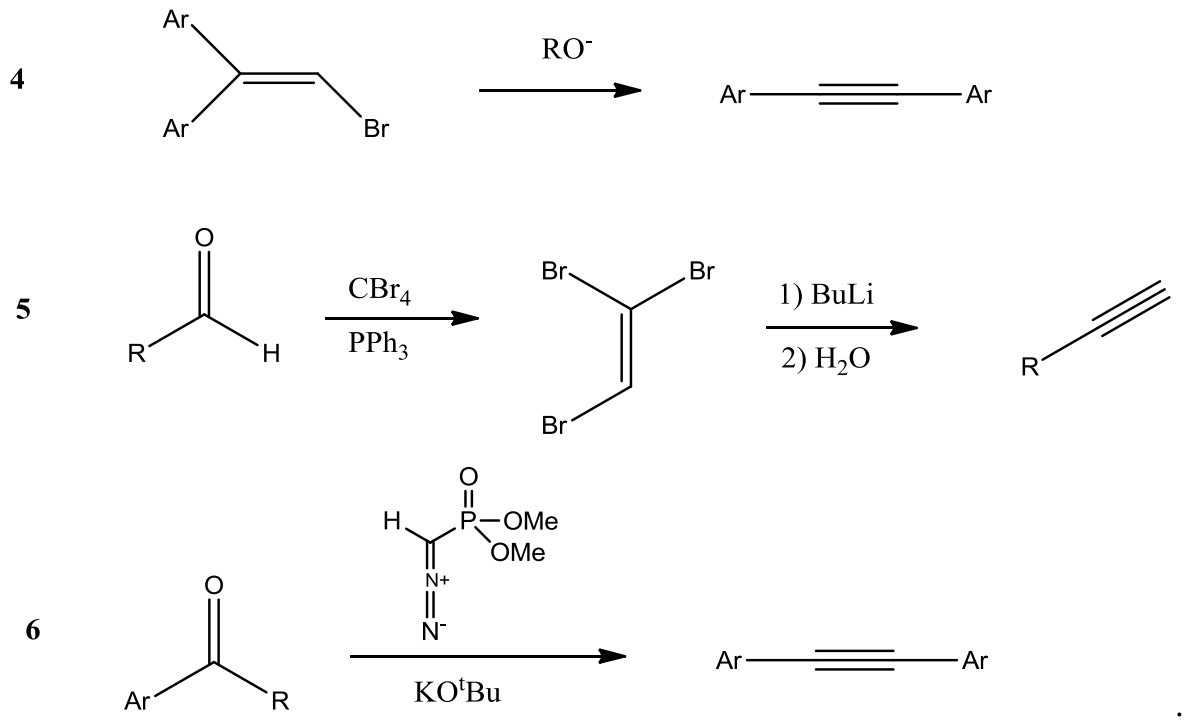

*Figure 5.5: Alkyne formation via the Frisch-Buttenberg-Weichell rearrangement of vinyl bromides (**4**), the Corey-Fuchs reaction using aldehydes (**5**) and the Seyferth-Gilbert homologation of ketones (**6**).*

The formation of terminal alkyne bonds is possible using the alkyne zipper reaction which involves the use of a strong base to isomerise the triple bond into a terminal position. Brown and Yamashita first reported this in 1975 using 1,3-diaminopropanide as an accelerant. [32] This is formed in situ from the addition of potassium hydride to 1,3-diaminopropane. This reaction proceeds via a series of alkyne-allene conversions which exist in equillibria until the alkyne is trapped as a stable terminal alkyne anion. This mechanism is shown in figure 5.6.

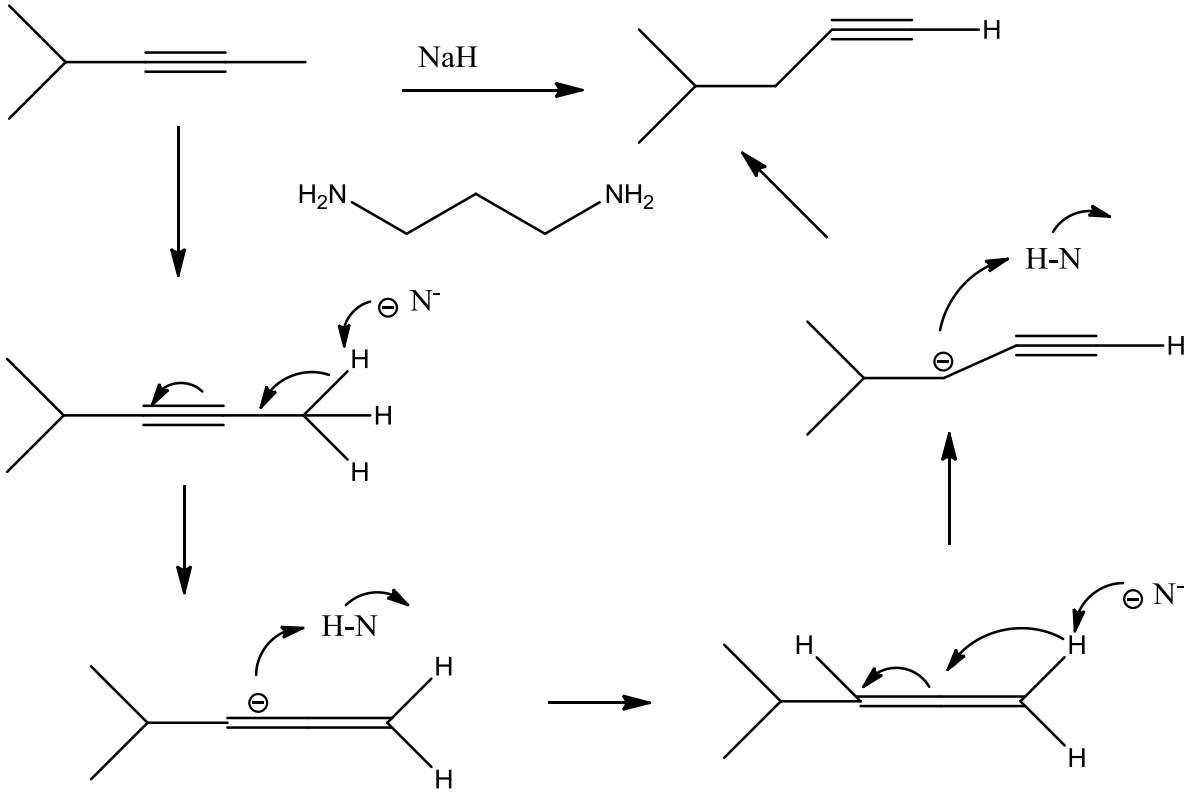

Figure 5.6: The mechanism for the alkyne zipper reaction.

5.1.2 Alkyne Reactions

Reactions of alkynes are of great interest as they are highly reactive building blocks for synthetic chemistry. Carbonylation of acetylene has been employed industrially since the mid 1950's to produce acrylic acid. This reaction was first discovered by Reppe [33, 34] of BASF and is still used to produce acrylic acid to this day, although a route to acrylic acid involving more readily available starting materials is the heterogeneously catalysed gas phase oxidation of propene. [35, 36]

It has been shown that varying the metal centre under comparable conditions allows for the production of several alternative compounds. Iron pentacarbonyl and ruthenium carbonyl produce hydroquinone whereas dicobalt octacarbonyl can produce both the *cis* and *trans* isomers of bis-furandione. [37]

Another well-known reaction of ethyne is the production of acetaldehyde via the addition of water to acetylene using Hg and H_2SO_4. [37] In contrast to this reaction, in which the product can partially oxidise to form acetic acid, the addition of alcohols leads to the formation of stable enol ethers, which are of great economic importance, and can also be prepared from acetylene using base catalysis. Noble metal catalysed alcohol addition leads to the formation of vinyl ether intermediates which then react to form acetaldehyde dialkyl acetals [37, 38] shown in figure 5.7.

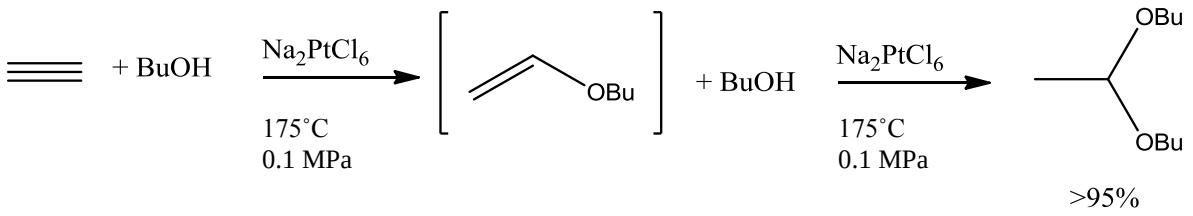

Figure 5.7: The formation of 1-(1-butoxyethoxy)butane from ethyne. [37]

Only in exceptional cases is it possible to isolate the enol ether. An example of this would be the addition of methanol to acetylenedicarboxylic esters, shown in figure 5.8. [37, 39]

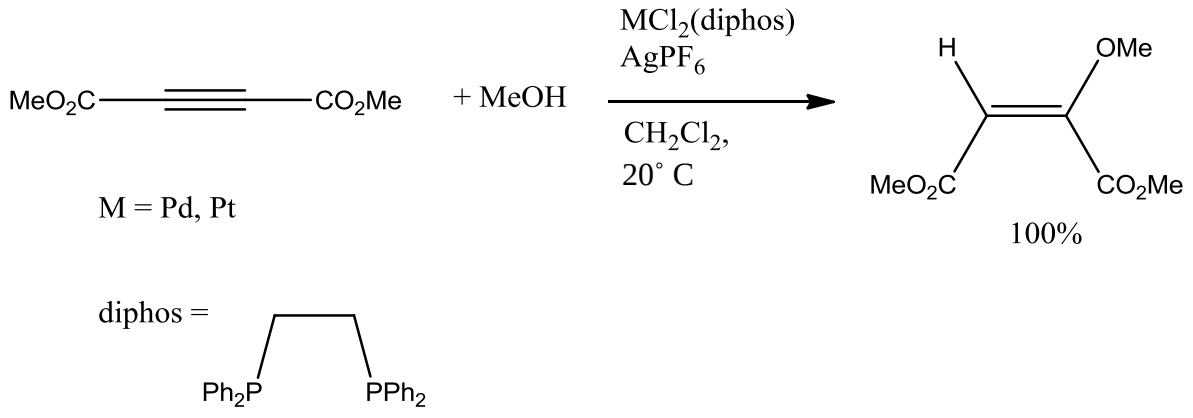

Figure 5.8: The formation of dimethyl 2-methoxymaleate from dimethyl but-2-ynedioate. [37]

The above-mentioned examples show the reaction of acetylene with a nucleophile to produce heterovinyl compounds; however, it is comparatively rare to find industrially

relevant additions of C-H acidic compounds to acetylenes. Examples include the addition of hydrocyanic acid to acetylene [40] or the zinc-catalysed addition of malonic ester derivatives to acetylene, [41] which is used in the synthesis of barbiturates.

In the case of C-vinylation reactions, there have been a few new reactions catalysed by transition metals. These include linking aldehydes with internal alkynes [42] and the addition of allyl halides to alkynes. [43] Allyl alcohols can also react with terminal alkynes to produce the corresponding ketones [44] It has also been shown that noble metals can isomerise the alkynes to form dienes. [45-47]

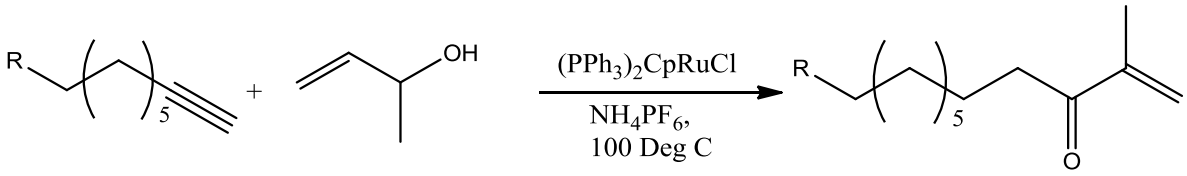

Figure 5.9: The formation of 2-methyldec-1-en-3-one from the reaction of but-3-en-2-ol and 1-octyne (where R = H).[37]

5.2 Aims

As was shown in chapter 3 and previously in the literature, Cole-Hamilton *et al* [48] have demonstrated that Pd_2dba_3/BDTBPMB/H^+, is a highly active and selective catalyst for the carbonylation of unsaturated alkenes to produce terminal carboxylic acid esters.

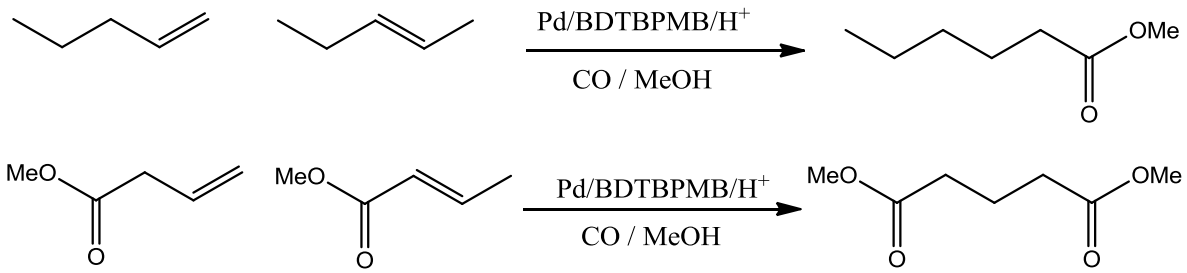

Figure 5.10: The methoxycarbonylation of alkenes and unsaturated esters using $Pd_2(dba)_3$/BDTBPMB.

Furthermore, separate studies by Cole-Hamilton *et al*. [49] have shown that it is possible selectively to produce α,ω-diesters via the alkoxycarbonylation of various fatty acid esters, figure 5.10.

As it has been shown previously that it is possible to achieve terminal selectivity from internal double bonds, [48] it was postulated that the methoxycarbonylation of alkynes could produce dicarbonylated products. Phenyl acetylene was of particular interest as previous studies determined that the additional steric bulk from the phenyl ring influenced the product distribution, resulting in the preferential formation of the linear mono-carbonylated product. This means that the methoxycarbonylation of phenyl acetylene is a potential waste free step in the formation of this and similar heck products.

Thereafter, various linear alkynes were studied to establish if these substrates could produce α,ω-diesters in a single cascade reaction.

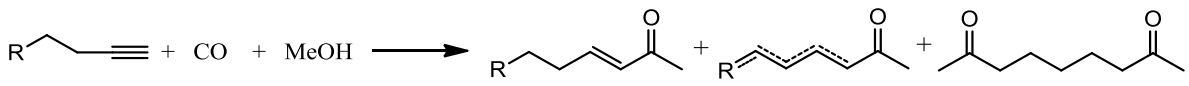

Figure 5.11: The methoxycarbonylation of a terminal alkyne, showing the first carbonylation product, the isomerisation of the internal double bond and the resulting α,ω-diester product.

If the first carbonylation, step were to occur in the terminal position it would be expected to generate an α,β-unsaturated ester. This would be followed by the isomerisation of the double bond to the opposite end of the chain where it would trapped and carbonylated to form the α, ω-diester. [49] This selectivity seemed possible because Pd/BDTBPMB has such a strong tendency to form linear products by a hydride mechanism. However, the strong tendency for palladium catalysed methoxycarbonylation to form branched products with alkyne substrates (carbomethoxy mechanism) and the fact that Pd/BDTBPMB can give branched products when using substrates such as styrene or vinyl acetate means that branched selectivity would also be possible, in which case the either or both of the products shown in Figure 5.12 would be formed. The previous studies of these products are discussed below.

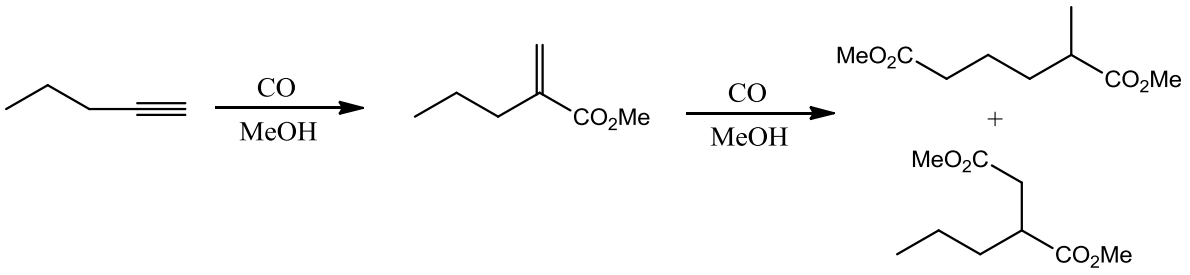

Figure 5.12: Possible course of the methoxycarbonylation of 1-pentyne if the first step were to give branched selectivity.

5.3 The Methoxycarbonylation of Phenyl Acetylene

The substrate explored within this study was phenyl acetylene. This is a particularly desirable reaction as the linear isomer products obtained via the alcoxycarbonylation of this substrate are cinnamates. These are highly desirable intermediates in organic synthesis owing to their facile conversion to numerous organic products such as phenyl aniline or phenyl succinic acid. It was previously shown by Claver and van Leeuwen [50, 51] that the presence of the phenyl group in styrene affects the product regioselectivity during methoxycarbonylation, therefore the study of phenyl acetylene would also allow for the study of the effect of the phenyl group on the production of these cinnamates. The reaction scheme is detailed below in figure 5.13.

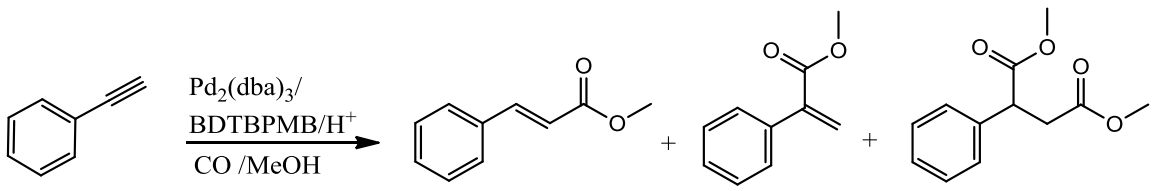

Figure 5.13: The methoxycarbonylation of phenyl acetylene which produces methyl cinnamate, methyl atropate and dimethyl 2-phenylsuccinate.

Cole-Hamilton *et al* [52] have shown that the methoxycarbonylation of phenyl acetylene, catalysed by Pd_2dba_3/BDTBPMB gives a high activity (>99.9% conversion). Furthermore they also show a preference for the production of the linear isomer, methyl cinnamate with a selectivity of 99 %. An interesting point to note was that under some reaction conditions,

the substrate underwent a double carbonylation to form dimethyl 2-phenylsuccinate, but they showed no evidence towards the formation of either dimethyl 2-benzylmalonate or dimethyl 2-methyl-2-phenylmalonate

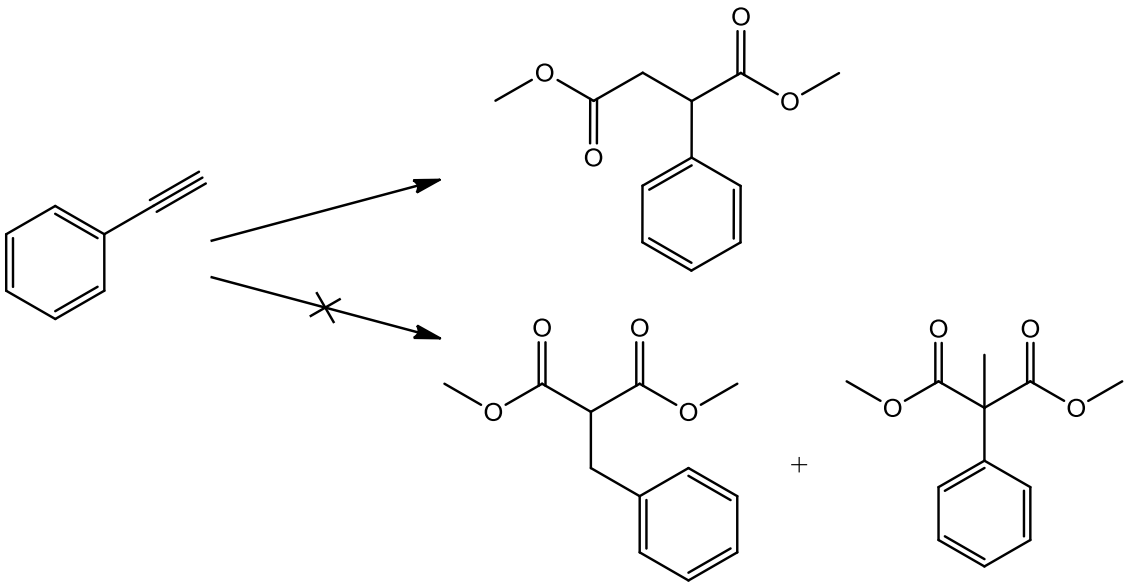

Figure 5.14: The possible products from the double methoxycarbonylation of phenyl acetylene. It was found that only the dimethyl 2-phenylsuccinate was formed.

This study has also shown that the reaction can be carried out at room temperature and runs to completion within 3 hours; furthermore running the reaction at room temperature lowers the yields of the di-substituted product. The reaction showed significantly lower yield and regioselectivity when the pressure was dropped to 2 bar and at lower palladium concentrations the reaction yielded high conversion and no dimethyl phenylsuccinate.

It was shown that the presence of the dimethyl 2-phenylsuccinate was not increased by carrying the reaction out over a longer time (14 h). This indicated that the second carbonylation only occurs from the branched product methyl atropate. This was then confirmed experimentally by studying the methoxycarbonylation of methyl cinnamate and methyl atropate separately. They found that 66 % methyl atropate is converted to dimethyl-phenylsuccinate within the reaction time; whereas there was no conversion under the same conditions from the methyl cinnamate and only 2 % of dimethyl 2-phenylsuccinate was obtained under higher palladium concentrations, indicating that the dimethyl succinate

product, shown in figure 5.15, is effectively formed via the methoxycarbonylation of methyl atropate.

.

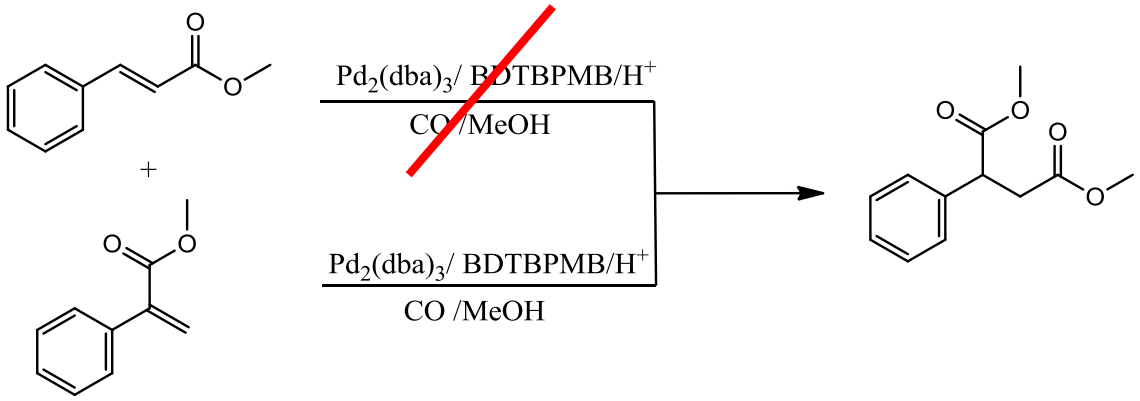

Figure 5.15: Formation of dimethyl-phenylsuccinate from methyl cinnamate or methyl atropate.

5.4 The Methoxycarbonylation of Linear Alkynes

Noble metal catalysed processes have allowed for the carbonylation of higher acetylenes to produce their corresponding acrylic acid derivatives. An example of this would be the methoxycarbonylation of propyne to produce methyl methacrylate by Drent.[2] This study involves the use of pyridyl-diphenylphosphine ligands to produce methyl methacrylate with selectivities up to 98.9% at 45°C. This study showed that when the 6-position on the pyridyl ring was functionalised, the selectivity towards methyl methacrylate formation increased to >99.9% from 89% as seen with triphenylphosphine, creating a 20 fold suppression of methyl crotonate formation. They provide evidence to suggest that the reaction follows the carbomethoxy mechanism, shown in figure 5.16, and that the pyridine group acts as a proton shuttle.

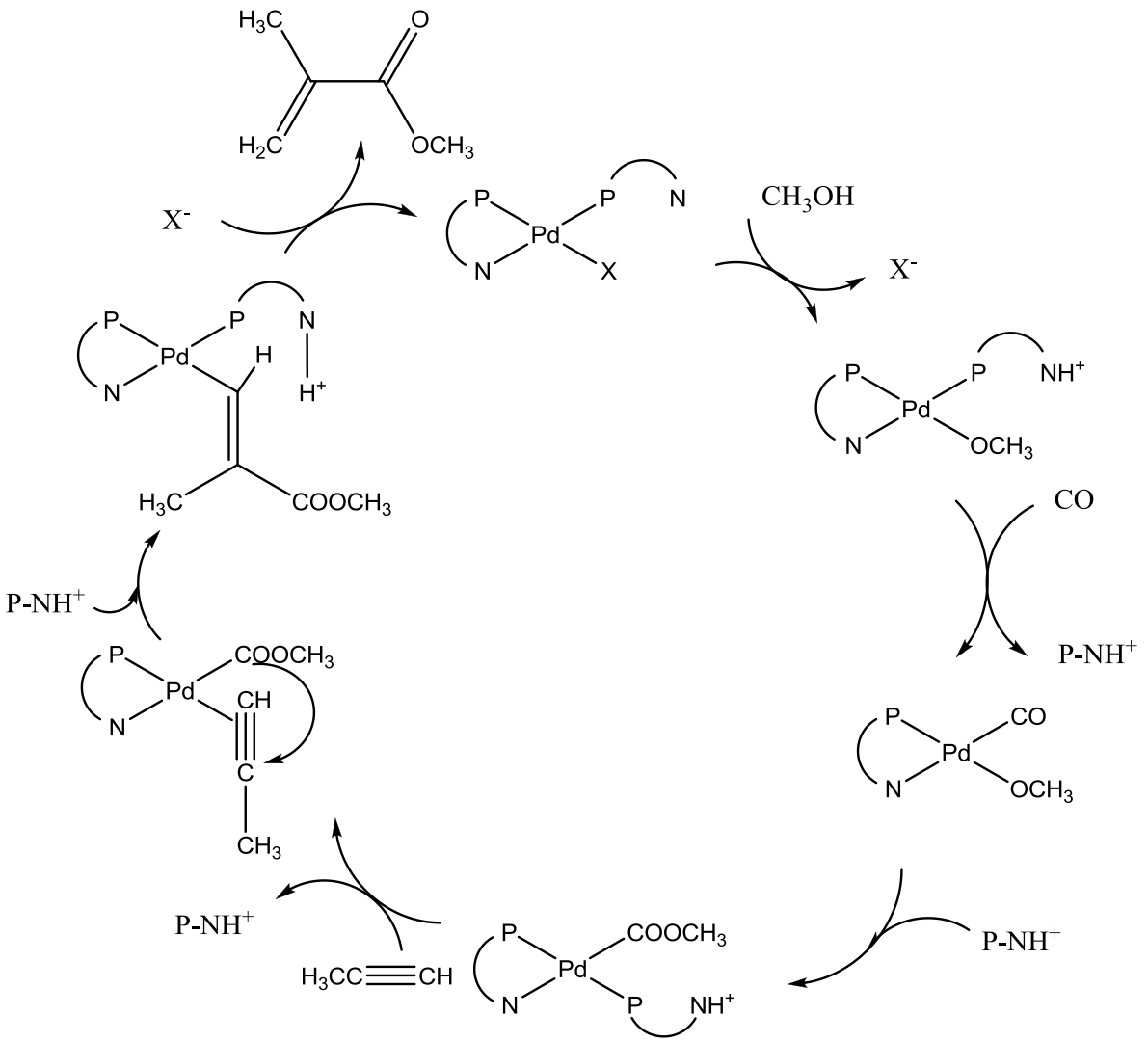

Figure 5.16: The proposed catalytic cycle for the palladium-methoxy/2-PyPPh$_2$- catalysed methoxycarbonylation of propyne. [2]

The initiation step of this reaction involves methanol addition to the $PdXL_2$ complex. This is followed by the neucleophillic attack by CO to displace the mono-coordinated P-N ligand. The subsequent migratory insertion of the CO into the palladium-methoxy bond produces a palladium carbomethoxy species with the carbomethoxy group coordinated *cis* to the phosphorus. The propyne displaces the mono-coordinated P-NH$^+$ ligand and is coordinated perpendicular to the square plane of the ligand coordination site to reduce steric hindrance. The propyne then undergoes migratory insertion into the palladium-carbomethoxy bond to form a palladium alkenyl species. This could be either 1-palladium-2-carbomethoxy-propene (linear) or 2-palladium-1-carbomethoxy-propene (branched). This step involves the rotation of the propyne into the square plane of the complex followed by the neucleophillic

attack by the carbomethoxy moiety. The vacant site created is then occupied by the mono-coordinated protonated P-NH^+ ligand. This insertion facilitates the protonation of the alkenyl bond to form the product and reinitiate the cycle.

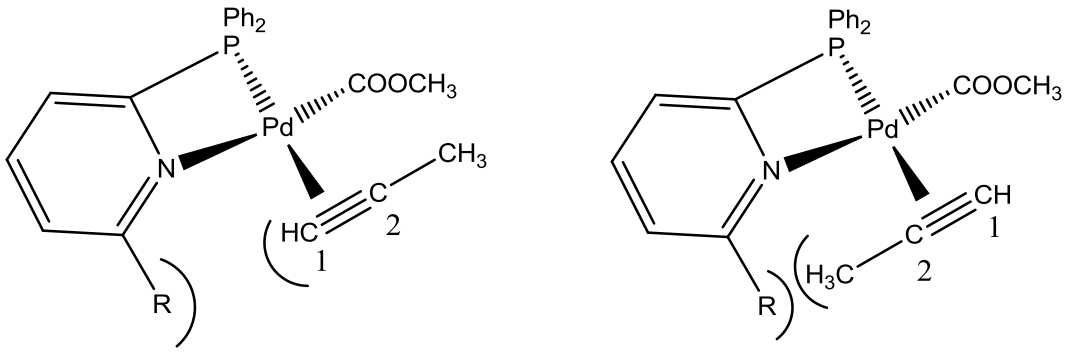

Figure 5.17: The spatial configurations for 1,2 and 2,1 insertion of propyne when using the 2-(6-CH_3-Py)PPh_2 ligand for the methoxycarbonylation of propyne.

The inclusion of substituents on the 6-position of the pyridyl ring results in a marked change in selectivity, suggesting that the product distribution is controlled by steric, rather than electronic factors. The introduction of the methyl group in the 6-position on the pyridyl ring limits the coordination space envelope, which in turn limits the route of migratory insertion. Drent *et al* [2] postulate that the mono-coordinated ligand is involved in the termination step of the cycle and as such the functionalisation of the 6-position on the pyridyl ring, will result in the methyl group of the propyne co-ordinating away from the functional group, which results in the formation of the 2-palladium-1-carbomethoxy-propene formation being inhibited, figure 5.17.

The 1,2-insertion step then would determine the regioselectivity of the product. The nature of the product gives an indication of the mechanistic pathway of the reaction. As the predominant product is methyl methacrylate, it can be postulated that the reaction proceeds by the above described carbomethoxy mechanism, as the same inhibition for the hydride mechanism would result in the selective formation of the linear methyl crotonate. The differences in these steps and their resulting product distributions are discussed later in figure 5.55.

5.5 Results

5.5.1 Functionalised Alkynes: Phenyl acetylene

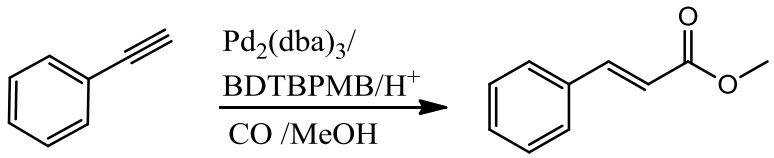

Figure 5.18: The methoxycarbonylation of phenyl acetylene.

Phenyl acetylene was of particular interest as studies [52] determined that the additional steric bulk from the phenyl ring influenced the product distribution The rate of the methoxycarbonylation were then compared to that of styrene.

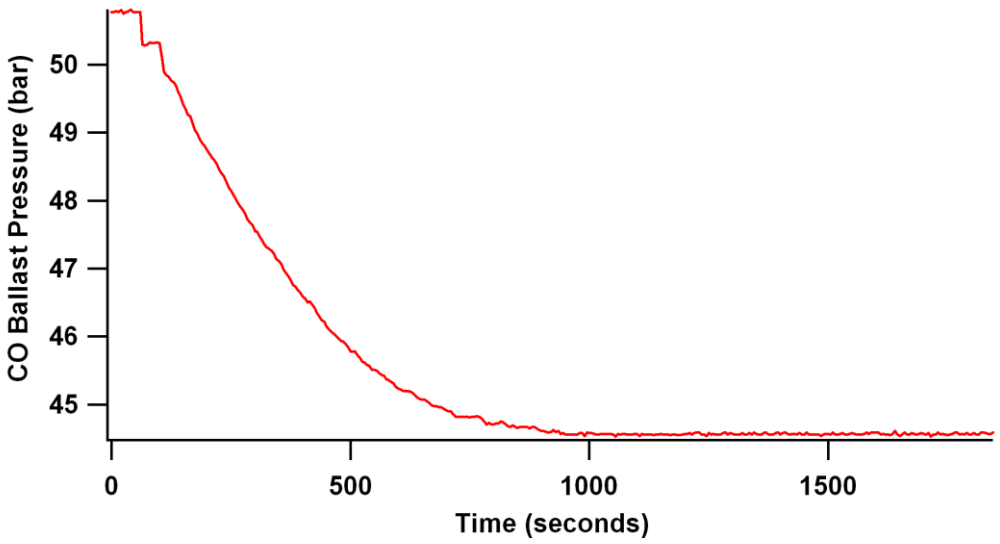

Figure 5.19: The methoxycarbonylation of phenyl acetylene in 10 ml of methanol under constant CO.

The reaction was run in a higher methanol concentration to establish the order with respect to the substrate concentration. The gas uptake curve is shown in Figure 5.19 and the graphical rate expression in Figure 5.20. The rate as a function of phenyl acetylene graph showed that at lower substrate concentrations there was a linear fit running through the origin indicating the reaction to be first order in substrate.

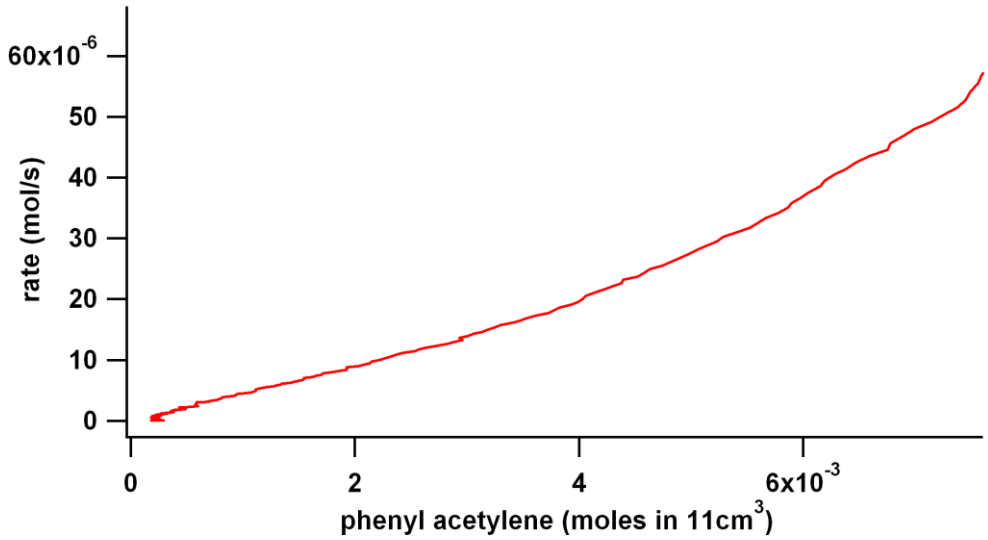

Figure 5.20: The rate as a function of the substrate concentration for the methoxycarbonylation of phenyl acetylene in 10 ml of methanol.

The natural log of the rate was then plotted against the natural log of the phenyl acetylene concentration to determine the order with respect to phenyl acetylene. The linear fit confirms that the reaction is first order at lower substrate concentrations and tends to higher order at higher concentrations.

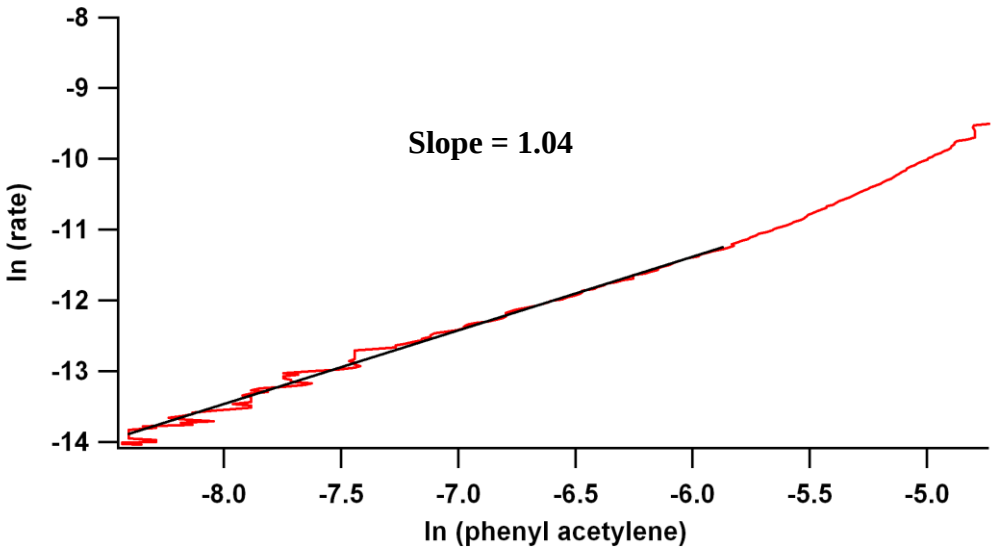

Figure 5.21: The natural log of the rate as a function of the natural log of the phenyl acetylene concentration for the methoxycarbonylation of phenyl acetylene in 10 ml of methanol.

The reaction was also run at lower methanol concentrations (2ml) to establish the order with respect to the methanol concentration. Once again, the rate was plotted against the substrate concentration and then the rate divided by the substrate concentration was plotted against the methanol concentration to determine the order with respect to methanol. The plots are shown in figure 5.22 and 5.23 respectively. As the order with respect to substrate is complex, the determination with order with respect to methanol concentration can only be determined for lower substrate concentrations when the reaction is known to be first order in substrate.

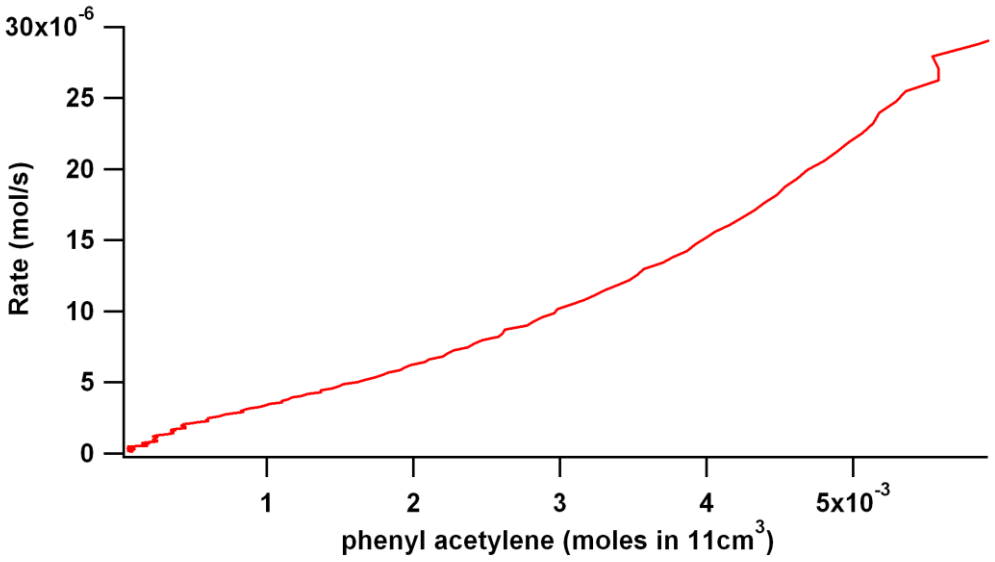

Figure 5.22: The rate as a function of the substrate concentration for the methoxycarbonylation of phenyl acetylene in 2 ml of methanol.

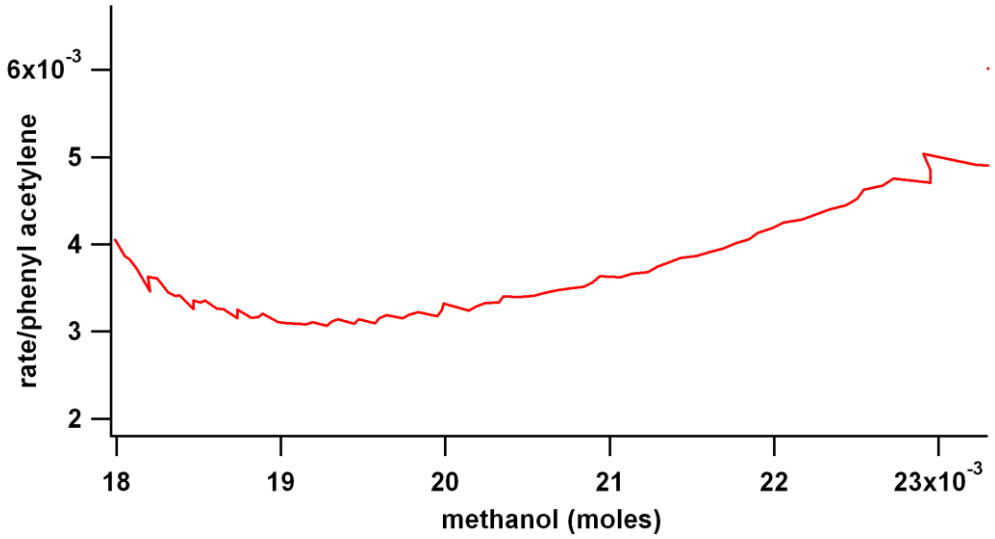

Figure 5.23: The rate divided by the substrate concentration as a function of the methanol concentration for the methoxycarbonylation of phenyl acetylene in 2 ml of methanol.

When the rate was divided by the substrate concentration and plotted against the methanol concentration, it was found that, at low substrate concentration, the rate was almost independent of methanol concentration. This suggests that the reaction is zero order in methanol concentration at lower substrate concentrations.

The system was then run under constant volume conditions to record the CO consumption as a function of time. The gas uptake curve for this reaction is shown in figure 5.24

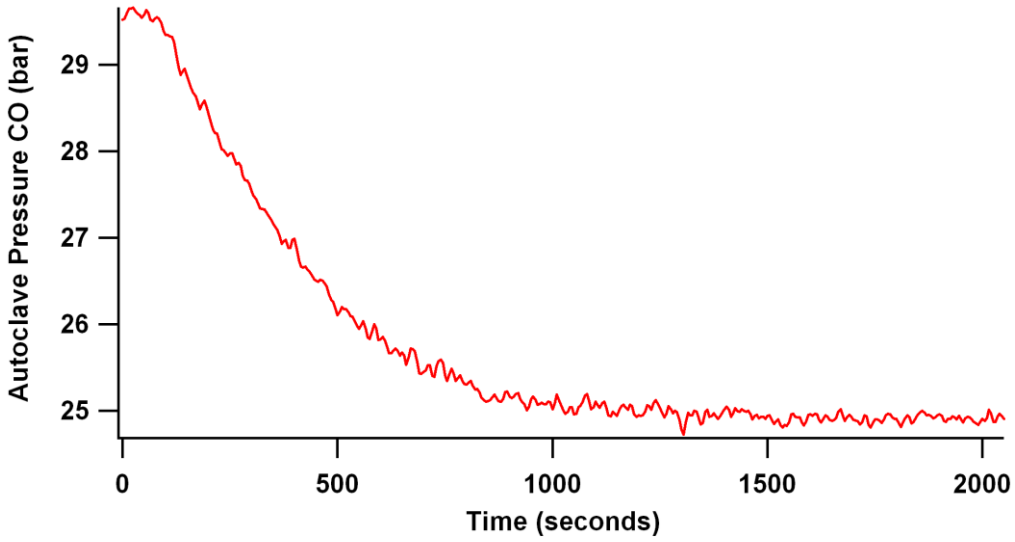

Figure 5.24: The methoxycarbonylation of phenyl acetylene in 10 ml of methanol in a constant volume system.

This reaction was carried out in the presence of 10 ml of methanol, which would result in pseudo zero order kinetics in methanol. The rate as a function of substrate concentration was then plotted to show the order in substrate concentration. In this instance, the reaction was found first order in substrate concentration throughout the reaction, which is shown in figure 5.25.

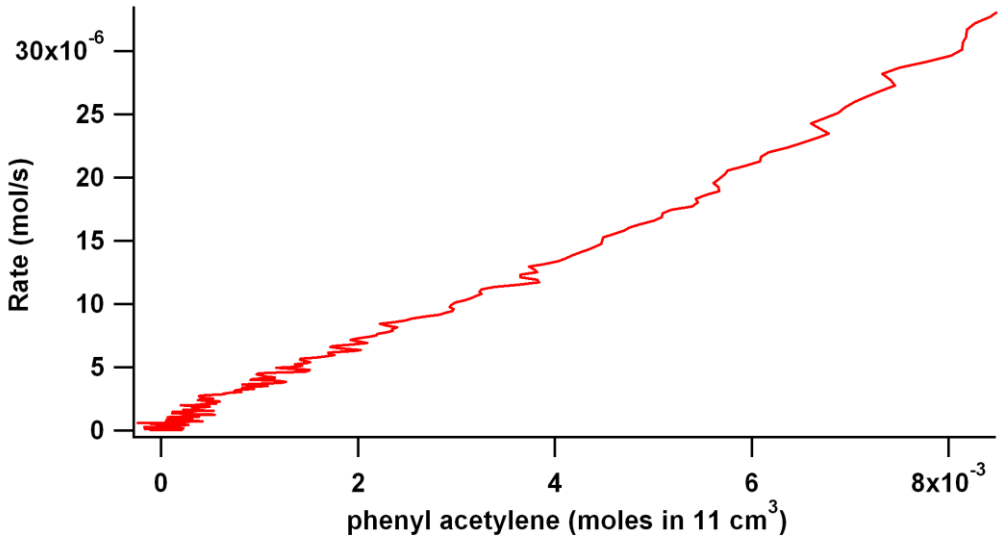

Figure 5.25: The rate as a function of the substrate concentration for the methoxycarbonylation of phenyl acetylene in 10 ml of methanol in a constant volume system.

As the reaction was run under constant volume conditions, the CO partial pressure was changing as a function of time. The apparent overall first order dependence combined with the already determined first order dependence of the rate on phenyl acetylene concentration suggests that the reaction may be zero order in pCO, at least at low substrate concentrations. This is confirmed by a plot of the rate divided by the phenyl acetylene concentration as a function of the partial pressure of CO, which approximates to a straight line parallel to the x axis (figure 5.26)

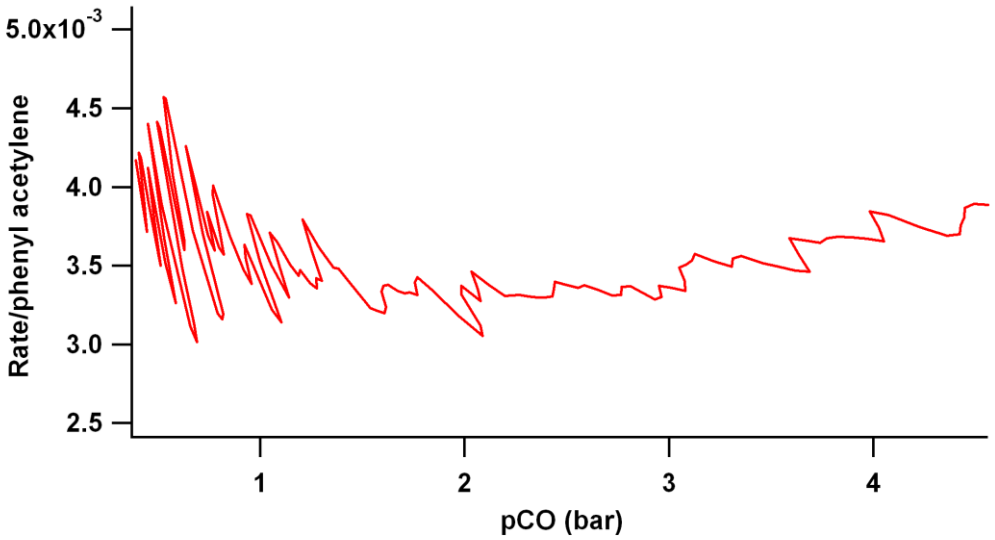

Figure 5.26: The rate, divided by the substrate concentration, as a function of the partial pressure of CO, for the methoxycarbonylation of phenyl acetylene in 10 ml of methanol in a constant volume reactor.

At lower concentrations of phenyl acetylene, the reaction is first order in phenyl acetylene, zero order in methanol and zero order in pCO. This suggests that the coordination of phenyl acetylene to the palladium is rate determining. All of the palladium remains in the catalytic cycle all of the time. In other words the equilibrium shown in figure 5.27 lies completely to the right; otherwise a negative dependence on CO should be observed.

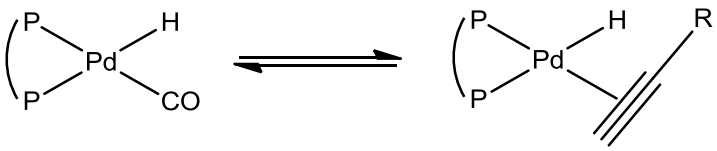

Figure 5.27: The hydrido carbonyl complex in equilibrium with hydrido alkyl complex for the methoxycarbonylation of styrene.

However we note that in the reaction run at constant volume, the initial pressure was 30 bar, and 100% conversion of substrate would result in only a 17% decrease in CO concentration. So a possible alternative explanation for the observed zero order in pCO is that the measurements are not sufficiently sensitive to pick up changes as a result of this small pressure drop and that the reaction is effectively run under pseudo zero order conditions in CO.

The selectivity towards the linear product, methyl cinnamate was found to be in excess of 99% throughout these reactions. The reaction was, therefore, proposed to follow the hydride mechanism. The mechanism and origin of selectivity is explored in more detail in section 5.5.

5.5.2 Comparison to Styrene

Several previous studies have selected styrene as the substrate of focus as it is the simplest aromatically functionalised alkene. For comparison to phenyl acetylene we have also studied this reaction. The plot of styrene concentration against time was fitted with a double exponential curve as shown in figure 5.28. The two observed exponentials are 0.00015 and 0.0013 mol/s. It was found that when the reaction was run overnight, it did not proceed to completion, showing that the carbonylation of styrene is, as expected, much slower than that of phenyl acetylene. The double exponential fit could imply that there is a change in order with respect to styrene as the reaction proceeds. The reaction was found to have a 69 % selectivity towards the linear product, methyl-3-phenylpropanoate. It therefore seemed logical to choose the simplest aromatically functionalised alkyne for this study, phenyl acetylene.

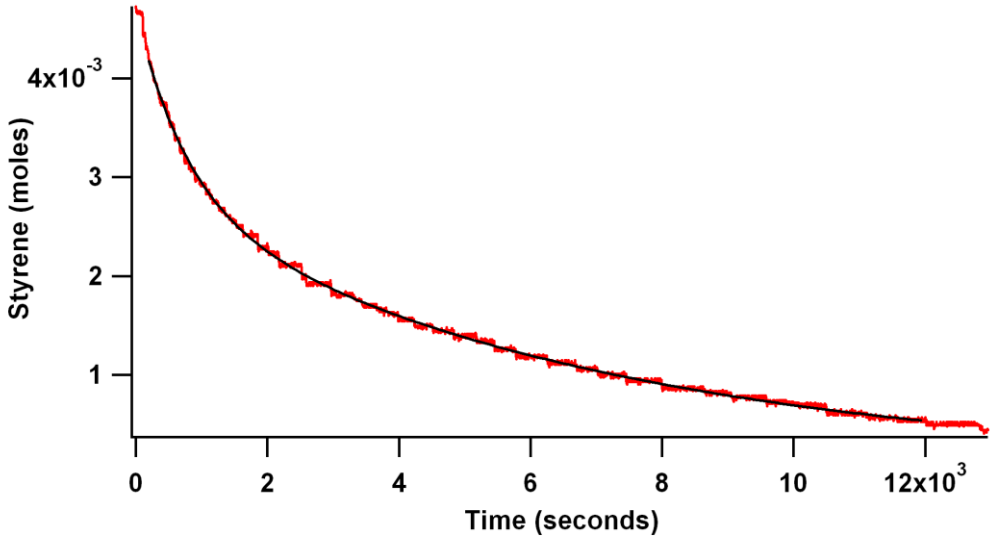

Figure 5.28: The methoxycarbonylation of styrene in a constant pressure reactor shown as the consumption of styrene as a function of time.

The reaction did not show a clear fit to a single exponential, particularly at higher substrate concentrations. The reaction was therefore checked using graphical rate equations similar to those used for the phenyl acetylene reactions.

The reaction was run in 10 ml of methanol, under constant pressure conditions, which gives pseudo zero order conditions in methanol and CO, allowing the order with respect to substrate to be determined.

The rate expression for the reaction is:

$$\text{Rate} = k\,[\text{styrene}]^{x}[\text{MeOH}]^{y}\text{pCO}^{z}$$

This can be simplified, owing to the pseudo zero order kinetics in methanol and zero order kinetics in pCO (constant pressure reaction), to:

$$\text{Rate} = k\,[\text{styrene}]^{x}$$

The rate was plotted as a function of styrene concentration and is shown in figure 5.29

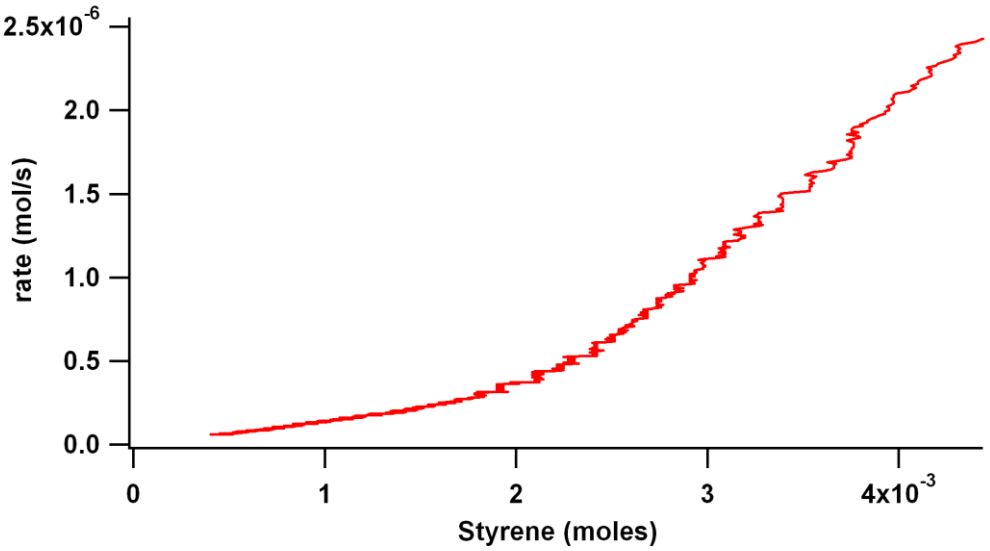

Figure 5.29: The rate as a function of substrate concentration for the methoxycarbonylation of styrene in 10 ml of methanol under constant pressure.

As the reaction showed a complex order in substrate, the natural log of the rate was plotted against the natural log of the styrene concentration to determine the order with both steps. This is shown in figure 5.30 with a linear fit at lower substrate concentrations showing the reaction is first order. A linear fit of the upper section of the graph indicates the reaction is initially 0.4 order in substrate concentration. This might suggest that the reaction is exhibiting saturation kinetics with a first order dependence at low substrate concentration tending towards zero order at higher substrate concentrations.

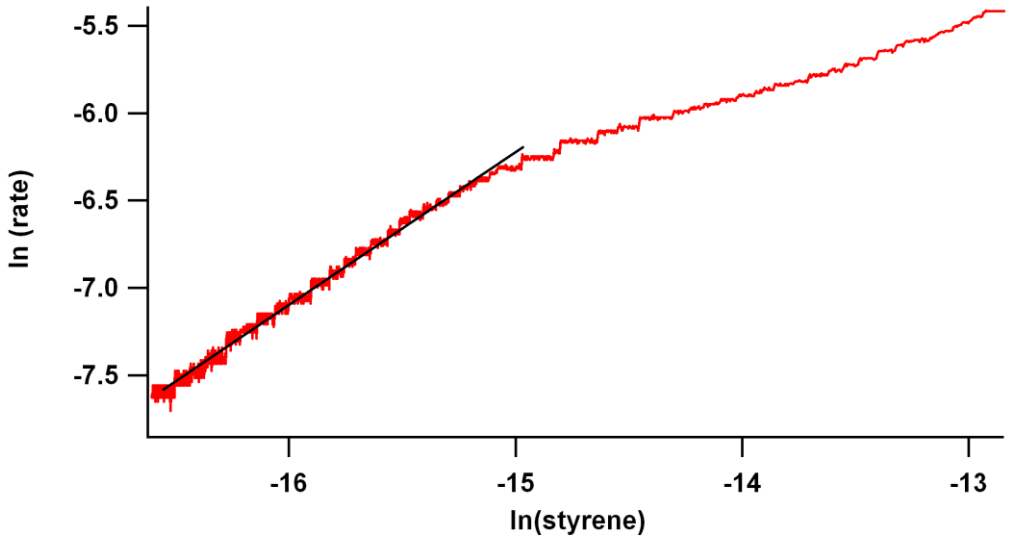

Figure 5.30: The log-log plot of the rate as a function of styrene concentration for the methoxycarbonylation of styrene.

When the methoxycarbonylation of styrene was compared to that of the phenyl acetylene, it was found that the phenyl acetylene reaction occurred much faster. The difference in the two reactions is shown in figure 5.31. This difference in reaction rate can be attributed to the ease of coordination of the triple bond as both reactions are run under pseudo zero order conditions in methanol and in pCO.

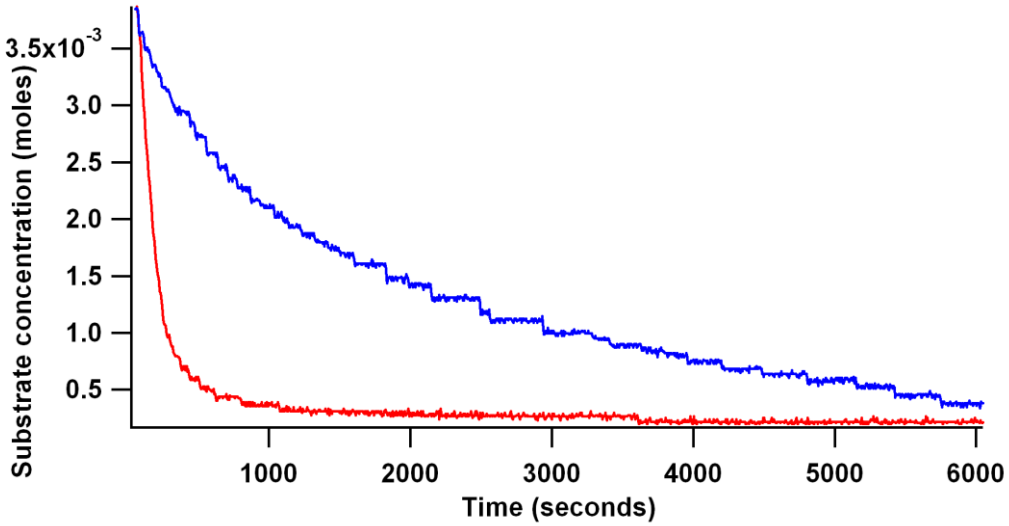

Figure 5.31: The substrate consumption comparison for the methoxycarbonylation of styrene (blue) and phenyl acetylene (red) as a function of time.

5.5.3 Linear Alkynes

It was postulated that the individual steps within the Pd/BDTBPMB/H^+ catalysed methoxycarbonylation of a linear alkynes could be studies separately. 1-octyne was initially used as the substrate with the aim of producing dimethyl decanedioate (Figure 5.32). This would potentially allow us to show the orders with respect to substrate and methanol for both carbonylation steps within the reaction.

Preliminary experiments were carried out to determine the product distributions for these reactions. These results are summarised in table 5. 1

Substrate	**[$Pd_2(dba)_3$] (mol %)**	**Time (h)**	**Ester Yield (%)**	**α,β-unsaturated ester (%)**	**Diester Yield (%)**	**α,ω-diester (%)**
1-butyne	0.1	0.5	100	83	0	0
1-butyne	0.1	3	0	0	>99	>99
1-pentyne	0.05	3	90	73	0	0
1-pentyne	0.25	3	0	0	>99	92
1-octyne	0.05	3	87	75	0	0
1-octyne	0.25	3	34	29	66	61
1-octyne	0.5	3	0	0	>99	85
1-octyne	0.25	14	0	0	>99	87

Table 5.1: The methoxycarbonylation of alkynes: Conditions: Substrate (9.1 mmol), [Pd_2dba_3] (as indicated), BDTBPMB/Pd mol ratio (6:1), MsOH/Pd ratio (30:1), T = 80ºC, pCO = 30 bar, MeOH (10 ml).

Initial batch reactions were run under constant pressure with higher concentrations of methanol to determine the order with respect to substrate for both steps of the reaction. The reactions were then run under lower methanol concentrations to establish the order in methanol.

5.5.3.1 Octyne

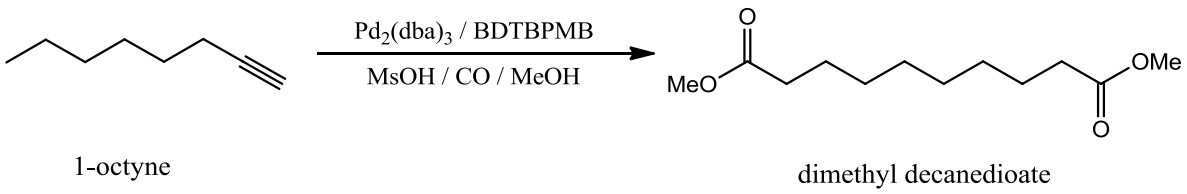

Figure5.32: The double methoxycarbonylation of 1-octyne.

The methoxycarbonylation of 1-octyne (1ml, 0.00678 mol) was run under the conditions detailed in chapter 6 and the consumption of CO as a function of time was recorded. This is shown in figure 5.33.

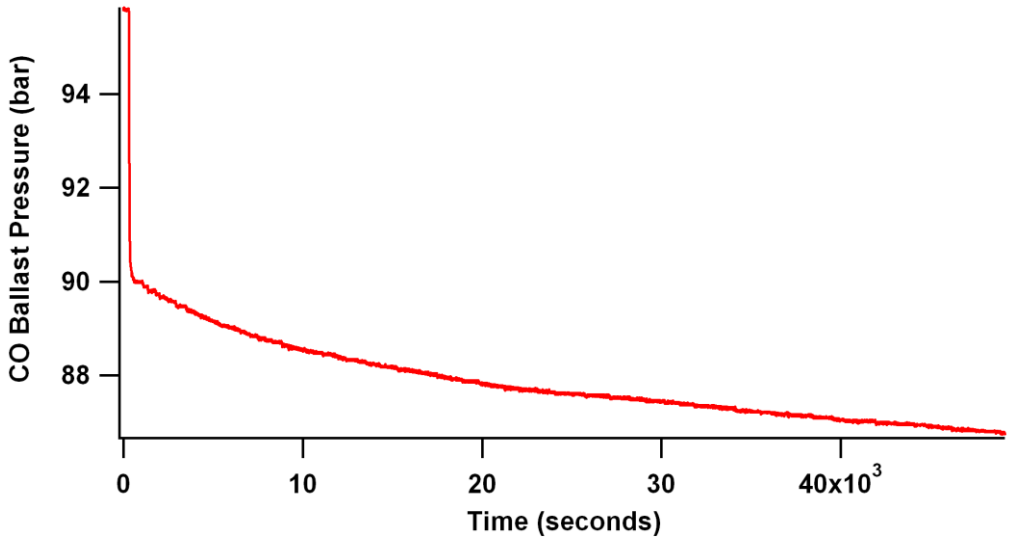

Figure 5.33: The methoxycarbonylation of 1-octyne in 10ml of methanol.

5.5.3.1.1: Octyne: Step One

It was found that, when the gas uptake for the methoxycarbonylation of 1-octyne was measured, the reaction progressed in two distinct stages. The first step of the reaction, the methoxycarbonylation of the triple bond, takes place very rapidly. This step was then

followed by a much slower second step which involves the tandem isomerisation and secondary methoxycarbonylation of the double bond of the methyl non-2-enoate intermediate. The double bond is trapped in the terminal position at the opposite end of the chain before methoxycarbonylation takes place.

It was found, when taking a closer look at the first step of the reaction that the methoxycarbonylation was very fast (complete within 1.5 min). The gas uptake plot is linear suggesting that this step of the reaction is gas transport limited.

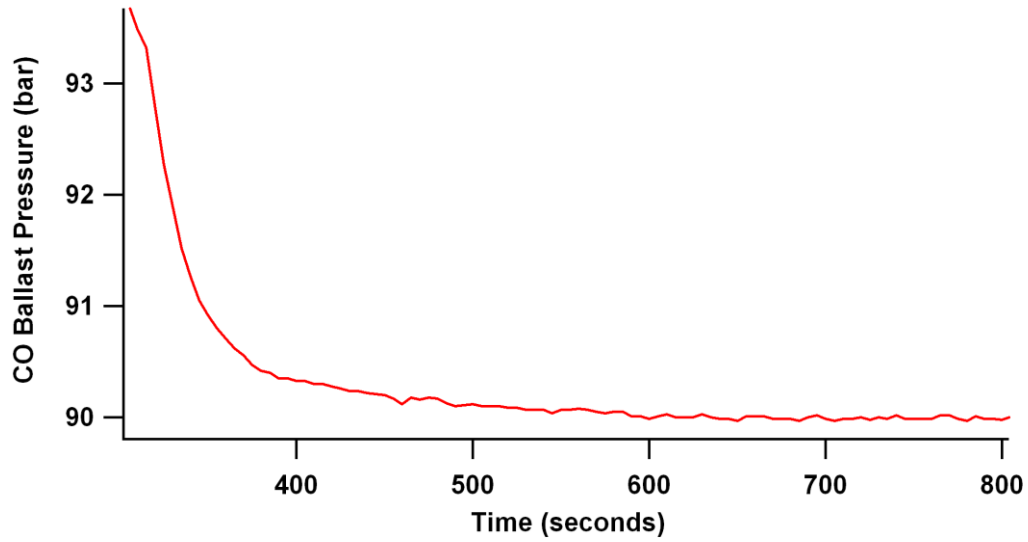

Figure 5.34: The first step of the methoxycarbonylation of 1-octyne in 10 ml of methanol. The initial slope is the injection of the substrate.

5.5.3.1.2 Octyne: The Second Step

As there was no way to quantify the rate of the first step of the reaction, the study was instead focussed on the second carbonylation step. The rate of the second step was thought to be limited by the rate of isomerisation of the double bond, produced from the first reaction, towards the terminal position at the opposite end of the chain. The initial experiment was run with 10 ml of methanol under constant CO pressure. The CO pressure in the ballast vessel from which the CO was being fed to the reactor as a function of time is shown in figure 5.35

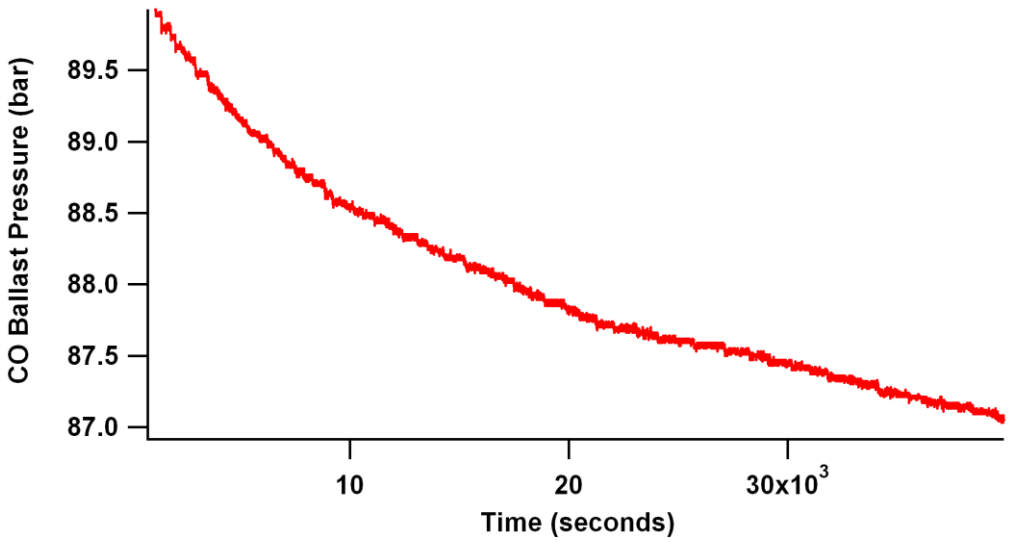

Figure 5.35: The second step of the methoxycarbonylation of methyl nonenoate with 10 ml of methanol.

The methyl nonenoate concentration was then plotted against time and was fitted with an exponential curve fit. The methyl nonenoate concentration against time and the methanol concentration against time are shown in figures 5.36 and 5.37. Note that methanol concentration only decreases by 3 % so it is safe to assume that the reaction is pseudo zero order in methanol.

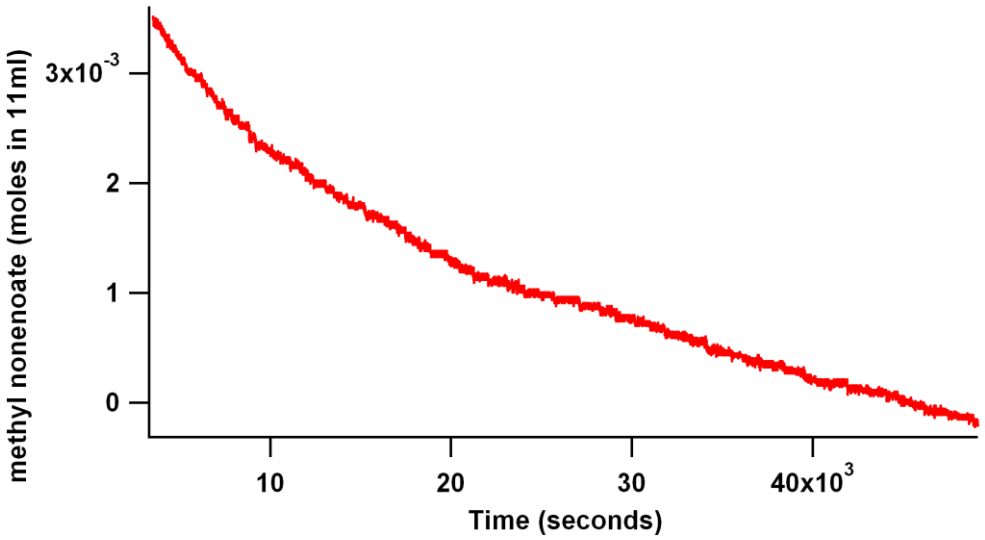

Figure 5.36: methyl nonenoate concentration as a function of time for the methoxycarbonylation of 1-octyne with 10 ml of methanol.

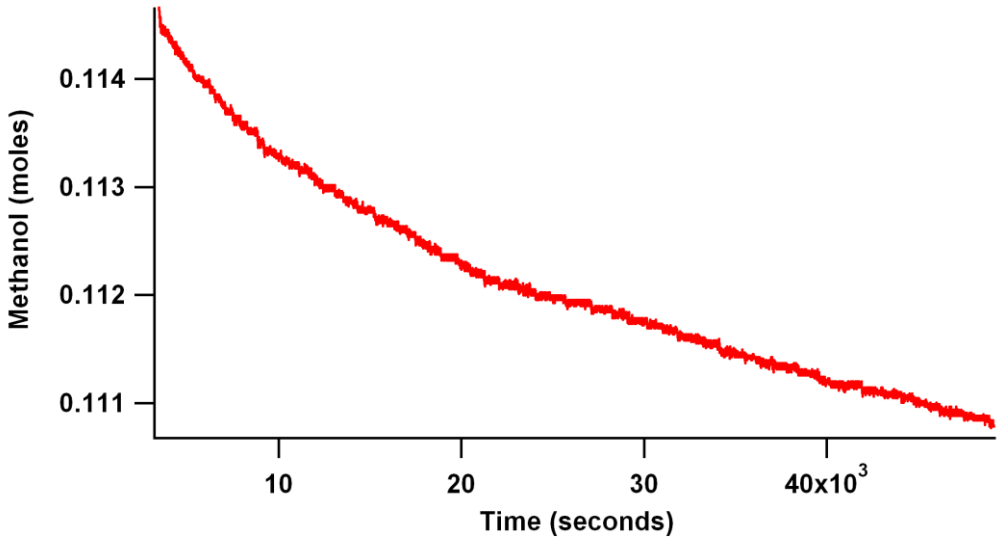

Figure 5.37: Methanol concentration as a function of time for the methoxycarbonylation of 1-octyne in 10ml of methanol.

The reaction rate was then plotted as a function of methyl nonenoate concentration and the reaction was shown to be first order in substrate concentration. This is shown in figure 5.38. This graph reads from right to left owing to the decrease in substrate concentration within this reaction.

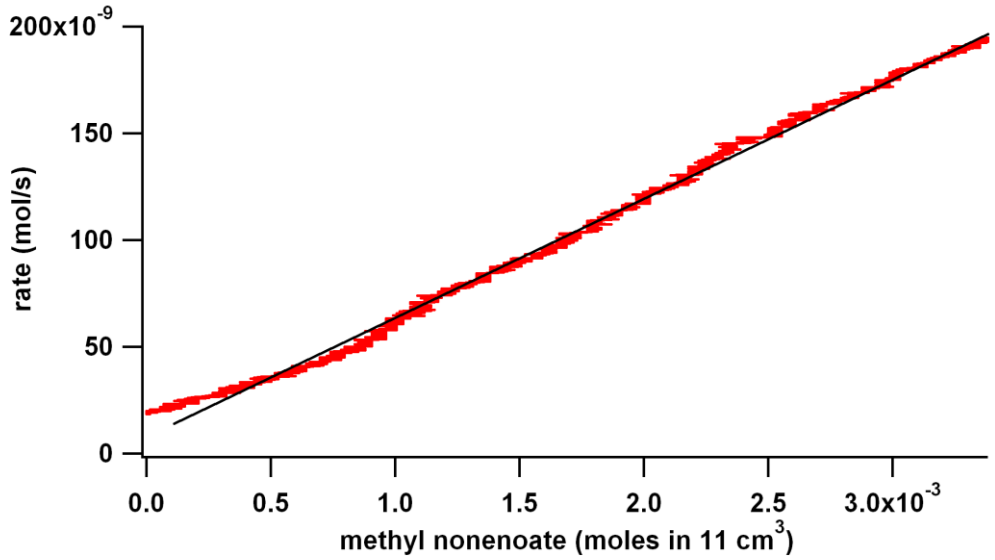

Figure 5.38: The rate as a function of methyl nonenoate concentration for the methoxycarbonylation of 1-octyne with 10 ml of methanol.

The amount of added methanol was varied between 10 and 4 ml and the reactions were run under the same conditions. It was found, when analysing the second steps of these reactions, that there was a large variability in the observed results. This has been attributed to running the reactions overnight. Figure 5.39 shows the involving 8 ml of methanol.

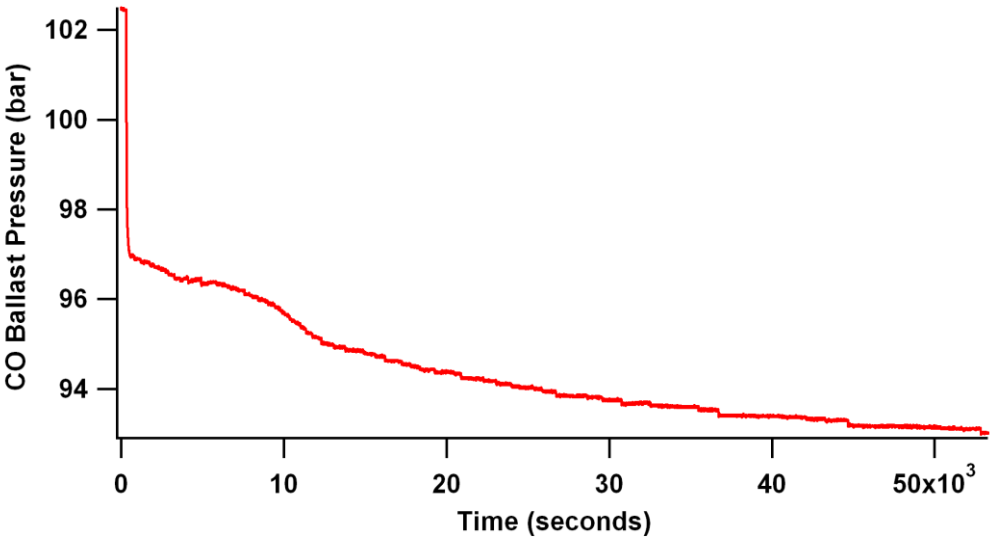

Figure 5.39: The methoxycarbonylation of 1-octyne in 8 ml of methanol.

When the reaction containing the 4ml of methanol was fitted with an exponential curve fit to establish the rate constant it was found that the rate was comparable to that of the 10 ml reaction.

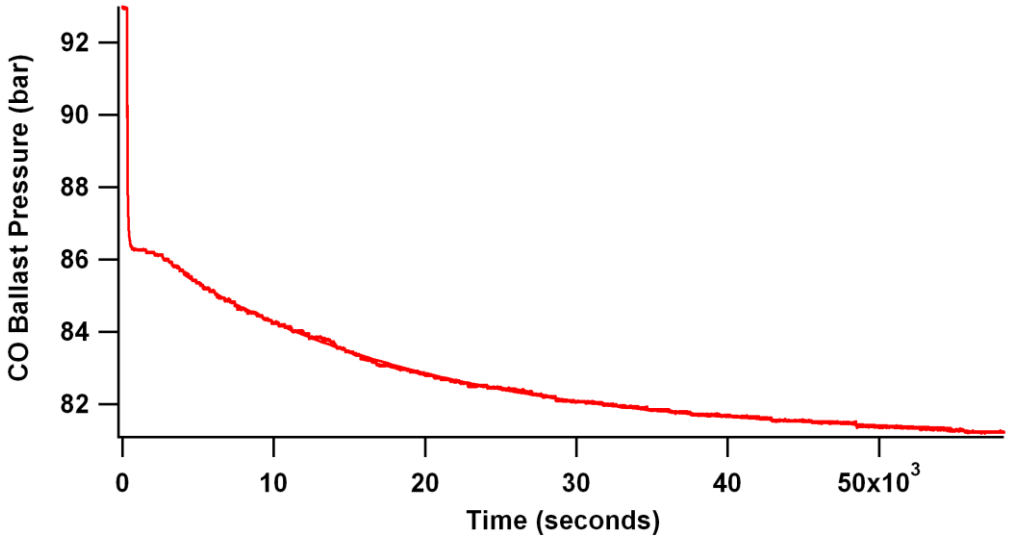

Figure 5.40: The methoxycarbonylation of 1-octyne in 4 ml of methanol.

The reactions involving 6 ml of methanol was also found to show a comparable rate to that of the 4 ml and 10ml reactions. This would indicate the second methoxycarbonylation step is zero order with respect to methanol concentration and the rate determining step was the isomerisation of the double bond from being conjugated with the ester group to the terminal position. The reaction with 4 ml of methanol was used to show the orders with respect to the substrate and methanol.

.

The rate expression for the reaction is:

$$\text{Rate} = k[\text{octyne}]^x[\text{MeOH}]^y p_{CO}{}^z$$

However, we have already established that the rate is first order in [octyne] (x = 1) and, since these reactions are carried out at constant pressure, we are working under zero order conditions for CO (z = 0).

The rate expression then reduces to

$$\text{Rate} = k'[\text{octyne}][\text{MeOH}]^y$$

The plot of rate as a function of substrate concentration is shown in figure 5.41. It is a straight line through the origin, suggesting that the overall order is 1 and hence that the order with respect to methanol is zero.

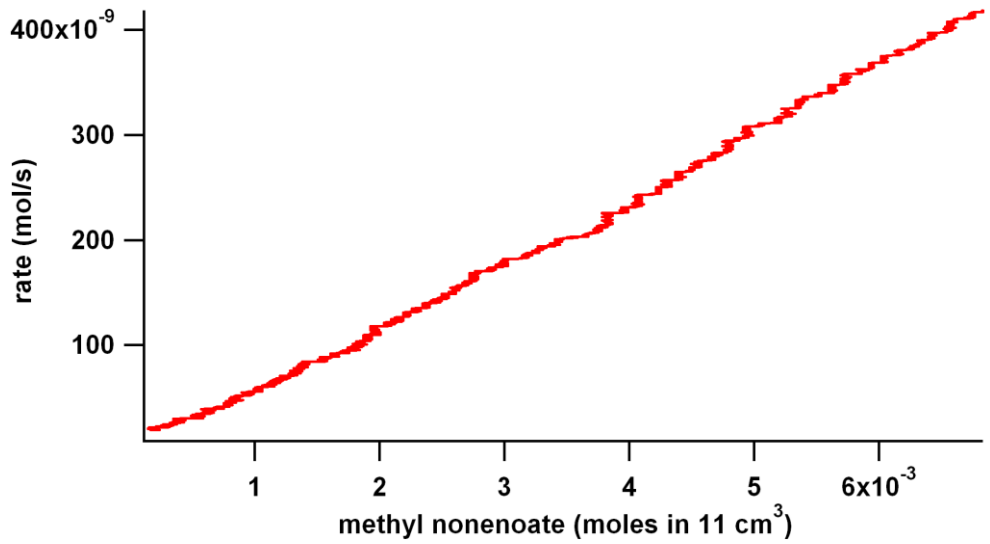

Figure 5.41: The reaction rate as a function of methyl nonenoate concentration to give the order with respect to methyl nonenoate concentration in 2 ml of methanol.

The rate divided by the methyl nonenoate concentration was plotted against the methanol to establish the rate in methanol and it was shown to be parallel to the x axis indicating zero order dependence in methanol concentration, figure 5.42.

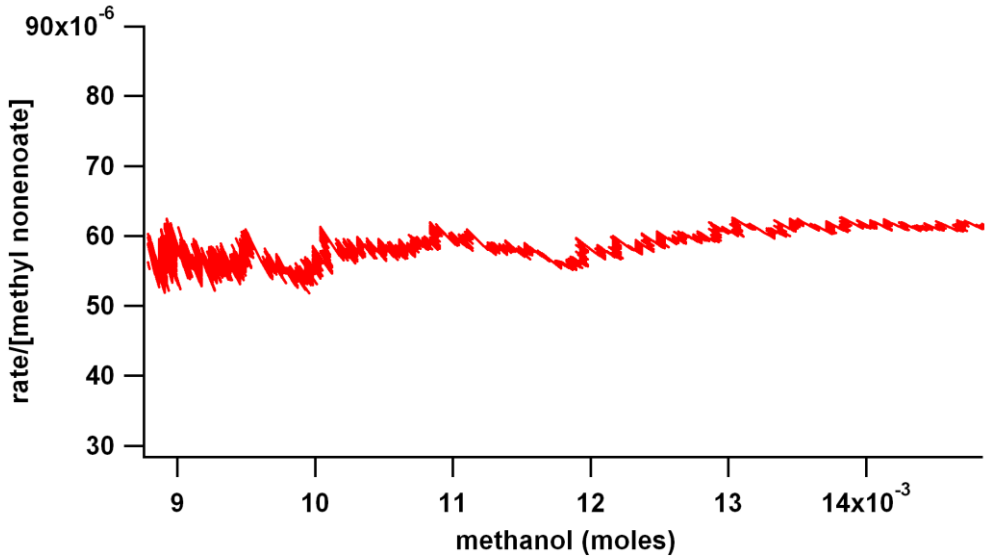

Figure 5.42: The reaction rate divided by the methyl nonenoate concentration as a function of methanol concentration to give the order with respect to methanol concentration for the methoxycarbonylation of 1-octyne in 4 ml of methanol.

5.5.3.2 Pentyne

When using octyne, it was noted that the reaction, required a long time (16 h) to carbonylate the second step of the reaction. It was postulated that if the chain length was shortened, the isomerisation steps required to create a terminal double bond would be less and as such, the second step of the reaction would proceed more quickly. However, it should be noted that in both cases conjugation of the double bond with the ester group needs to be broken.

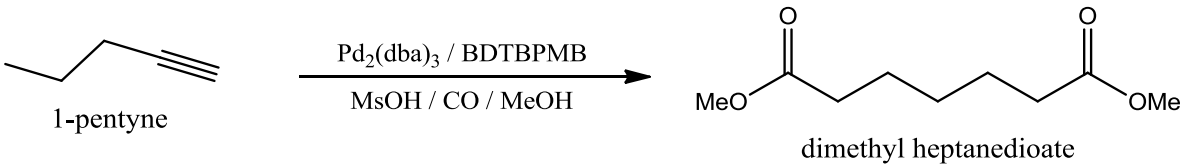

Figure 5.43: The methoxycarbonylation of pentyne to produce dimethyl hepantedioate.

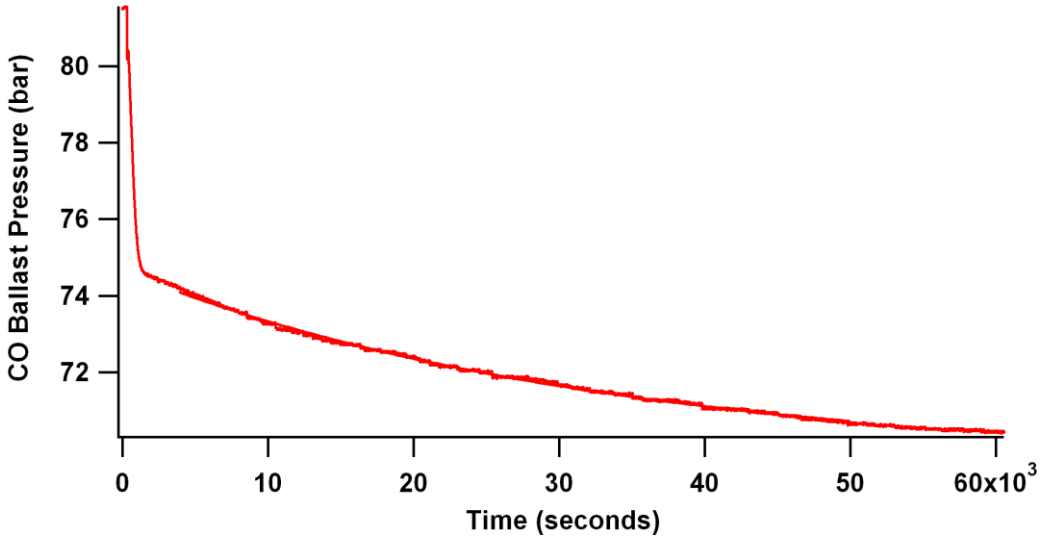

Figure 5.44: The double methoxycarbonylation of 1-pentyne.

The methoxycarbonylation of 1-pentyne was run overnight to establish the rate of the second step of the reaction, and again the reaction was monitored using gas uptake. It was again found that the first step proceeded very rapidly and was mass transport limited and that again the second step was very much slower (comparable to that with 1-octyne).

The methoxycarbonylation of 1-pentyne in 10 ml of methanol was used to determine the order in methyl hexenoate concentration. It was found that the reaction was first order in substrate. This is shown in figure 5.45.

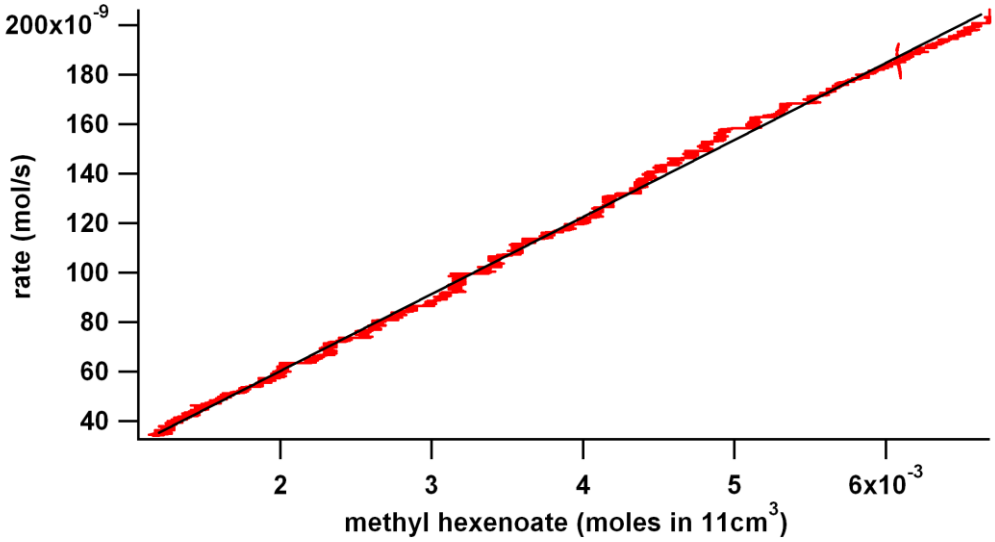

Figure 5.45: The rate as a function of the substrate concentration for the methoxycarbonylation of methyl hexenoate in 10 ml of methanol.

The reaction was fitted with a straight line which runs through the origin confirming that the reaction is first order in substrate. The methoxycarbonylation of methyl hexenoate in 4 ml of methanol was used to determine the order in methanol concentration. The reaction rate was plotted as a function of methyl hexenoate concentration and found to fit to a straight line running through the origin. This graph, figure 5.45, showed that the reaction was first order in substrate.

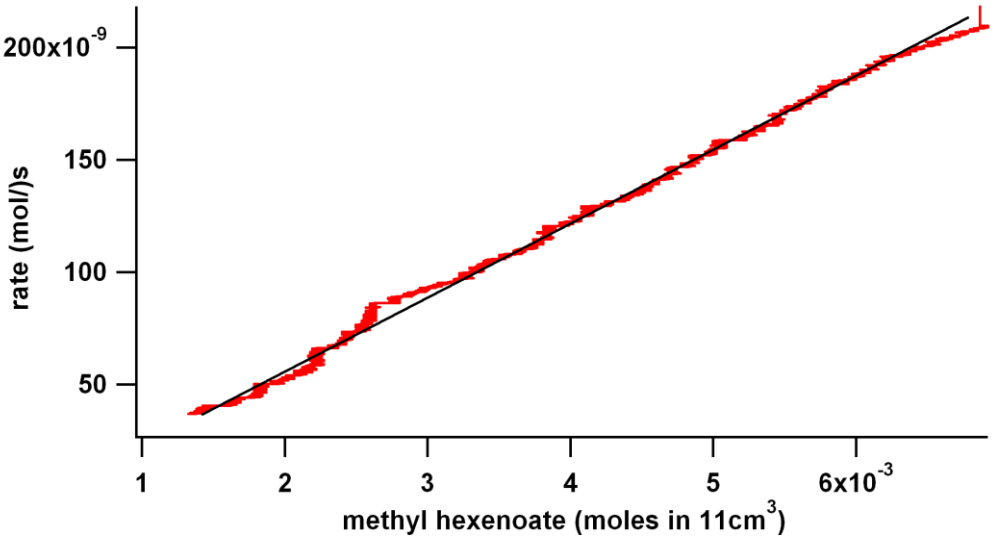

Figure 5.46: The rate as a function of the substrate concentration for the methoxycarbonylation of 1-pentyne in 4 ml of methanol.

The rate divided by the substrate concentration as a function of the methanol concentration was then plotted to show the reaction to be zero order in methanol concentration. The very long reaction times mean that significant temperature changes occur in the ballast vessel and these are probably responsible for the unusual shape of the plot at low methanol concentration.

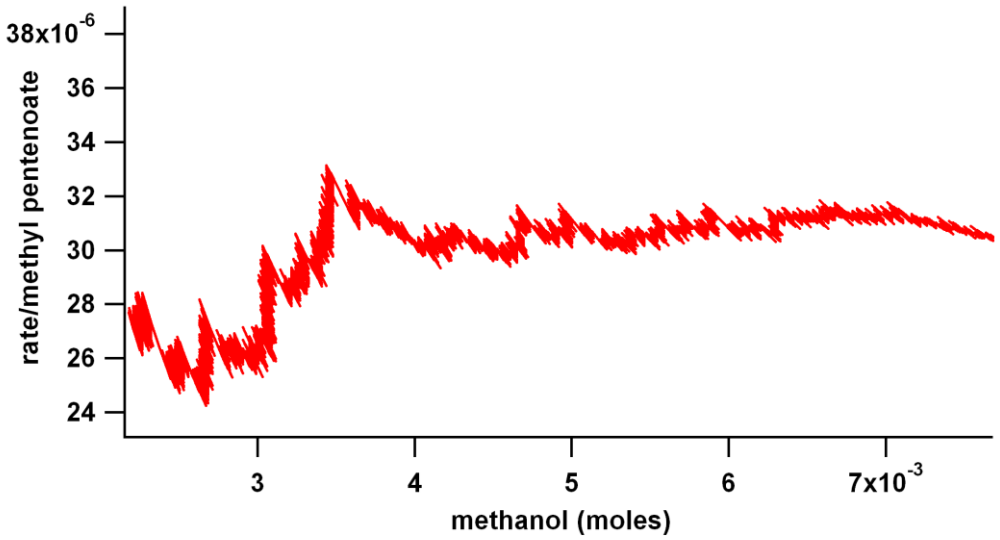

Figure 5.47: The reaction rate divided by the methyl hexenoate concentration as a function of methanol concentration to give the order with respect to methanol concentration for the methoxycarbonylation of 1-pentyne in 2 ml of methanol.

5.5.3.3 Substrate Comparison

As both systems (pentyne and octyne methoxycarbonylation) have been found to be zero order in methanol concentration, but first order in substrate, it is reasonable to propose that the rate determining step of the second methoxycarbonylation step is isomerisation of the double bond to the terminal position. This might be expected to result in the an increase in rate for the methoxycarbonylation of methyl hexenoate compared to methyl nonenoate, owing to the lower number of isomerisation steps required to produce a terminal double bond. The CO consumption per mole of alkyne consumed for both 1-octyne and 1-pentyne are shown in figure 5.48. In each case the first methoxycarbonylation step was ignored as mass transport limitations meant that it was difficult to extract any information from the observed uptakes. For the second step, the rates are comparable (pseudo first order rate constants of 5 $x10^{-5}$ for octyne and 4 x 10^{-5} for pentyne) perhaps suggesting that the actual rate determining step is that involving removal of the double bond from conjugation with the ester group in the α,β-unsaturated ester.

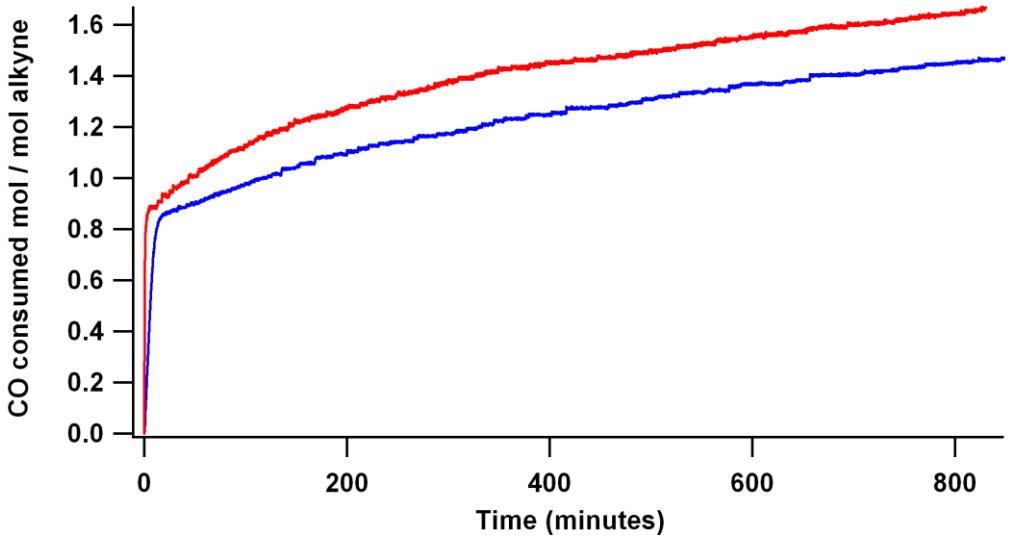

Figure 5.48: The comparison of the CO uptakes in the methoxycarbonylation of 1-octyne (red) and 1-pentyne (blue).

5.5.3.4 1-butyne

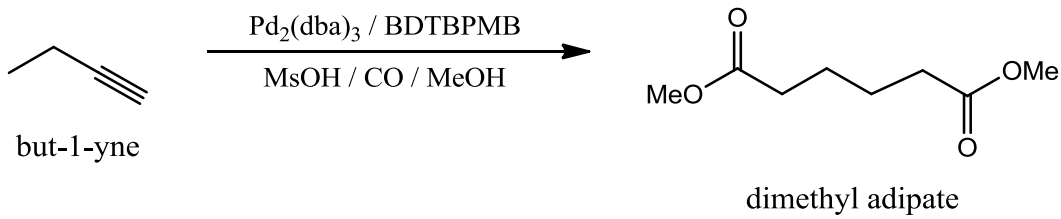

Figure 5.49: The double methoxycarbonylation of but-1-yne.

The methoxycarbonylation of 1-butyne was of particular interest as the linear product of the dual carbonylation, dimethyl 1,6- hexandioate is one of the precursors of nylon 6.6. Despite this, the volatility of this substrate meant that it was a particularly difficult substrate to manipulate under the conditions used with the reactor set up. However, slight modifications to the methodology used meant that some results were produced.

It was found that 1-butyne reacts extremely rapidly (gas transport limited) to give methyl 2-pentenoate with 83% selectivity, together with unconjugated linear isomers and small

amounts of the branched product, methyl 2-methyl-2-butenoate. It was found that after longer reaction times (3 hours), dimethyl 1,6-hexandioate was produced with excellent yield and selectivity (both >99%) This is shown in table 5.1.

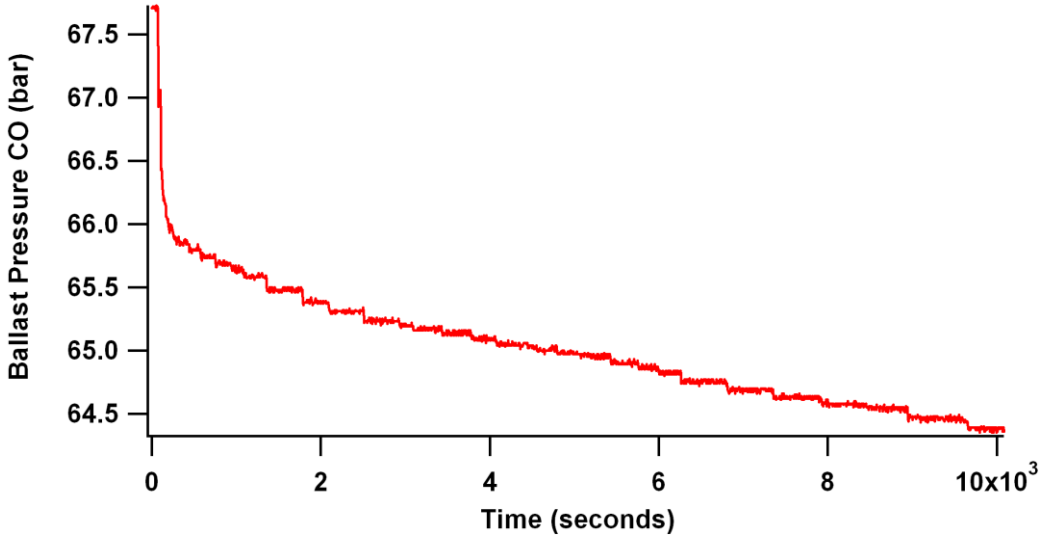

Figure 5.50: Gas uptake plot of the methoxycarbonylation of 1-butyne.

5.5.4 Internal alkynes

Previous studies by Cole-Hamilton *et al*, [48, 49, 53] have shown that palladium complexes containing 1,2-bis(di*tert*butylphosphinomethyl)benzene can effectively methoxycarbonylate a substrate irrespective of the position of the double bond on a chain, even when the double bond is in a conjugated position and/or far from the unsubstituted end of the chain. It was of interest to know what would happen with internal alkynes, since isomerisation of the triple bond is not usually very accessible in internal alkynes. The gas uptake and product distribution of 2-butyne and 4-octyne were studied, to determine the impact of chain length on product distribution.

5.5.4.1 2-butyne

The methoxycarbonylation of 2-butyne, gave a mixture of the two dicarbonylation products, dimethyl 2-methylpentane-1,5-dioate and dimethyl 2-ethylbutane-1,4-dioate.

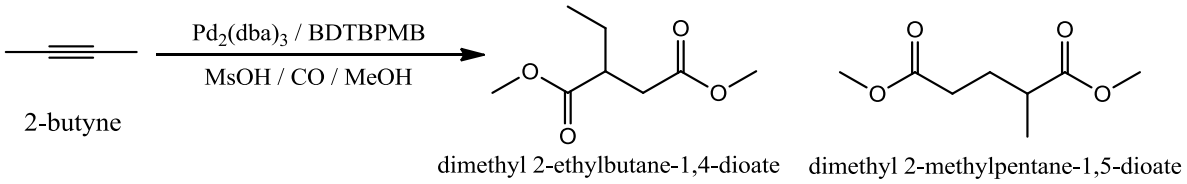

Figure 5.51: The double methoxycarbonylation of but-2-yne in 10 ml of methanol at pCO of 30 bar and 80˚C.

This reaction was also followed using gas uptake. If the reaction was stopped after 3 hours, small amounts of methyl 2-methylbutenedioates were observed (Figure 5.52).

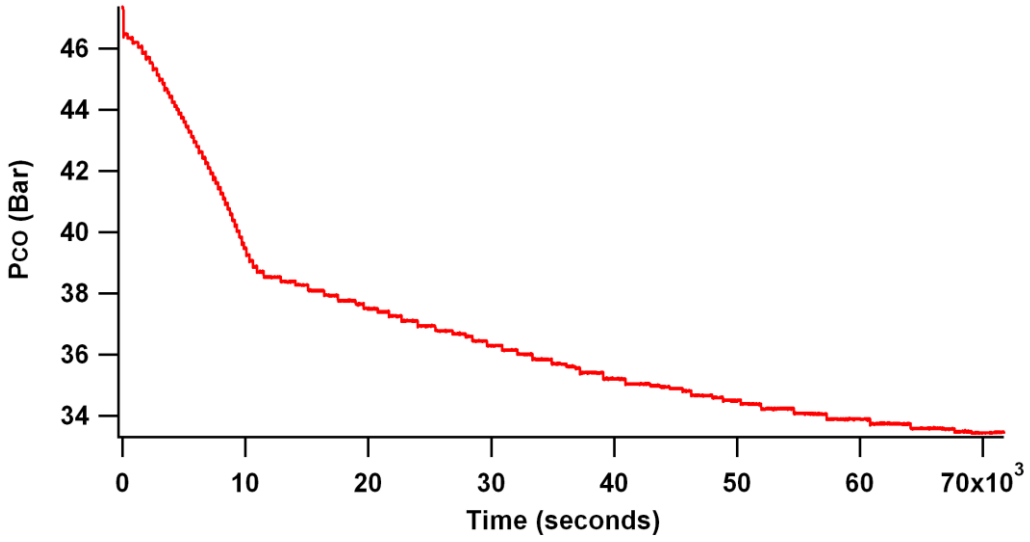

Figure 5.52: Gas uptake plot of the methoxycarbonylation of 2-butyne.The two stages of the reaction are clearly visible. The first step is again very rapid despite the triple bond being located in the middle of the chain.

Evidently, the double bond in the intermediate unsaturated ester migrates to either end of the chain where it is trapped and carbonylated. It was found that isomerisation away from the quaternary centre rather than past it is preferred.

5.5.4.2 4-Octyne

When considering longer chain internal alkynes, it was postulated that this two step reaction could be hindered by the increased chain length and its effects on the capability for the catalyst to carry out the isomerisation step. The methoxycarbonylation of 4-Octyne yielded exclusively the α,β-unsaturated mono ester, methyl 2-propylhex-2-enoate.

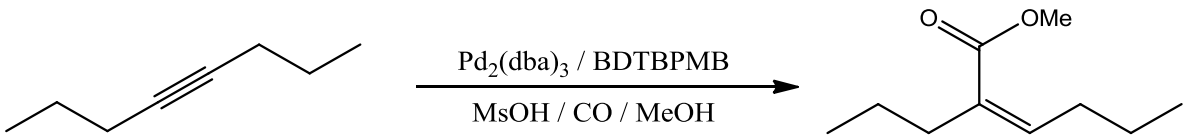

Figure 5.53: The methoxycarbonylation of 4-octyne

No isomers of this product were detected, presumably because the tri-substituted conjugated double bond is thermodynamically favoured. The failure to observe dicarbonylation products means that the equilibrium concentration of terminal alkene as a result of isomerisation is extremely small owing to the blocking of the isomerisation by conjugation and steric factors.

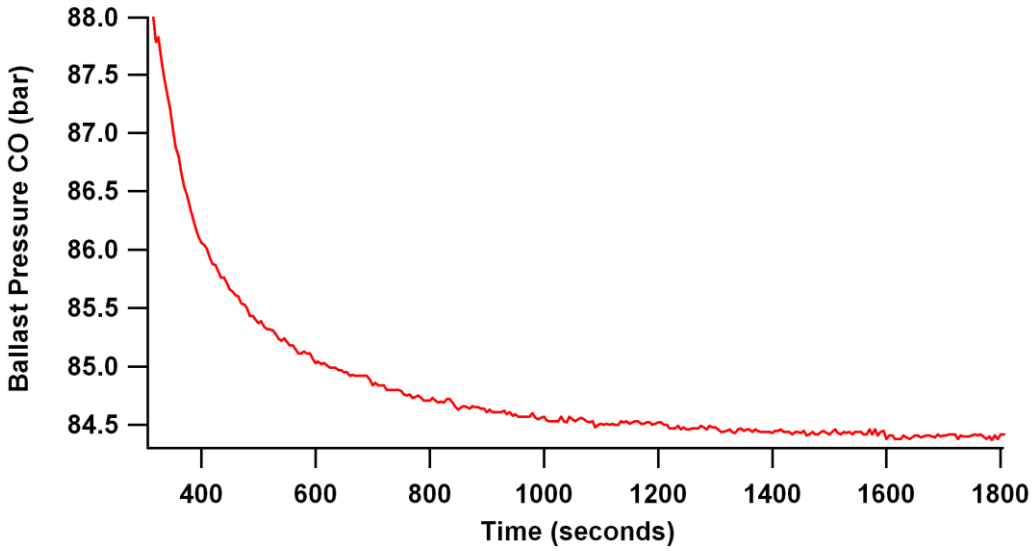

Figure 5.54: Gas uptake plot of the methoxycarbonylation of 4-octyne.

The gas uptake plot of this reaction is shown in figure 5.54, and shows that again the carbonylation of the alkyne is a very fast step and over within minutes. The initial uptake appears zero order in 4-octyne concentration and as the substrate is consumed, the order changes to first order. When the reaction was run for longer times, none of the di-substituted product was seen in the crude mixture.

5.6 Discussion

The methoxycarbonylation of alkynes when catalysed by palladium complexes based on BDTBPMB led mainly the generation of linear products. To understand the reason for the change in product distribution compared with that of most literature examples brought on by utilising this system, the mechanism must be taken into consideration. As has previously been described by Eastham *et al* [54, 55] there are two distinct mechanistic pathways known for methoxycarbonylation reactions, the hydride and alkoxy (carbomethoxy) mechanisms. These are shown in figure 5.55.

The alkoxy mechanism starts off when the phenyl acetylene reacts with an acylpalladium species **2** (formed by the coordination and insertion of CO to the alkoxypalladium species **1**). This then generates the intermediates **3** and **4,** which, in turn undergo a reaction with

methanol to produce the final linear and branched products **6** and **5**, and regenerate the alkoxypallidium species **6**. The hydride mechanism starts with the protonation of the pre-catalyst to produce a catalytically active palladium hydride species, **8**. The palladium hydride then migrates onto the phenyl acetylene to produce species **9** and **10**. These then undergo CO insertion and methanolysis to produce the final products **5** and **6** and regenerate the palladium hydride species, **8**.

The main difference between these two reaction mechanisms is the C-C bond formation. The steric bulk brought on by the ligand attached to the palladium centre results in the 1, 2-insertion to give intermediates **3** and **9** being considered more favourable than 2, 1-insertion to give **4** and **10**. The palladium will orientate itself as far from the phenyl group as possible to reduce the overall steric hindrance. This 1, 2-insertion leads to different regiochemistry in the final product dependant on which mechanism takes place within the reaction.

It can therefore be explained that the alkoxy mechanisms generates the branched products whereas the hydride mechanism produces linear products. This suggests that; when methoxycarbonylation is catalysed by palladium complexes bearing ligands such as diphenyl-2-pyridylphosphine; the reaction follows the alkoxy mechanism and forms the branched product [2a, b, 3a] whereas when the reaction is catalysed by palladium complexes based on BDTPMB. The predominant mechanism in operation is the hydride, leading the formation of linear isomer. As with alkenes, it seems that the hydride mechanism is preferred, when using BDTBPMB as the ligand to palladium.

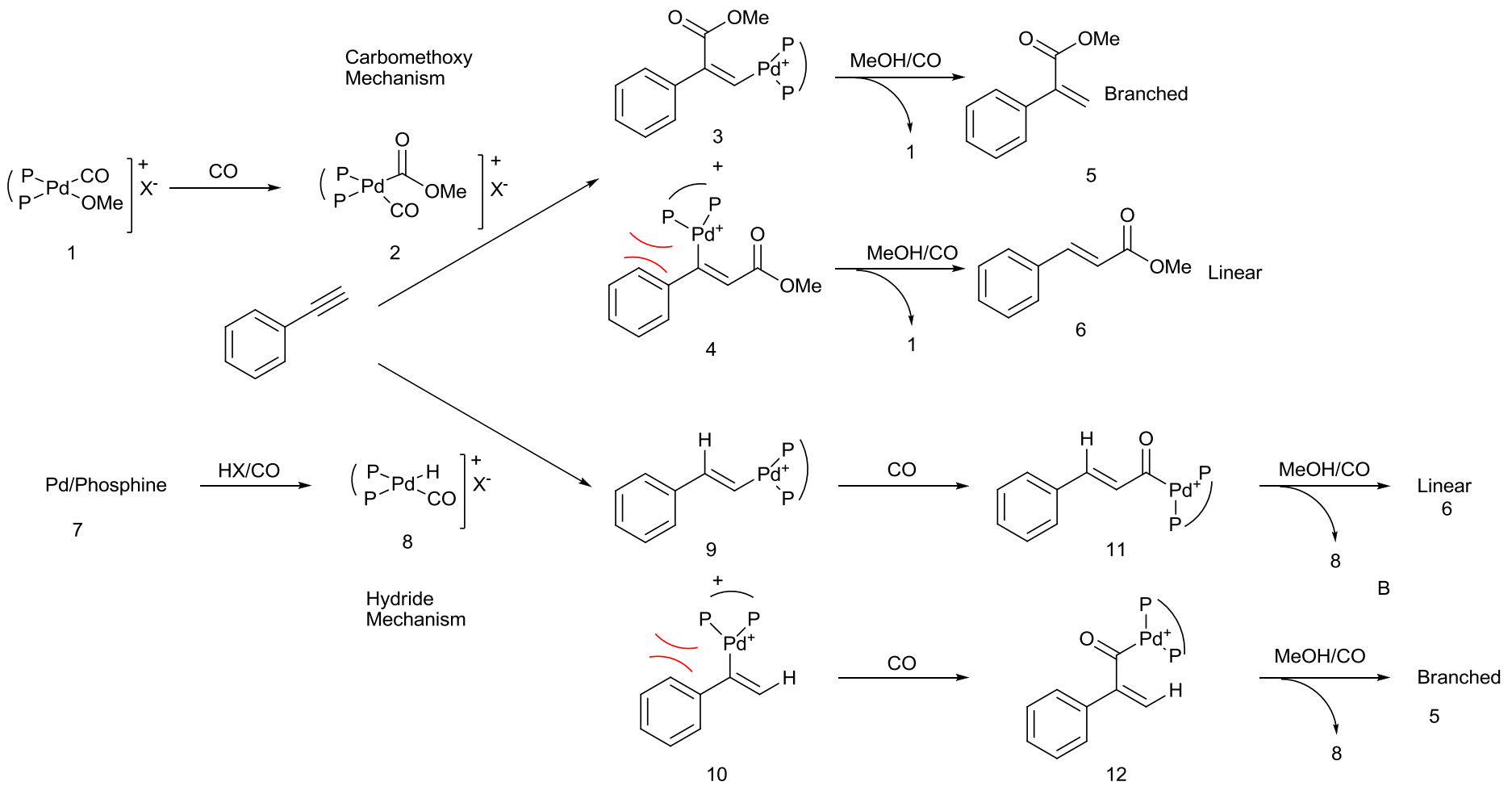

Figure 5.55: The mechanistic pathways of the methoxycarbonylation of phenyl acetylene showing how different mechanistic pathways result in different final product distributions. It is found that the alkoxy mechanism results in predominantly branched product formation whereas the hydride mechanism results in predominantly linear products.

5.7 References

1 E. Drent, P. Arnoldy, and P. H. M. Budzelaar, *J. Organomet. Chem.*, 1993, **455**, 247.
2 E. Drent, P. Arnoldy, and P. H. M. Budzelaar, *J. Organomet. Chem.*, 1994, **475**, 57.
3 E. Drent, W. W. Jager, and J. C. L. Suykerbuyk, 1995.
4 E. Drent and D. H. L. Pello, 1995.
5 E. Drent and W. W. Jager, USA, 1998.
6 A. Dervisi, P. G. Edwards, P. D. Newman, and R. P. Tooze, *J. Chem. Soc., Dalton Trans.*, 2000, 523.
7 A. Dervisi, P. G. Edwards, P. D. Newman, R. P. Tooze, S. J. Coles, and M. B. Hursthouse, *J. Chem. Soc., Dalton Trans.*, 1999, 1113.
8 B. E. Ali and H. Alper, *J. Mol. Cat.*, 1991, **67**, 29.
9 K. Itoh, M. Miura, and M. Nomura, *Tetrahedron Lett.*, 1992, **33**, 5367.
10 Y. Kushino, K. Itoh, M. Miura, and M. Nomura, *J. Mol. Cat.*, 1994, **89**, 151.
11 M. T. Reetz, R. Demuth, and R. Goddard, *Tetrahedron Lett.*, 1998, **39**, 7089.
12 A. Scrvanti, V. Beghetto, E. Campagna, M. Zanato, and U. Matteoli, *Organometallics*, 1998, **17**, 630.
13 S. Jayasree, A. Seayad, S. P. Grupte, and R. V. Chaudhari, *Cat. Lett.*, 1999, **58**, 213.
14 A. Scrivanti, V. Beghetto, M. Zanato, and U. Matteoli, *J. Mol. Cat. A. Chem.*, 2000, **160**, 331.
15 M. Akao, S. Sugawara, K. Amino, and Y. Inoue, *J. Mol. Cat. A. Chem.*, 2000, **157**.
16 A. Scrivanti, U. Matteoli, V. Beghetto, S. Antonaroli, R. Scarpelli, and B. Crociani, *J. Mol. Cat. A. Chem.*, 2001, **170**, 51.
17 M. L. Clarke, D. J. Cole-Hamilton, D. F. Foster, A. M. Z. Slawin, and J. D. Woolins, *J. Chem. Soc., Dalton Trans.*, 2002, 1618.
18 J. J. M. d. Pater, E. P. Maljaars, E. d. Wolfe, M. Lutz, A. L. Spek, B. Deelman, C. J. Elseveir, and G. V. Koten, *Organometallics*, 2005, **24**.
19 T. Hiyama, N. Wakasa, T. Ueda, and T. Kusumoto, *Bull. Chem. Soc. Jpn.*, 1990, **63**, 640.
20 H. Yu and H. Alper, *J. Org. Chem.*, 1997, **62**, 5684.
21 K. Tezuka, Y. Ishizaki, and Y. Inoue, *J. Mol. Cat. A. Chem.*, 1998, **129**, 199.
22 Y. Fukuta, I. Matsuda, and K. Itoh, *Tetrahedron Lett.*, 2001, **42**, 1301.
23 A. F. Littke and G. C. Fu, *Angew. Chem: Int. Ed.*, 2002, **41**.
24 I. P. Beletskaya and A. V. Cheprakov, *Chem. Rev.*, 2000, **100**, 3009.
25 A. B. Dounay and L. E. Overman, *Chem. Rev.*, 2003, **103**, 2945.
26 M. A. Fox and J. K. Whitesell, 'Organic Chemistry', Jones and Bartlett Publishers, 1997.
27 K. N. Campbell and B. K. Campbell, *Org. Synth.*, 1963, **4**, 763.
28 G. Kobrich, *Angew. Chem: Int. Ed.*, 1965, **4**, 49.
29 E. J. Corey and P. L. Fuchs, *Tetrahedron Lett.*, 1972, **13**, 3796.
30 D. Seyforth, R. S. Marmor, and P. Hilbert, *J. Org. Chem.*, 1971, **36**, 1379.
31 J. C. Gilbert and U. Weerasooriya, *J. Org. Chem.*, 1982, **47**, 1837.
32 C. A. Brown and A. Yamashita, *J. Am. Chem. Soc.*, 1975, **97**, 891.
33 W. Reppe, *Liebigs Ann. Chem.*, 1953, **582**, 1.
34 A. Muller, 'New Synthesis with Carbon Monoxide', ed. J. Falbe, Springer, 1980.

[35] B.Blumenberg, *Nachr. Chem. Tech. Lab*, 1984, 480.
[36] N. v. Kutepow, 'Ullmann's Encyclopedia of Industrial Chemistry', 1973.
[37] C. D. Frohling and C. W. Kohlpaintner, 'Applied Homogeneous Catalysis with Organometallic Compounds', ed. B. Cornils and W. A. Herrmann, Wiley-VCH, 1996.
[38] W. Reppe, *Justus Leibigs Ann. Chem.*, 1856, **601**, 84.
[39] D. Steinborn, T. Rosenstock, H. Mosinski, and R. Nuenthel, *Proc. Conf. Coord. Chem.*, 1991, **13**, 265.
[40] Y. Kataoka, O. Matsumoto, M. Ohashi, and T. Yamagata, *Chem. Lett.*, 1994, 1283.
[41] 'Propylene and its Industrial Derivatives', ed. D. J. Hadley and E. G. Hancock, Halstead Press, 1973.
[42] W. Reppe, *Liebigs Ann. Chem.*, 1956, **601**, 88.
[43] T. Tsuda, T. Kujor, and T. Saegusa, *J. Org. Chem.*, 1990, **55**, 2554.
[44] B. M. Trost, G. Dyker, and R. J. Kulawiec, *J. Am. Chem. Soc.*, 1990, **112**, 7809.
[45] B. M. Trost and U. Katzmaier, *J. Am. Chem. Soc.*, 1992, **114**.
[46] B. M. Trost and C.-J. Li, *J. Am. Chem. Soc.*, 1994, **116**, 3167.
[47] B. M. Trost and C.-J. Li, *J. Am. Chem. Soc.*, 1994, **116**, 10819.
[48] C. Jimenez-Rodriguez, D. F. Foster, G. R. Eastham, and D. J. Cole-Hamilton, *Chem. Commun.*, 2004, 1720.
[49] C. Jimenez-Rodriguez, G. R. Eastham, and D. J. Cole-Hamilton, *J. Chem. Soc., Dalton Trans.*, 2005, 1826.
[50] I. d. Rio, C. Claver, and P. W. N. M. v. Leeuwen, *Eur. J. Inorg. Chem.*, 2001, **11**, 2719.
[51] C. Godard, B. K. Munoz, A. Ruiz, and C. Claver, 2008, 853.
[52] A. A. Nunez-Magro, L. M. Robb, P. J. Pogorzelec, A. M. Z. Slawin, G. R. Eastham, and D. J. Cole-Hamilton, *Chem. Sci.*, 2010, **1**, 723.
[53] C. Jimenez-Rodriguez, G. R. Eastham, and D. J. Cole-Hamilton, *Inorg. Chem. Commun.*, 2005, **8**, 878.
[54] W. Clegg, G. R. Eastham, M. R. J. Elsegood, B. T. Heaton, J. A. Iggo, R. P. Tooze, R. Whyman, and S. Zacchini, *Organometallics*, 2002, **21**, 1832.
[55] G. R. Eastham, B. T. Heaton, J. A. Iggo, R. P. Tooze, R. Whyman, and S. Zacchini, *Chem. Commun.*, 2000, 609.

Chapter 6: Experimental

6.1 Chemicals and Equipment

All manipulations of air-sensitive materials were performed in oven-dried glassware using standard Schlenk line and catheter tubing techniques, under a dry and deoxygenated nitrogen atmosphere. All liquids and solutions were transferred via syringe or cannula through a septum. The nitrogen was dried through a chromium (II) silica glass column.

The precious metal complexes $Pd_2(dba)_3$, $Rh(CO)_2(acac)_2$ and $RhCl_3(H_2O)$ were purchased from Alfa Aesar. Triphenylphosphine, 1-octyne, 1-pentyne, 1-butyne, 2-butyne, phenylacetylene and vinyl acetate from Aldrich and used as received. All gases used were purchased from BOC. 1,2-bis(di-*tert*-butylphosphinomethyl)benzene was provided by Lucite International.

All solvents were purchased from Fischer Scientific. Toluene was dried and degassed over sodium under an argon atmosphere. Methanol was refluxed over magnesium and distilled under argon. 1-butyne, 2-butyne and 1-pentyne were stored at 0 ˚C under nitrogen and phenylacetylene and vinyl acetate were stored under nitrogen in a freezer in a flask wrapped in aluminium foil to exclude light.

1-octene was purchased from Acros. Before use, it was treated to remove hydroperoxides, which have been known to form into alkenes once they have been exposed to air and can cause unwanted oxidation of products during reactions.[1] The octene was degassed by bubbling argon through it for 30 minutes. The octene was then transferred via cannula to a Schlenk tube containing a saturated solution of ferrous ammonium sulphate in water. The Schlenk tube was then shaken, the phases were allowed to separate and the organic phase was removed via cannula and run through a degassed column packed with alumina, under a stream of argon before being collected and stored under argon.

Gas chromatographic analysis was carried out on a Hewlett-Packard 5890 series gas chromatograph equipped with both a flame ionisation detector (GC-FID) and a Hewlett-Packard 5890 series mass selective detector for qualitative analysis (GC-MS). The gas

chromatograph has a Hewlett-Packard Chemstation installed for the determination of peak areas by electronic integration. Both the GC-MS and GC-FID determination of products employed a Supeclo^{TM} MDN-35 [bonded and crosslinked, 35% phenyl / 65% methylpolysiloxane] fused silica capillary column 30m x 0.25 mm x 0.25 μm film thickness. The carrier gas used was helium and the flow rate for GC-MS was 0.8 cm^3 min^{-1}. The method for MS was 40˚C for 5.6 minutes, then a ramp rate of 20˚C min^{-1} up to 120˚ and hold for 2.4 minutes before ramping the temperature at a rate of 20˚C min^{-1} to 300˚C and holding for 11 minutes.

6.2 Catalysis Reactions

6.2.1 Example of a Reaction in a High-Pressure Autoclave

The standard procedure for the use of a high-pressure autoclave is described. The substituent quantities vary depending on the reaction being carried out and will be shown for each individual experiment detailed below.

Tris(dibenzylideneacetone)dipalladium (47.5 mg, 0.05 mmol) was weighed into a Schlenk tube in a glove box along with 1,2-bis(di-*tert*-butylphosphinomethyl)benzene (197 mg, 0.5 mmol). The flask was then removed from the glove box and attached to a Schlenk line. Methanol (10 cm^3) was added followed by methanesulphonic acid (32 μl, 0.5 mmol). The mixture was heated gently and stirred until the entire solid had dissolved. The resulting solution was transferred via cannula to a degassed Hastelloy autoclave fitted with a PTFE o-ring, which contained a magnetic stirrer and had been previously cleaned with acid, water and acetone and dried in an oven.

Vinyl acetate (1 cm^3, 25 mmol) was injected under a flow of gas into the autoclave, which was then closed and pressurised to 20 bar. The autoclave was heated to 80 ˚C and the pressure to 30 bar. The system was sealed and left to stir for the desired length of time. Once the reaction time had elapsed, the heating jacket was removed and the autoclave cooled. The CO was then vented and the sample was then stored until analysed.

6.2.2 Gas Experiments: Batch Reactor

Catalyst solutions were made up as stated in the sections below and they were then used in a batch autoclave following the procedure outlined below. The individual component parts are detailed below and shown in figure 6.1.

The reactor setup incorporates the following components: a cylinder attachment (1); a pressure transducer to record the reservoir pressure (2); a mass flow controller (3) to regulate the gas flow into the reactor autoclave; substrate injector (4); a needle valve to open/closed the autoclave reactor from the rest of the reactor set up – allowing for the change from constant pressure to constant volume experiments (5); a screw cap seal for injecting/venting the catalyst solution for *in-situ* catalyst formation within the reactor (6); a pressure transducer for recording the pressure within the reactor throughout the reaction (7); a variable speed stirrer (8) and an electronically controlled heating jacket (9).

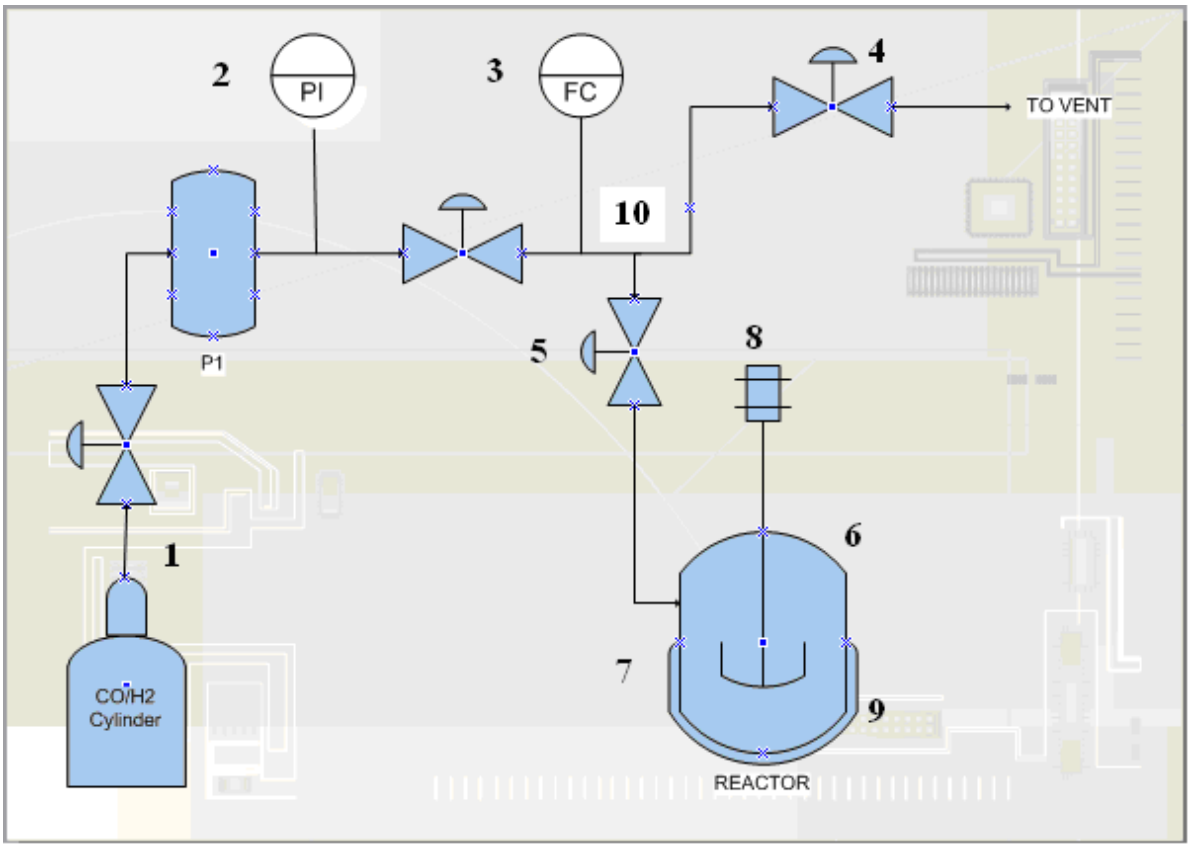

Figure 6.1: A schematic of the reactor

A gas cylinder (CO, H_2, 1:1 syngas, 2:1 syngas) was attached to the reactor via a high pressure cylinder head and stainless steel, flexible, high pressure tubing(1). The autoclave was fitted with a PTFE O-ring seal and fixed into place. The head of the autoclave was fitted with a removable cap, (6) which was then was then put into place to seal the autoclave. The reactor was purged with gas (10 bar) three times. This is done by venting the pressure through the cap (6). The catalyst solution was injected, through the cap, into the autoclave under a stream of gas and the autoclave was once again closed. The reactor was purged with gas twice, the stirrer (8) was then turned on and the system purged two further times. The required pressure was then set using the mass flow controller (3) and the reactor was brought to pressure (approximately 3 bar below the required pressure to allow for heat expansion) and then closed (5). The heating jacket was then fixed to the autoclave and the temperature and ramp rate set using the temperature regulator. The heater (9) was switched on and the reactor was left to come up to temperature.

As the autoclave was heated, the reaction substrate was added to the injector (4) via the pressure release valve. This was then sealed and the injector brought up to pressure. Once at temperature the reactor was left for ten minutes to ensure the mixture was at equilibrium and then the connector valve (5) was opened to allow the substrate into the autoclave. If the reactor was running as a constant pressure system this valve was left open, whereas if the reactor was being run under constant volume conditions, the valve was closed once the autoclave was pressurised to the set pressure. The data from the pressure transducers (P1, shown as 2 in figure 6.1 and P2, shown as 7 in figure 6.1) was recorded every five seconds using a data logger and stored using a computer equipped with Pico data recording software.

6.3 The Hydrogenation of 1-Octene:

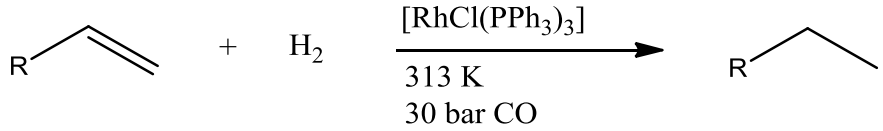

Wilkinson's catalyst, $[RhCl(PPh_3)_3]$ (10 mg, 0.01 mmol) was weighed into a Schlenk tube in a glove box. The flask was then removed from the glove box and attached to a Schlenk

line. Toluene (10 cm^3) was added and the mixture was heated gently and stirred until the entire solid had dissolved. The resulting solution was transferred using a syringe into the reactor under a flow of H_2. 1-octene (1 cm^3, 12.5 mmol) was injected under a positive pressure of gas into the autoclave as detailed in section 6.2.2.

6.4 The Hydroformylation of 1-Octene

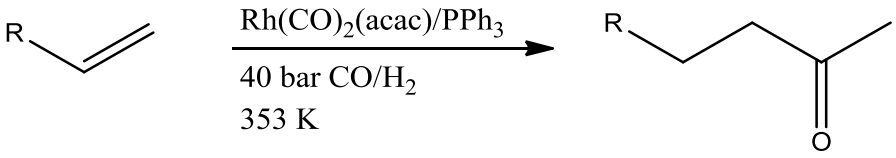

$Rh(CO)_2(acac)$ (12.9 mg, 0.05 mmol) was weighed into a Schlenk tube in a glove box along with triphenylphosphine (1.1 mg, 0.288 mmol) The flask was then removed from the glove box and attached to a Schlenk line. Toluene (10 cm^3) was added and the mixture was heated gently and stirred until the entire solid had dissolved. The resulting solution was transferred using a syringe into the reactor under a flow of 1:1 H_2/CO. 1-octene (1 cm^3, 12.5 mmol) was injected under a positive pressure of gas into the autoclave as detailed in section 6.2.2.

6.5 The Methoxycarbonylation of 1-Octyne

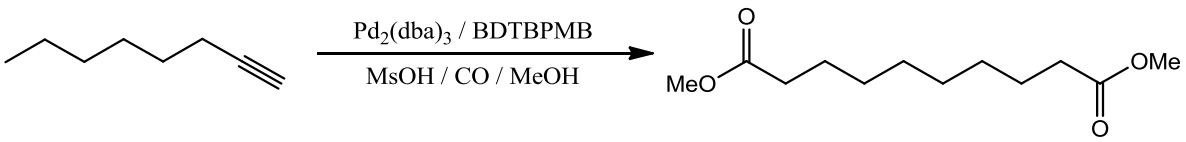

Tris(dibenzylideneacetone)dipalladium (20.67 mg, 0.0227 mmol) was weighed into a Schlenk tube in a glove box along with 1,2-bis(di-*tert*-butylphosphinomethyl)benzene (53.5 mg, 0.1365 mmol). The flask was then removed from the glove box and attached to a Schlenk line. Methanol (10 cm^3) was added followed by methanesulphonic acid (44 μl, 0.6825 mmol) and the mixture was heated gently and stirred until all the solid had dissolved. The resulting solution was transferred using a syringe into the reactor under a

flow of CO. 1-octyne (1 cm^3, 12 mmol) was injected under a positive pressure of gas into the autoclave as detailed in section 6.2.2.

6.6 The Methoxycarbonylation of 1-Pentyne

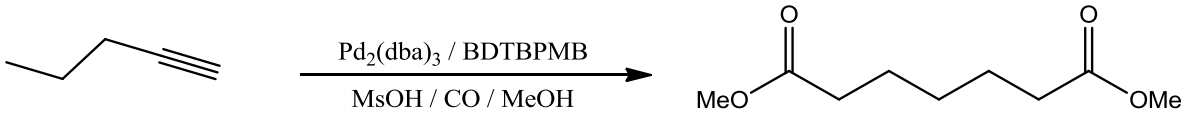

Tris(dibenzylideneacetone)dipalladium (20.67 mg, 0.0227 mmol) was weighed into a Schlenk tube in a glove box along with 1,2-bis(di-*tert*-butylphosphinomethyl)benzene (53.5 mg, 0.1365 mmol). The flask was then removed from the glove box and attached to a Schlenk line. Methanol (10 cm^3) was added followed by methanesulphonic acid (44 µl, 0.6825 mmol) and the mixture was heated gently and stirred until the entire solid had dissolved. The resulting solution was transferred using a syringe into the reactor under a flow of CO. 1-pentyne (1 cm^3, 21 mmol) was injected under a positive pressure of gas into the autoclave as detailed in section 6.2.2.

6.7 The Methoxycarbonylation of 1-Butyne/2-Butyne

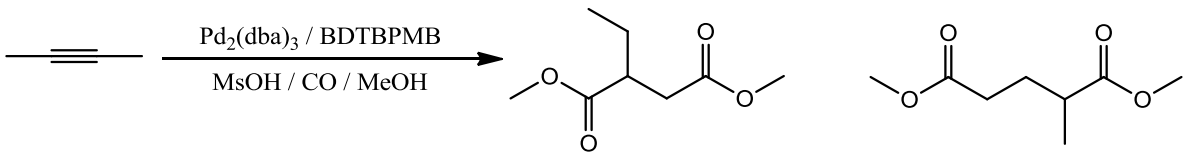

Tris(dibenzylideneacetone)dipalladium (20.67 mg, 0.0227 mmol) was weighed into a Schlenk tube in a glove box along with 1,2-bis(di-*tert*-butylphosphinomethyl)benzene (53.5 mg, 0.1365 mmol). The flask was then removed from the glove box and attached to a Schlenk line. Methanol (10 cm^3) was added followed by methanesulphonic acid (44 µl, 0.6825 mmol) and the mixture was heated gently and stirred until the entire solid had dissolved. The resulting solution was transferred using a syringe into the reactor under a flow of CO. Butyne (1 cm^3, 27 mmol) was injected, using a gas tight syringe, to account for

the volatility of the substrate, under a positive pressure of gas into the autoclave as detailed in section 6.2.2.

6.8 The Methoxycarbonylation of Vinyl Acetate

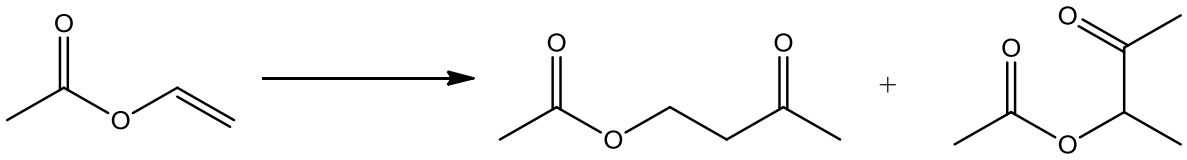

Tris(dibenzylideneacetone)dipalladium (47.5 mg, 0.05 mmol) was weighed into a Schlenk tube in a glove box along with 1,2-bis(di-*tert*-butylphosphinomethyl)benzene (197 mg, 0.5 mmol). The flask was then removed from the glove box and attached to a Schlenk line. Methanol (10 cm^3) was added followed by methanesulphonic acid (32 μl, 0.5 mmol) and the mixture was heated gently and stirred until the entire solid had dissolved. The resulting solution was transferred using a syringe into the reactor under a flow of CO. Vinyl acetate (1 cm^3, 25 mmol) was injected under a positive pressure of gas into the autoclave as detailed in section 6.2.2.

6.9 The Methoxycarbonylation of Phenylacetylene

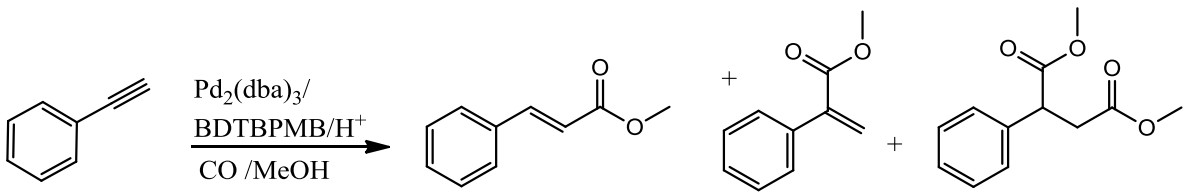

Tris(dibenzylideneacetone)dipalladium (4.2 mg, 0.0046 mmol) was weighed into a Schlenk tube in a glove box along with 1,2-bis(di-*tert*-butylphosphinomethyl)benzene (22 mg, 0.055 mmol). The flask was then removed from the glove box and attached to a Schlenk line. Methanol (10 cm^3) was added followed by methanesulphonic acid (9 μl, 0.138 mmol) and the mixture was heated gently and stirred until the entire solid had dissolved. The resulting solution was transferred using a syringe into the reactor under a flow of CO. Phenyl acetylene (1 cm^3, 10.5 mmol) was injected under a positive pressure of gas into the autoclave as detailed in section 6.2.2.

6.10 Determination of the Orders with Respect to Individual Reacting Components

In order to determine the orders with respect to each of the reacting components, the above experiments had certain components changed.

6.10.1 Determination of the Order with Respect to Methanol

Tris(dibenzylideneacetone)dipalladium (47.5 mg, 0.05 mmol) was weighed into a Schlenk tube in a glove box along with 1,2-bis(di-*tert*-butylphosphinomethyl)benzene (197 mg, 0.5 mmol). The flask was then removed from the glove box and attached to a Schlenk line. Methanol (2, 4, 6, 8 or 10 cm^3) was added and Toluene (8, 6, 4 and 2cm^3 respectively) was added to make the total "solvent" volume 10 cm^3. Methanesulphonic acid (32 μl, 0.5 mmol) was then added and the mixture was heated gently and stirred until all the solid had dissolved. The resulting solution was transferred using a syringe into the reactor under a flow of CO. Vinyl acetate (1 cm^3, 25 mmol) was injected under a positive pressure of gas into the autoclave as detailed in 6.2.2.

6.10.2 Determination of the Order with Respect to Substrate

Tris(dibenzylideneacetone)dipalladium (47.5 mg, 0.05 mmol) was weighed into a Schlenk tube in a glove box along with 1,2-bis(di-*tert*-butylphosphinomethyl)benzene (197 mg, 0.5 mmol). The flask was then removed from the glove box and attached to a Schlenk line. Methanol (8-10 cm^3) was added followed by methanesulphonic acid (32 μl, 0.5 mmol) and the mixture was heated gently and stirred until the entire solid had dissolved. The resulting solution was transferred using a syringe into the reactor under a flow of CO. Vinyl acetate (2, 1.5, 1 and 0.5 cm^3, 12.5-50 mmol) were injected under a positive pressure of gas into the autoclave as detailed in above.

6.10.3 Determination of Order with Respect to Gas

When determining the order with respect to a particular gas it is possible by the means of the mass flow controller attached to the reactor to vary the pressure of the gas for the length of the reaction. When there is more than one reactant gas present, a different method of preparation was used, which is detailed in 6.10.4.

6.10.4 Hydroformylation: 2 or More Gases

A gas cylinder (H_2 or CO) was attached to the reactor via a high pressure cylinder head and stainless steel, flexible, high pressure tubing. The autoclave was fitted with a PTFE O-ring seal and fixed into place. The cap, which is fitted to the head of the autoclave, was put into place to seal the autoclave. The reactor was purged with gas, (10 bar) three times through the cap. The catalyst solution was injected into the cap of the autoclave under a stream of gas and the autoclave was closed. The reactor was purged with gas (10 bar) twice, the stirrer was then turned on and the system was purged a further two times. The required pressure was set using the mass flow controller and the reactor was brought to pressure (the pressure throughout these experiments was set at 20 bar) and then closed (using valve 5 shown in figure 6.1). The cylinder was closed, the head was vented and replaced by the next required gas cylinder (either CO or H_2, the opposite of which was added primarily). The cylinder was then pressurised and the mass flow controller was set to the appropriate pressure (for 15 bar of the second gas, the mass flow controller would be set to 35 bar). The connecting pipe work was vented three times before the autoclave was brought up to pressure and closed.

The heating jacket was fixed to the autoclave and the temperature and ramp rate set using the temperature regulator. The heater was switched on and the reactor was left to come up to temperature. Whilst the reactor was heating the second gas cylinder was closed and vented and replaced by a cylinder of 1:1 ratio synthesis gas. The mass flow controller was set to 5 bar over the pressure in the autoclave (during heating 35 bar of CO/H_2 mix expanded up to 5 bar). The reaction substrate was added to the injector via the pressure release valve under a stream of gas (shown as part 5 in figure 5.2). This was then sealed and the injector brought up to pressure with CO/H_2 mix. The additions of substrate and the pressure measurements procedures were the same as for the single gas reactions.

[1] P. W. N. M. v. Leeuwen, 'Rhodium Catalysed Hydroformylation', Kluwer Academic Publishers, 2000.

Chapter 7: Conclusions and Further Work

7.1: Conclusions

A homogeneous batch reactor, fitted with equipment to continuously monitoring temperature and pressure, can be used to record the progress of reactions incorporating gases. Gas uptake analysis can be used to successfully determine the overall orders with respect to the individual reacting components within these reactions.

It was found that, in a two component reaction, such as the hydrogenation of an alkene, the orders with respect to each component can be determined in two experiments. The rhodium catalysed hydrogenation of 1-octene is first order in substrate and zero order with respect to the partial pressure of hydrogen. These findings tie in with previous studies which have shown that the reaction proceeds via the formation of a hydride species before the coordination of the alkene. The coordination of the alkene is the rate determining step within the reaction.

The rhodium catalysed hydroformylation of 1-octene involves three reacting components changing simultaneously. When each of these reacting components is looked at individually it is possible to determine the order with respect to each reacting component. It was found that the order with respect to substrate was 1, the order with respect to the partial pressure of hydrogen was 0.1 and the order with respect to the partial pressure of CO was found to be -0.4. This allowed for the postulation that the catalytic cycle follows the dissociative mechanism and that the rate determining step for the reaction is the insertion of the alkene. It was difficult to deconvolute the individual orders with respect to CO and H_2 simply using reaction progress kinetic analysis.

Additional complication is added when considering the methoxycarbonylation of vinyl acetate as this involves one gas and two liquid reacting components, one of which is the solvent for the reaction. The reaction was found to be first order in vinyl acetate concentration and first order in methanol concentration suggesting methanolysis is the rate determining step within the catalytic cycle. It was found that the order with respect to the partial pressure of CO was negative. The negative order in CO is thought to be as a result of

CO removing palladium from the catalytic cycle to form the resting complex $[PdH(CO)BDTMPMB]^+$. This would also explain the first order dependence on vinyl acetate.

The methoxycarbonylation of phenylacetylene gave insight into the impact of steric hindrance on the final product formation and product distribution. The formation of methyl cinnamate in almost quantitative yields showed that the steric bulk of the ligand gave rise to a preferential formation of the linear product. This also meant that the potential second methoxycarbonylation to form dimethyl 2-phenylsuccinate was prevented as the double bond was not accessible for coordination. The formation of only the linear product also highlighted the reaction proceeded via the hydride mechanism as steric interactions involved in the carbomethoxy mechanism would result in the preferential formation of the branched product, methyl atropate.

At low phenylacetylene concentrations, the reaction was found to be first order in substrate concentration, zero order in methanol and zero order in pCO. It is proposed that, under these conditions, the substrate coordination is rate determining and that all of the palladium is involved in the catalytic cycle.

The methoxycarbonylation of 1-octyne, 1-pentyne and 1-butyne incorporated the learning from the alkene and carboxylic acid methoxycarbonylation previously studied in the Cole-Hamilton group.[1-3] The initial methoxycarbonylation at the α-terminal position produced an α,β-unsaturated carboxylic acid ester. The tandem isomerisation reaction resulted in the double bond being isomerised out to the opposite terminal position before being trapped there and carbonylated to form a α,ω-diester product. This allowed for the formation of the diesters in a one pot reaction without the generation of waste.

The first step of this reaction was found to be exceedingly fast and was mass transport limited. This meant that very little information could be extracted about the kinetics associated with the first step of this reaction. The second step was then found to be limited by the rate of isomerisation rather than carbonylation. The similarity in rate constant observed for this step for both pentyne and octyne was interpreted as suggesting that the actual rate determining step is the removal of the double bond from conjugation with the ester group in the α,β-unsaturated ester.

The methoxycarbonylation of linear alkynes produced predominantly linear products which again showed that the reaction proceeded via the hydride mechanistic pathway. The predominant products are dictated by the steric hindrance impacted on the substrate from the catalytically active species containing the bulky phosphine groups. This results in 1,2-insertion being the more sterically favourable in the C-C bond formation step and as such, the linear product would be the dominant product when the catalytic cycle follows the hydride mechanism.

Internal alkenes were found to isomerise to a terminal position before they underwent methoxycarbonylation. This would not be possible with internal alkynes and therefore 2-butyne and 4-octyne were studied to determine the product distribution and the impact of the chain length. The methoxycarbonylation of the 2-butyne resulted in the formation of two dicarbonylated products, with the isomerisation away from the quaternary centre preferred to the isomerisation past it. However, the methoxycarbonylation of 4-octyne produced only the monocarbonylated product suggesting that the concentration of terminal double bonds formed by isomerisation of the tri-substituted conjugated double bond is vanishingly small.

7.2: Further Work

As this thesis shows, this analysis method is an effective tool for elucidating kinetic information from homogeneous reactions which involve gases. It is possible to determine orders with respect to various reacting components with considerably less reactions than previous kinetic investigations.

The method is shown to work effectively and some of the limits of the method have also been established. Future work can focus on establishing the extremes of this technique, as well as potentially combining this technique with various others such as nuclear magnetic resonance spectroscopy (NMR), Ultraviolet-visual spectroscopy (UV-vis) and gas chromatography-mass spectrometry (GCMS) to elucidation kinetic information and mechanisms for a number of homogeneous reactions which incorporate gases.

The learning from the methoxycarbonylation of alkynes can be combined with previous work in the Cole-Hamilton group[4-6] to allow for the study of the aminocarbonylation of alkynes.

As the alkyne reactions are very active and selective towards the linear products, the potential for moving these batch processes into continuous flow processes could be explored.

7.3 References

1 C. Jimenez-Rodriguez, G. R. Eastham, and D. J. Cole-Hamilton, *Inorg. Chem. Commun.*, 2005, **8**, 878.

2 C. Jimenez-Rodriguez, G. R. Eastham, and D. J. Cole-Hamilton, *J. Chem. Soc., Dalton Trans.*, 2005, 1826.

3 C. Jimenez-Rodriguez, D. F. Foster, G. R. Eastham, and D. J. Cole-Hamilton, *Chem. Commun.*, 2004, 1720.

4 C. Jimenez-Rodriguez, P. J. Pogorzelec, G. R. Eastham, A. M. Z. Slawin, and D. J. Cole-Hamilton, *J. Chem. Soc., Dalton Trans.*, 2007, 4160.

5 A. A. Nunez-Magro, G. R. Eastham, and D. J. Cole-Hamilton, *Chem. Commun.*, 2007, 3154.

6 A. A. Nunez-Magro, L. M. Robb, P. J. Pogorzelec, A. M. Z. Slawin, G. R. Eastham, and D. J. Cole-Hamilton, *Chem. Sci.*, 2010, **1**, 723.